Integration of Product Recovery in Microbial Advanced Biofuel Production: Overcoming Emulsification Challenges

Proefschrift

ter verkrijging van de graad van doctor
aan de technische universiteit delft,
op gezag van de rector magnificus prof. ir. K.Ch.A.M. Luyben
voorzitter van het College voor Promoties,
in het openbaar te verdedigen op donderdag
7 januari 2016 om 15.00 uur.

Door

Arjan Sebastiaan HEERES
Bioprocestechnoloog, geboren te Vlissingen, Nederland

This dissertation has been approved by the
promotors: Prof. dr. ir. L.A.M. van der Wielen and Prof. dr. ir. J.J. Heijnen,
and copromotor: Dr. M.C. Cuellar Soares.

Composition of the doctoral committee:

Rector Magnificus	Chairman
Prof. dr. ir. L.A.M. van der Wielen	Delft University of Technology
Prof. dr. ir. J.J. Heijnen	Delft University of Technology
Dr. M.C. Cuellar Soares	Delft University of Technology
Independent members:	
Prof. dr. B. Bühler,	Helmholtz Center for Environmental Research Leipzig and University of Halle, Germany
Prof. dr. ir. R.M. Boom	Wageningen University
Prof. dr. R.F. Mudde	Delft University of Technology
Dr. K.R. Benjamin	Amyris Inc., USA
Prof. dr. ir. H.J. Noorman	Delft University of Technology, reserve member

The research for this thesis was performed at the Department of Biotechnology, Faculty of Applied Sciences, Delft University of Technology, the Netherlands.

This work was carried out within the BE-Basic R&D Program, which was granted a FES subsidy from the Dutch Ministry of Economic affairs, agriculture and innovation (EL&I).

Cover design by: Karlijn van Etten
Printed and bound in The Netherlands by Gildeprint.
ISBN 978-94-6186-583-0

Summary

This thesis is the result of the first PhD research project executed within the Delft Integrated Recovery Column (DIRC) project, funded by BE-Basic. About a decade ago, the first reports came out of genetically engineered microorganisms that produced significant amounts of long chain hydrocarbons, which could be used as advanced biofuels. However, cost reductions in both the microbial production and in the used process technology are required to create an economically feasible alternative. In the microbial production of advanced biofuels, the product is secreted and oil droplets are formed in the fermentation broth. Components in the fermentation broth, originating from the feed or the microorganism, can cause droplet stabilisation. This results in formation of a stable emulsion and hinders the recovery of the product. The present recovery process (centrifugation and de-emulsifiers) is expensive and does not allow complete cell recycling. These problems also apply to other multiphase fermentations. Therefore the DIRC project was conceived, aiming at developing cheaper process technology that can be applied at an industrial scale to make the production of advanced biofuels more economically feasible.

At the start of the PhD project, the knowledge about the possible causes of emulsion formation and the properties of the formed emulsions in advanced biofuel fermentations was limited. The first goal was to study the likeliness of emulsions in these processes and to come with a model emulsion that van be used to characterise the stability and behaviour of these emulsions. The second goal was to develop an oil recovery process that avoids the use of usually toxic de-emulsifiers, has low energy requirements and investment costs (no centrifugation), and can be integrated with the fermentation. The latter can reduce costs by:

- Lower equipment costs – When the separation is integrated with the fermentation, only one piece of equipment is needed.
- Easier product recovery – Continuous removal of the product from the fermentation broth reduces the residence time of the product droplets in the fermentation broth. This

reduces the time available for the droplet stabilisation to take place, lowering emulsion stability.

- A cell recycle – A separation method without (usually toxic) de-emulsifiers leaves cell viability intact. When such a separation method is then integrated with the fermentation, the cells can be recycled directly, leading to smaller fermenters and higher yields.

In the recovery of the advanced biofuel, coalescence of the secreted product droplets is the most important mechanism, leading to larger droplets and formation of an oil layer. A literature study (Chapter 2) showed that a wide variety of components in fermentation processes can hinder coalescence, by causing interface stabilisation or inducing repulsion between droplets. These components can originate from the feedstock (e.g., hydrolysed cellulosic biomass) or be released by the microorganism (e.g., proteins, glycolipids, glycoproteins). Experimental measurements using microfluidics and stirred vessels confirmed the finding of the literature study, showing that some fermentation broth components (e.g., mannoproteins, HMF) indeed influence coalescence and slow down this process several orders of magnitude (Chapter 3).

Product emulsification has been mentioned in patent literature on the microbial production of advanced biofuels, such as farnesene. In that process, most of the cells and water are removed from the emulsion by a first centrifugation step and a concentrated emulsion is obtained. In the second step, coalescence into a continuous oil layer is forced by centrifugation with addition of chemical de-emulsifiers (e.g., surfactants such as Triton X114).

Gravity separation is a cheap separation alternative for the first centrifugation step, but the droplet size in the fermentor has to be large enough. A regime analysis showed that process conditions can be chosen in a way that droplet coalescence is favoured, making gravity separation possible (Chapter 4). However, integration of gravity separation with the fermentation requires a separate, gas-free compartment, in which droplets rise to form a concentrated emulsion.

The used model emulsion (hexadecane/water/yeast derived protein) quickly separated by gravity, resulting in a concentrated emulsion instead of a single oil phase. A separation method leading to a continuous oil layer was developed that uses gas bubbles to induce coalescence of stabilised droplets into a continuous oil layer (Chapter 5). By changing the properties of the gas phase (gas flow, nozzle diameter), the rate at which this continuous oil layer was formed could be influenced, showing possibilities for optimisation. This separation method eliminates the need for harsh process conditions or de-emulsifiers, so this method fits the earlier mentioned requirements.

In conclusion, this thesis shows that challenges in product recovery are serious for advanced biofuels production and will oppose challenges in other multiphase fermentation processes as well. A separation method was developed that shows potential to improve advanced biofuel production. Next steps towards an integrated advanced biofuel fermentation and separation are to apply the gas bubble induced coalescence method in a fermentation process, to optimise the fermentation conditions to minimise the emulsion formation, and to develop and scale-up an integrated reactor in which the fermentation and gas bubble induced oil recovery are integrated. These aspects are currently being addressed within the DIRC project.

Samenvatting

Dit proefschrift is het resultaat van het eerste promotieonderzoek uitgevoerd binnen het *Delft Integrated Recovery Column* (DIRC) project, gefinancierd door BE-Basic. Ongeveer tien jaar geleden kwamen de eerste berichten over genetisch gemodificeerde micro-organismen die significante hoeveelheden koolwaterstoffen produceren met lange koolstofketens. Dit soort moleculen zijn zeer vergelijkbaar met de moleculen in de huidige transportbrandstoffen, in tegenstelling tot bijvoorbeeld ethanol, en kunnen dus beschouwd worden als geavanceerde biobrandstoffen. Echter, de kosten van deze microbiële productie moeten omlaag gebracht worden voordat het een economisch haalbaar alternatief is. Tijdens de microbiële productie van deze geadvanceerde biobrandstoffen wordt het product in de fermentatie door de cellen uitgescheiden en vormt het kleine oliedruppels in het fermentatiebeslag. De oppervlakte actieve stoffen aanwezig in het fermentatiebeslag kunnen de oliedruppels stabiliseren, waardoor er emulsies gevormd worden en de scheiding van het product gehinderd wordt. In het huidige productieproces worden meerdere centrifugatiestappen gebruikt in combinatie met chemische emulsiebrekers, wat voor hoge kosten zorgt en het compleet recyclen van de cellen onmogelijk maakt. Het DIRC project richt zich op het ontwikkelen van goedkopere procestechnologie die op industriële schaal gebruikt kan worden om de productie van geavanceerde biobrandstoffen economisch haalbaar te maken.

Aan het begin van het promotieonderzoek was de kennis over de mogelijke oorzaken van emulsievorming en de emulsie-eigenschappen beperkt. Het eerste doel was om de emulsies in deze processen te bestuderen en om met behulp van een model emulsie methodes te ontwikkelen om de emulsies te karakteriseren. Het tweede doel was om een scheidingsproces te ontwikkelen zonder chemische emulsiebrekers, met lage energiebehoeften, met lage investeringskosten (dus geen centrifuge), en met de mogelijkheid van integratie met de fermentatie. Het integreren van de twee processen kan leiden tot lagere productiekosten door:

- Lagere apparatuurkosten – Wanneer de scheiding en fermentatie geïntegreerd worden is slechts één apparaat nodig.
- Eenvoudiger scheiding – Als het product continu verwijderd wordt uit het fermentatiebeslag, dan wordt de verblijftijd van de oliedruppels in het fermentatiebeslag verkort. De tijd die dan beschikbaar is voor het stabiliseren van de druppels wordt verminderd, wat kan leiden tot een verlaagde emulsiestabiliteit.
- Het recyclen van de cellen – Met een scheidingsmethode zonder chemische emulsiebrekers kunnen de cellen levensvatbaar blijven. Als de scheiding dan geïntegreerd wordt met de fermentatie kunnen de cellen gerecycled worden en is er minder substraat voor de groei van biomassa nodig.

De belangrijkste stap in het scheiden van de geavanceerde biobrandstof is coalescentie van de oliedruppels, wat leidt tot grotere druppels, die gemakkelijker te scheiden zijn, en de vorming van een olielaag. Een literatuurstudie (Hoofdstuk 2) laat zien dat een breed scala aan componenten in fermentatieprocessen coalescentie kunnen hinderen, doordat ze het druppeloppervlak stabiliseren of afstoting tussen druppels veroorzaken. Deze componenten kunnen afkomstig zijn uit de grondstof voor de biobrandstof (bijvoorbeeld in een oplossing van gehydrolyseerde cellulose) of worden losgelaten door de micro-organismen (bijvoorbeeld eiwitten, glycolipiden, glycoproteïnen). Experimenteel werk bevestigt wat in de literatuur studie was gevonden, dat sommige componenten (bijv mannoproteïnen) coalescentie sterk kan laten afnemen (Hoofdstuk 3).

Een voorbeeld van de vorming van emulsies in de productie van geavanceerde biobrandstoffen kan gevonden worden in patentliteratuur die de microbiële productie van farneseen betreft. In dat proces worden in een eerste scheidingsstap het merendeel van de cellen en water verwijderd en wordt een geconcentreerde emulsie verkregen. In de tweede stap vindt coalescentie van de geconcentreerde emulsie tot een continue olielaag, gedwongen door een tweede centrifugatie met toevoeging van chemische emulsiebrekers (bijvoorbeeld oppervlakteactieve stoffen zoals Triton X114).

Scheiding met behulp van de zwaartekracht kan een goedkoop alternatief zijn voor de eerste centrifugatiestap, maar dan moet de druppelgrootte in de fermentor voldoende groot zijn. Uit een regime analyse blijkt dat het mogelijk is om procescondities te kiezen zodat coalescentie van druppels bevorderd wordt, en scheiding van de gevormde grotere druppels met behulp van de zwaartekracht mogelijk zou zijn (Hoofdstuk 4). Echter, voor de integratie van zwaartekrachtscheiding met de fermentatie is een afzonderlijk, gas-vrij compartiment nodig in de fermentor, waarin druppeltjes kunnen scheiden tot een geconcentreerde emulsie.

In het gebruikte model mengsel (hexadecaan/water/eiwit afkomstig van bakkersgist) scheidden de oliedruppels onder invloed van de zwaartekracht snel tot een geconcentreerde emulsie, echter een continue oliefase wordt niet gevormd. Om tot een continue olielaag te komen is een scheidingswerkwijze ontwikkeld die gasbellen gebruikt om coalescentie van druppeltjes in de emulsie naar een continue olielaag te induceren (Hoofdstuk 5). Door de eigenschappen van de gasfase aan te passen (gasdebiet, de diameter van het beluchtingsgat), kan de snelheid waarmee deze continue olielaag werd gevormd worden beïnvloed en zijn er dus mogelijkheden voor optimalisatie. Met deze scheidingsmethode zijn extreme procesomstandigheden of chemische emulsiebrekers niet meer nodig en voldoet de scheidingsmethode aan eerder genoemde eisen.

Dit proefschrift richt zich op de uitdagingen in het scheiden van geavanceerde biobrandstoffen van het fermentatiebeslag, maar de resultaten van het werk zijn ook van toepassing op andere meerfase fermentatieprocessen. Een scheidingsmethode is ontwikkeld die het mogelijk maakt de productie van geavanceerde biobrandstoffen te verbeteren. Volgende stappen naar een geïntegreerde fermentatie en scheiding van geavanceerde biobrandstof zijn het toepassen van de gasbel-geïnduceerde coalescentie in een fermentatieproces, het optimaliseren van de fermentatie condities om de emulsievorming te minimaliseren, en het ontwikkelen en opschalen van de geïntegreerde reactor waarin de fermentatie en de nieuwe methode van de gasbel-geïnduceerde coalescentie zijn geïntegreerd. Deze aspecten worden momenteel onderzocht binnen het DIRC project.

Contents

Chapter 1. Introduction

1.1 Renewable energy resources

Global warming, public health, environmental preservation, energy security, fossil fuel depletion; these are just a few of the reasons why the attention for renewable energy keeps increasing and it is applied more and more. Biofuels have an important role in the transition to renewable energy sources. At this moment, bioethanol is already widely used in the United States, Brazil, and the European Union to blend with gasoline and replace part of the fossil based gasoline in transportation fuels [1]. A next step for urban road transport would be to make the switch to electric engines or hydrogen, eliminating local emissions completely. In the aviation market, these possibilities do not exist due to payload restrictions and here, biofuels can provide a renewable alternative for fossil based kerosene [2]. Aviation fuels have very strict requirements with respect to energy density, cold-flow properties, freezing point, and thermal stability, and therefore it is expected that liquid hydrocarbon fuels will remain to be used [3].

1.2 Aviation biofuels

Currently, five different technologies for production of aviation biofuels are being developed, each in a different stage of maturity. Some of the fuels are already produced at a commercial scale and used in commercial flights, others are still in the research and development stage.

1.2.1 Hydrotreated esters and fatty acids

The conversion of oils or fats (triglycerides) into biodiesel by transesterification with methanol or ethanol is a route to convert oil/fat waste streams into biofuels. However, the resulting biofuels do not meet the standards set for jet fuel properties, especially in terms of their freezing and cloud points in mixtures, making them unsuitable for the application as aviation biofuel [4]. An improved fuel can be obtained by hydrotreating the fatty acids, esters,

or directly treating the triglycerides. In this process, a combination of high hydrogen pressure and a catalyst results in the removal of oxygen from the fatty acids and the saturation of double bonds present in the molecule [5]. The produced hydrotreated esters and fatty acids (HEFA) are linear alkanes that can be upgraded further to meet the requirements for jet fuels. In July 2011, the ASTM approved the use of HEFA as jet biofuel as a drop in fuel up to 50% of the total mixture [6]. Neste Corporation is the main producer of this type of biofuels, having provided fuel for over 1000 commercial flights up to now [7]. The feedstock supply proves to be the main challenge for this process, with the limited availability of waste oils and fats. For further growth of this process, other sustainable sources for triglycerides need to be developed, for instance lipids from microalgae or oleaginous yeast.

1.2.2 Fischer Tropsch

The second process that acquired ASTM approval for the produced biofuel is based on the Fischer-Tropsch process. This process is applied at a commercial scale to produce liquid fuels from coal (Sasol) or natural gas (Shell), via synthesis gas. Biomass can also be converted into synthesis gas by different gasification methods, giving different compositions of the synthesis gas, which could cause difficulties in the Fischer-Tropsch process itself [8]. At this moment, the Fischer-Tropsch process is not commercially operated using biomass feedstocks, but when syngas production from the biomass can be further optimised it could become cost competitive in 2020 [9].

1.2.3 Alcohol to jet fuel

The production of alcohols by fermentation is well established in industry, especially ethanol produced by fermentation is widely available, but also (iso-)butanol can be produced by fermentation. After dehydration of the alcohols, the resulting olefins can be oligomerised to form molecules with a longer carbon chain. Further processing, for instance hydrogenation or cracking, results in the final product that can be used as jet biofuel [10]. Several companies have demonstrated these processes up to pilot scale: Lanzatech and Swedish Biofuel AB

(ethanol, http://www.lanzatech.com/), BYOGY and Qatar Airways (ethanol, http://www.byogy.com/), and Gevo and the US airforce (*iso*-butanol) [11]. Currently, the jet fuels produced from alcohols are in the process of obtaining ASTM approval, which is expected to be granted in the near future [10].

1.2.4 Hydrotreated depolymerized cellulosic jet fuel

Biomass can also be directly converted into a bio-crude oil mixture by pyrolysis or liquefaction [12]. The first step in both processes is to grind the feedstock into small particles, which is preceded by a drying step in pyrolysis. Then, the particles are quickly heated to 650-800 K in pyrolysis or 525-725 K in liquefaction. Compared to pyrolysis, liquefaction requires a catalyst (sodium carbonate in water), higher pressures (5-20 atm), and a longer residence time. These differences result in higher process costs for liquefaction, but the bio-crude product contains a lower amount of oxygen and therefore requires less upgrading [13]. Further hydrogenation of the bio-crude is necessary to remove this oxygen and saturate double bonds in the molecules. The complex composition of the feedstock and the unselective chemistry yield a complex product mixture with a wide range of carbon chains. By a distillation step, the different fractions in the product can be separated (lights, gasoline, kerosene, and diesel). One of the main challenges for this process is to have a sustainable source of the hydrogen that is required for the upgrading of the bio-crude.

1.2.5 Direct fermentation of sugar to jet fuel

Another method to convert the sugars from biomass into aviation biofuel is by fermentation with genetically engineered microorganisms. Several long carbon chain biofuels have been produced by *Saccharomyces cerevisiae* and *Escherichia coli*: alkenes and alkanes (C13-C17) [14, 15], sesquiterpenes (C15) such as farnesene and bisabolene [16, 17], and 'high chain' alcohols (C12-C18) [18]. Of these compounds, the production of farnesene is most mature and this process has been commercialised by Amyris (www.amyris.com). This company started with producing a precursor for the anti-malarial drug artemycin by

implementing the isoprenoid pathway in yeast [19], but small adaptations in the pathway led to a microorganism that produced significant quantities of *trans*-β-farnesene. For this fermentation, product titers above 100 g/L have been reported [20]. After hydrogenation to farnesane, the product can be used as a jet fuel. In 2014, the ASTM approved the use of farnesane into kerosene blends up to 10% [6]. The current production process of farnesane is too expensive to create an economically feasible alternative for fossil based kerosene. However, large amounts of glucose based feedstock are available for this process.

1.3 Opportunities in fermentative advanced biofuel production: the dream process

Because the different technologies are in different stages of maturity, making a fair comparison is difficult. However, by looking at the nature of the processes, several advantages of advanced biofuel production by fermentation can already be pointed out. The use of fermentation at very large scale has been proven for the production of ethanol, switching to production of other biofuels could be regarded as a next step forward. Comparing the fermentation process to the physical-chemical technologies, the process conditions (pressure, temperature) are mild so the equipment and operating costs will be lower. Furthermore, the products are nearly insoluble in water and product droplets are formed in the fermentation broth when the biofuel is secreted by the microorganism. The density difference between the aqueous and organic phase ranges from 0.11 to 0.24 kg/L (Table 1), creating the possibility for a simple gravity separation process.

Table 1. Different advanced biofuels that can be produced by fermentation, their densities [21], and the density differences with water (1 kg/L).

Compound	Chemical formula	Density (kg/L)	Density difference (kg/L)
Tridecane	$C_{13}H_{28}$	0.76	0.24
Heptadecane	$C_{17}H_{36}$	0.78	0.22
Farnesene	$C_{15}H_{24}$	0.84	0.19
Bisabolene	$C_{15}H_{24}$	0.89	0.11
Dodecanol	$C_{12}H_{25}OH$	0.83	0.17
Octadecanol	$C_{18}H_{37}OH$	0.81	0.19

Amyris is one of the companies that saw the potential of this production route and was the first to commercialise the fermentative production of advanced biofuels. After laboratory and pilot experiments in the United States, a full scale production facility was constructed in Brazil, where farnesene is produced from sugarcane syrup. The product is used as *Diesel de Cana* ™ in São Paulo city busses, contributing to the sustainability targets of the city of São Paulo (www.amyris.com). Due to the high production costs, farnesane is not commercially used in aviation fuels yet and Amyris decided to focus on hydrocarbon applications in higher value markets instead, such as lubricants, cosmetics, and fragrances.

A production process can be proposed from patent data and publically available information (Figure 1). Using a genetically engineered yeast strain, sugars are aerobically converted into farnesene in 200 m^3 fermenters (www.amyris.com). This results in a four phase fermentation mixture (cells/aqueous liquid/organic product/gas). In the first centrifugation step, water and part of the cells are removed and a concentrated emulsion is obtained (cream). After addition of chemical de-emulsifiers, a second centrifugation step results in recovery of an organic product phase [22]. The obtained product can then be hydrogenated to saturate the double bonds in the molecule and form the farnesane end product.

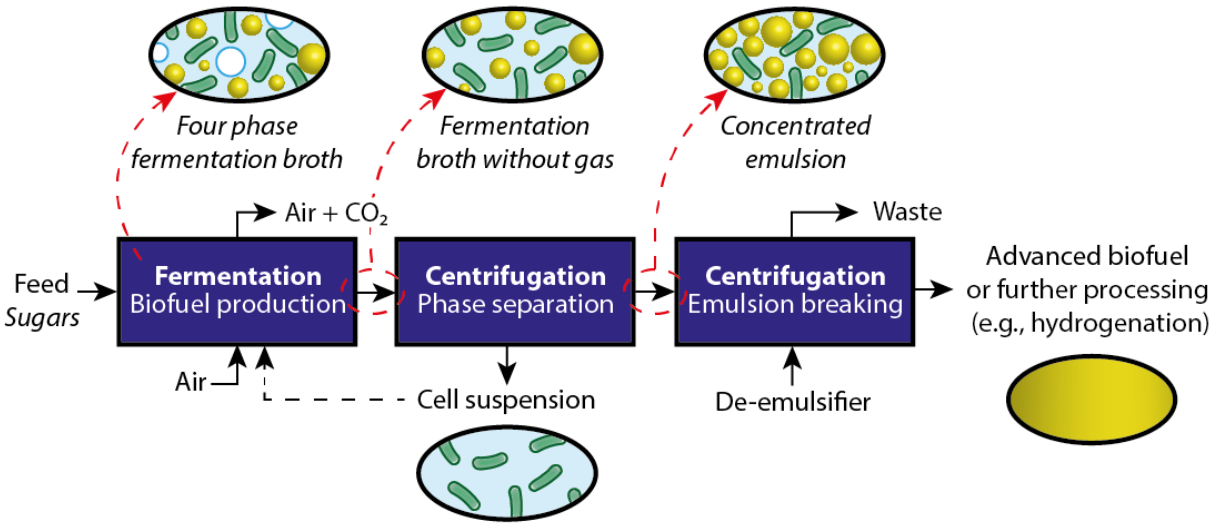

Figure 1. The status quo of advanced biofuel production.

Looking at the current production process, several opportunities can be identified for process improvement and the decrease of process costs:

- Use of a cheaper feedstock – In the production of bio-ethanol, several companies (e.g., POET-DSM, Abengoa, DuPont) have built plants in which cellulosic parts of the corn plant are used to produce ethanol instead of the corn itself. Implementing similar biotechnology in advanced biofuel fermentations will lead to lower substrate costs.
- Development of an anaerobic metabolic pathway – The current aerobic metabolic pathway for farnesene production has a theoretical yield of 23.8 g farnesene per 100 g of glucose [23]. When external electron acceptors (such as oxygen) are eliminated in the pathway, the following process reaction is obtained:

$$3.5\ C_6H_{12}O_6 \rightarrow C_{15}H_{24} + 6\ CO_2 + 9\ H_2O \quad (1)$$

From this reaction, we can calculate the Gibbs free energy of the anaerobic formation of farnesene, using the values from Table 2.

Table 2. The Gibbs free energy of formation of the compounds in reaction for anaerobic farnesene formation [24, 25].

Compound	Gibbs free energy of formation (kJ/mol)
Glucose	-917.22
Farnesene	372
Carbon dioxide	-394.359
Water	-237.18

This reaction has a Gibbs free energy change of –275 kJ/$mol_{glucose}$, which is comparable to the anaerobic production of ethanol (-235 kJ/$mol_{glucose}$) [24], indicating that this process would be thermodynamically feasible. This anaerobic process would increase the theoretical yield with 36%, to 32.4 g farnesene per 100 g glucose, offering a significant reduction in substrate requirements for the process. Furthermore, strain stability could increase. In the aerobic pathway, degeneration of the strain occurs

because the microorganisms without the farnesene pathway will have a growth advantage over the farnesene producing microorganisms and will outcompete them. In the anaerobic process, the growth advantage is with the higher farnesene producers, so degeneration does not occur.

- Alternative separation methods – Substituting the centrifugation steps by a cheaper method will decrease the investment costs. With the typical density differences between the aqueous and organic phase (Table 1), gravity separation could be a candidate for achieving the phase separation and to obtain a concentrated emulsion. However, additional step(s) to break this concentrated emulsion and form a continuous oil layer will be required. This additional separation step should not be energy intensive and avoid the need of chemical de-emulsifiers. These de-emulsifiers add to the material costs, are potentially toxic to the microorganism, and could end up in the product. When the de-emulsifiers can be avoided, the cells will also remain viable and they could be recycled, lowering the amount of substrate required for microbial growth and allowing smaller fermentors.
- Continuous operation and unit integration – When strain degeneration can be limited by implementing an anaerobic pathway, the overall productivity of the process could be increased by operating the process in a continuous mode. Furthermore, the capital costs for fermentation and separation equipment could be reduced by integrating the two processes into a single unit. Also when the product is removed continuously, the surface active components will have less time to stabilise the emulsion and the separation process could become easier.

An economic analysis of the process showed that the price of the feedstock is the main parameter determining the product price [26], so improving yields and using cheaper feedstocks will clearly benefit the overall economy of the process. Besides the potential in improvements on the microbial side (use of cheap feedstock, high yield with an anaerobic pathway), the economic analysis showed that improvements in the downstream processing

and unit integration could provide an important contribution to lowering the production costs as well. Additionally, process technology that does not require chemical de-emulsifier eliminates the negative environmental impact of those compounds [26]. When the afore mentioned improvements are implemented in the current production process, a "dream" process for advanced biofuels would be obtained (Figure 2).

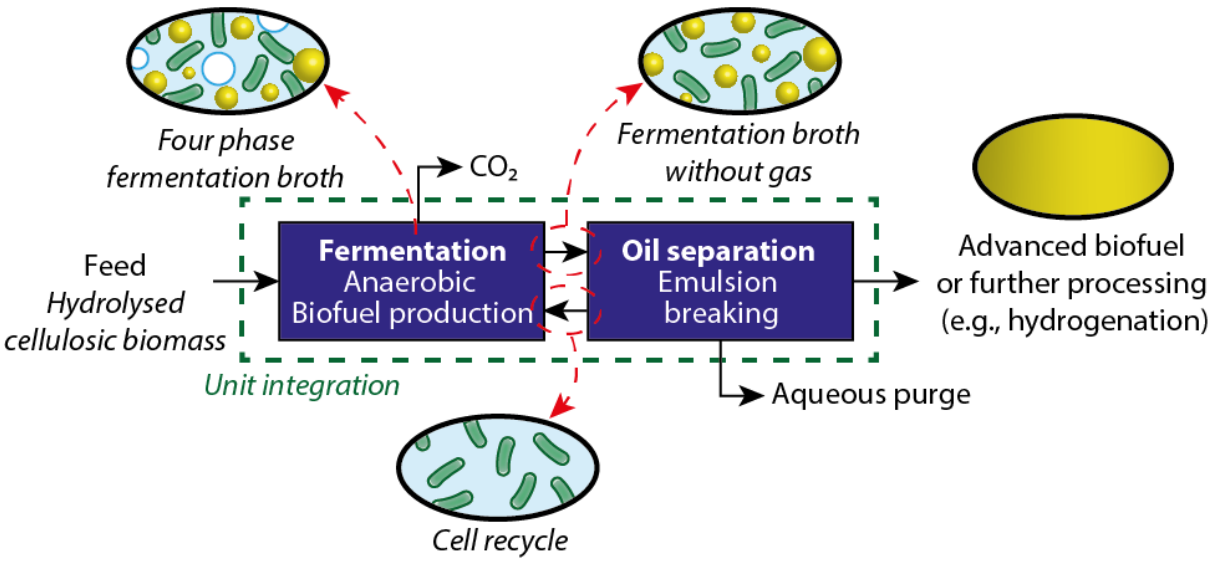

Figure 2. The "dream" process for advanced biofuel production, with impressions of the composition of the different flows (not drawn to scale).

Further research is required before all the mentioned improvements can be implemented in the process. In several groups, research is done on developing and optimising the microbial pathways to increase the metabolic yields or using alternative feedstocks (hydrolysed cellulosic biomass instead of sugars) [27, 28]. On the other hand, reports in literature on improving the process technology have been very limited up to now [29] and this area still has to be explored.

1.4 Product recovery without centrifugation and de-emulsifiers

Because the hydrocarbon product is immiscible with water, the secreted product droplets form a second liquid phase in the fermentation broth [14]. This offers the potential benefit of a very simple product recovery: droplets will rise up due to the density difference

and the accumulated droplets will coalesce into a continuous oil layer, which can then be removed. However, this has not been demonstrated and the fact that the current product recovery seems to rely on two centrifugation steps and addition of de-emulsifiers suggests otherwise. Since the product is secreted by the microorganism [23], the initial droplet size can be expected to be small. Since larger droplets will rise quicker due to the larger buoyancy force, the increase of the droplet size by coalescence is crucial. However, surface active components present in the fermentation broth can prevent coalescence by stabilising the oil/water interface and preventing the complete separation of the aqueous and organic phase. These challenges will have to be addressed to improve the product recovery to come to more economic production of advanced biofuels.

1.5 Delft Integrated Recovery Column reactor

In 2008, the Delft Integrated Recovery Column (DIRC) project was started based on the idea that production of advanced biofuels by microorganisms showed tremendous potential, but the challenges in product recovery were underestimated. In the DIRC reactor, the fermentation would be integrated with an alternative separation method (e.g., tilted plate settlers, flotation, hydrocyclones), resulting in a low cost reactor for advanced biofuel production. These first ideas were captured in a patent [30]. This PhD project was part of the overall DIRC project, focussing on the development of alternative separation methods and the exploring the opportunities for integration of the separation with fermentation. Parallel to this project, a research project has been started which studies the influence of the fermentation conditions on the product recovery and how the separation can be enhanced tuning these conditions. For further valorisation of the scientific findings of the DIRC project and commercialization of the technology, Delft Advanced Biorenewables (DAB, www.DelftAB.com) was founded as a spin out company of Delft University of Technology.

1.6 Thesis outline

Because reports on the challenges in product recovery of advanced biofuels from fermentation broths have been very limited in literature, the thesis will first continue with a detailed discussion of the potential causes of emulsion formation in fermentations with a second liquid phase and the process technology solutions to overcome these challenges (Chapter 2). Knowing which components hinder or enhance product recovery could provide directions for optimisation of the composition of the fermentation broth, making the product recovery easier. In Chapter 3, the effect of a selection of fermentation broth components on coalescence is studied. Multiple experimental approaches are used to acquire experimental information on the extent to which coalescence, and thereby the separation process, can be impacted by these components. Subsequently, the focus is shifted towards process integration and product recovery methods. A passive gravity separation is the most simple method to achieve phase separation and substitution of the first centrifugation step by passive gravity separation could reduce the process costs. Whether sufficient droplet coalescence can be achieved in the fermentor to facilitate gravity separation and whether gravity separation can be integrated with the fermentation was studied by a regime analysis (Chapter 4). As is suggested by the emulsion breaking step using de-emulsifiers and centrifugation, additional measures are required to recover the product as a pure organic phase instead of a concentrated oil/water emulsion. To achieve the separation of emulsified droplets, a method was developed that makes use of gas bubbles to induce coalescence of the emulsified oil droplets and causes the formation of a separate organic product phase (Chapter 5). Then in the last part of this thesis, the general conclusions from this research and the challenges that still have to be addressed will be discussed.

References

1. Demirbas, A., *Political, economic and environmental impacts of biofuels: a review.* Appl. Energy, 2009. 86(S1): p. S108-S117.
2. Daggett, D., et al., *Alternative Fuels and Their Potential Impact on Aviation*, in *25th Congress of the International Council of the Aeronautical Sciences*. 2006: Hamburg, Germany.
3. Marsh, G., *Biofuels: aviation alternative?* Renew. Energy Foc., 2008. 9(4): p. 48-51.
4. Hileman, J.I., P.E. Donohoo, and R.W. Stratton, *Energy Content and Alternative Jet Fuel Viability.* J. Propul. Power, 2010. 26(6): p. 1184-1196.
5. Lestari , S., et al., *Transforming Triglycerides and Fatty Acids into Biofuels.* ChemSusChem, 2009. 2(12): p. 1109-1119.
6. ASTM-D7566-14c, *Standard Specification for Aviation Turbine Fuel Containing Synthesized Hydrocarbons*. ASTM International, West Conshohocken, PA, 2014.
7. Lehmus, P., *Large scale chemical conversion of oils and residues in Rotterdam*, in *European Biofuels Technology Platform – 6th Stakeholder Plenary meeting*. 2014: Brussels.
8. Tijmensen, M.J.A., et al., *Exploration of the possibilities for production of Fischer Tropsch liquids and power via biomass gasification.* Biomass Bioenerg., 2002. 23(2): p. 129-152.
9. Chum, H.L., et al., *Conversion Technologies for Biofuels and Their Use*, in *Bioenergy & sustainability: bridging the gaps*, G.M. Souza, et al., Editors. 2015, SCOPE: Sao Paulo.
10. Karatzos, S., J.D. McMillan, and J.N. Saddler, *The Potential and Challenges of Drop-in Biofuels*. 2014, IEA Bioenergy.
11. Johnston, G., *Gevo - Alcohol to Jet (ATJ)*, in *Paris Air Show*. 2013: Paris.
12. Mohan, D., C.U. Pittman, and P.H. Steele, *Pyrolysis of Wood/Biomass for Bio-oil: A Critical Review.* Energy Fuels, 2006. 20(3): p. 848-889.
13. Alonso, D.M., J.Q. Bond, and J.A. Dumesic, *Catalytic conversion of biomass to biofuels.* Green Chem., 2010. 12(9): p. 1493-1513.
14. Schirmer, A., et al., *Microbial biosynthesis of alkanes* Science, 2010. 329: p. 559-562.
15. Howard, T.P., et al., *Synthesis of customized petroleum-replica fuel molecules by targeted modification of free fatty acid pools in Escherichia coli.* PNAS, 2013. 110: p. 7636-7641.
16. Peralta-Yahya, P.P., et al., *Identification and microbial production of a terpene-based advanced biofuel.* Nat. Commun., 2011. 2: p. 483.
17. Wang, C., et al., *Metabolic engineering of Escherichia coli for α-farnesene production.* Metab. Eng., 2011. 13(6): p. 648-655.
18. Steen, E.J., et al., *Microbial production of fatty-acid-derived fuels and chemicals from plant biomass.* Nature, 2010. 463(7280): p. 559-562.

19. Westfall, P.J., et al., *Production of amorphadiene in yeast, and its conversion to dihydroartemisinic acid, precursor to the antimalarial agent artemisinin.* PNAS, 2012. 109(3): p. E111-E118.
20. George, K.W., et al., *Isoprenoid drugs, biofuels, and chemicals - artemisinin, farnesene, and beyond*, in *Biotechnology of isoprenoids*, J. Schrader and J. Bohlmann, Editors. 2015, Springer International: Heidelberg. p. 355-390.
21. Patai, S., J. Zabicky, and Z. Rappoport, *Physical constants of organic compounds*, in *Handbook of chemistry and physics*, R.C. Weast, Editor. 1973, CRC Press: Cleveland, Ohio.
22. Tabur, P. and G. Dorin, *Method for purifying bio-organic compounds from fermentation broth containing surfactants by temperature-induced phase inversion*. US Patent 20120040396, 2012.
23. Chandran, S.S., J.T. Kealey, and C.D. Reeves, *Microbial production of isoprenoids.* Proc. Biochem., 2011. 46(9): p. 8-8.
24. Heijnen, J. and J. Van Dijken, *In search of a thermodynamic description of biomass yields for the chemotrophic growth of microorganisms.* Biotechnol. Bioeng., 1992. 39(8): p. 833-858.
25. Cueto-Rojas, H.F., et al., *Thermodynamics-based design of microbial cell factories for anaerobic product formation.* Trends Biotechnol., 2015. 33(9): p. 534–546.
26. Martinelli, F.G., *Design of a bioprocess for the production of microbial biojetfuel*. 2013, TU Delft: Delft.
27. Wenger, J.W., et al., *Minimizing the cost of cellulosic-biomass-derived Amyris diesel by combining non-native sugar catabolism and xylose isomerase pathways.* SBFC 2014, Clearwater, FL, US, 2014.
28. Runguphan, W. and J.D. Keasling, *Metabolic engineering of Saccharomyces cerevisiae for production of fatty acid-derived biofuels and chemicals.* Metab. Eng., 2014. 21(0): p. 103-113.
29. Cuellar, M.C. and L.A.M. van der Wielen, *Recent advances in the microbial production and recovery of apolar molecules.* Curr. Opin. Biotechnol., 2015. 33(0): p. 39-45.
30. Van der Wielen, L.A.M. and J.J. Heijnen, *Process for the continuous biological production of lipids, hydrocarbons or mixtures thereof.* EP 2196539 (A1), 2010.

Chapter 2. Microbial advanced biofuels production: overcoming emulsification challenges for large-scale operation

Abstract

Isoprenoids and alkanes produced and secreted by microorganisms are emerging as an alternative biofuel for diesel and jet fuel replacements. In a similar way as for other bioprocesses comprising an organic liquid phase, the presence of microorganisms, medium composition, and process conditions may result in emulsion formation during fermentation, hindering product recovery. At the same time, a low-cost production process overcoming this challenge is required to make these advanced biofuels a feasible alternative. In this chapter, we review the main mechanisms and causes of emulsion formation during fermentation, because a better understanding on the microscale can give insights into how to improve the large-scale processes and the process technology options addressing these challenges.

This chapter has been published as:

A.S. Heeres, C.S.F. Picone, L.A.M. van der Wielen, R.L. Cunha, M.C. Cuellar, *Microbial advanced biofuels production: overcoming emulsification challenges for large-scale operation,* Trends in Biotechnology 2014. 32 (4), p. 221-229.

2.1 Microbial production of advanced biofuels

Increases in the world population and global prosperity cause an increased global energy demand. To reduce the dependence on fossil energy, targets for the incorporation of renewable energy are being set worldwide. Biofuels are expected to make a significant contribution in achieving these goals. Commercial production of bioethanol is well established in the United States and Brazil and biodiesel produced from vegetable oils is also emerging [1]. However, their fuel properties and feedstock requirements have some inherent drawbacks.

Currently, microorganisms are being developed that produce and secrete molecules similar to fossil fuels, so called advanced or drop-in biofuels. The focus is on engineering of well-known industrial microorganisms (mostly *Escherichia coli* and *Saccharomyces cerevisiae*) and photosynthetic organisms (mostly cyanobacteria), enabling the production of isoprenoid-derived compounds or fatty acid (FA)-derived alkanes and alkenes.

Isoprenoids are molecules composed of multiple isoprene blocks and are abundant throughout nature. By the mevalonate (MEV) pathway or the deoxy-D-xylulose 5-phosphate (DXP) pathway, the two building blocks are formed: isopentenyl pyrophosphate and dimethylallyl pyrophosphate. By linking these blocks, a range of molecules can be formed, with varying applications, for instance artemisinic acid, a precursor for an anti-malarial therapeutic [2], and different sesquiterpenes, which are applied in flavours and fragrances [3]. With metabolic yields increasing, isoprenoids become interesting for biofuels application. Farnesenol [4], farnesene [5, 6] and bisabolene [7] have good fuel properties, but these molecules have multiple double bonds and require a hydrogenation step to improve their fuel quality. For farnesene, this route has been demonstrated at pilot and production scale (www.amyris.com).

Alkanes and alkenes can be produced microbially by the fatty acid (FA) pathway. In cyanobacteria, intermediates in the FA synthesis chain (acyl protein carriers) are reduced and decarboxylated, forming hydrocarbons [8]. This pathway was implemented in *E. coli* to further tailor alkane productivity. By directly using the free FAs in the cell, product

composition can directly be adapted by adjusting the type of free FAs present in the cell [9, 10]. This approach has led to the formation of C13 to C17 hydrocarbons up to pilot scale [11].

In both these routes, the product is secreted by the cells, resulting in a multiphase mixture consisting of cells, aqueous fermentation medium, oil droplets, and fermentation gas bubbles, as sketched in Figure 1. Product secretion eliminates the need for cell disruption in product recovery, potentially simplifying downstream processing and lowering production costs, which is a key factor for making advanced biofuels a feasible alternative for fossil fuels (Appendix A). However, not much is known about the secretion mechanism, but considering the size of the cells producing the biofuel, the initial droplet size after secretion can be expected to be smaller than the cell size, so in the order of micrometres.

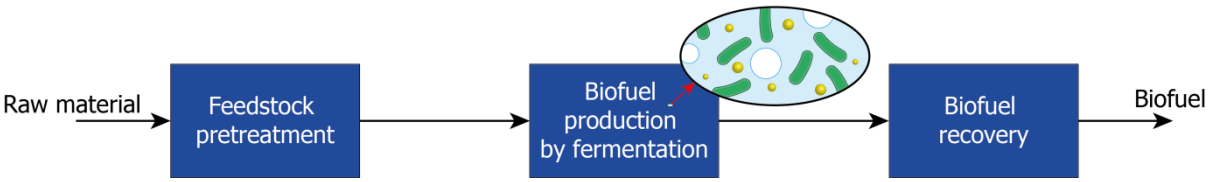

Figure 1. A simplified block diagram of the production of advanced biofuels. In the inset is a sketch of the multiphase mixture obtained during fermentation (not to scale)

The presence of the product as a second liquid phase may result in unconventional process configurations for biotechnology, where most products are water soluble or solids. To go from the product droplets – dispersed in the broth under fermentation conditions – to the formation of a continuous oil phase, several steps are required (Appendix B). When any of these steps is impeded, a stable emulsion is formed, as has already been described in advanced biofuel production [12]. Emulsion formation hinders product recovery; therefore, it is a key aspect for the large-scale implementation of advanced biofuels. In this review, we first discuss the potential causes of emulsion formation during fermentation, followed by process technology solutions that might be applied at a large scale to overcome emulsification challenges.

2.2 Emulsion stabilisation in bioprocesses

An emulsion is a thermodynamically unstable system formed by one immiscible liquid dispersed in another. With no stabilising components present, the emulsion will phase separate in the two liquids (Appendix B). In a process involving microorganisms, a wide range of stabilising components can be present. The next sections discuss potential causes of emulsion stabilisation in bioprocessing; which components specific for bioprocesses stabilise the droplet interface and which decrease the droplet mobility (Table 1).

Table 1. A summary of emulsion stabilisers that could be present in fermentation processes and their corresponding stabilisation mechanisms.

Emulsion stabiliser	Component Class	Stabilising mechanism	References
Salts pH control	Ions	Induce electrostatic repulsion between the droplets, hindering coalescence	[13]
Lipopeptides Phospholipids	Charged biosurfactants	Induce electrostatic repulsion between the droplets, lower interface tension, both hindering coalescence	[14-16]
Glycolipids	Uncharged biosurfactants	Steric interface stabilisation, lower interface tension, both hindering coalescence	[17, 18]
Lipoproteins Glycoproteins Proteins	Bioemulsifiers	Steric interface stabilisation, hindering coalescence	[19, 20]
Polysaccharides Viscous feedstocks	Bioemulsifiers	Viscosity increase of the continuous phase, hindering of creaming	[21, 22]
Microbial cells Other (colloidal) particles	Surface active particles	Mechanical interface stabilisation, hindering coalescence	[23, 24]

2.2.1 Stabilisation of the interface

The interface stability is enhanced by the presence of surface active components (SACs), originating from the substrate or produced by the microorganisms (biosurfactants/bioemulsifiers), or by the presence of surface active particles (e.g., cells). Their

stabilisation mechanisms are summarised in Appendix C. In Appendix D, the occurrence of emulsions in other multiphase fermentations is shortly described.

Biosurfactants and bioemulsifiers: Depending on the microorganism type and metabolism, different SACs are produced that change the interfacial properties of the emulsion. The SACs are produced as a protection mechanism or to increase the substrate availability when there is a second liquid phase present [25, 26]. Due to their high biodegradability, lower toxicity, and emulsifying properties at specific conditions (at extreme temperatures, pH, and salinity), SACs offer an alternative for the traditional surfactants and their isolation has been extensively studied [27-29]. These compounds are divided into two main classes: biosurfactants and bioemulsifiers. The biosurfactants are compounds with high surface active properties and usually low molecular weight [30]. The bioemulsifiers also show surface active properties, but they commonly do not decrease the surface and interfacial tension appreciably [27]. They are usually high-molecular-weight compounds, such as polymers, polysaccharides, lipopolysaccharides, or lipoproteins [25, 31]. However, some compounds show intermediate characteristics and may act as both biosurfactant and bioemulsifier. Both biosurfactants and bioemulsifiers can be produced intracellularly, secreted, or attached to the cell membrane [32]. The most common biosurfactants and bioemulsifiers found in bioprocesses are glycolipids, lipopeptides/lipoproteins, phospholipids, and polymeric surfactants [33].

Glycolipids are combinations of carbohydrates and long-chain aliphatic acids or hydroxy aliphatic acids [17]. Microorganisms secrete glycolipids to make hydrocarbons or other hydrophobic substrates available for cell metabolism [34]. Rhamnolipids are the best known glycolipids, showing strong surface active properties. They are composed by one or two hydrophilic rhamnose moieties and a hydrophobic FA. Several Gram-negative proteobacteria are capable of producing rhamnolipids and the emulsifying power depending on the substrate type [35]. Rhamnolipids are effective in stabilising emulsions containing vegetable oils, as well as long-chained hydrocarbons and aromatic compounds [18], but these molecules fail to emulsify short-chain hydrocarbons (<C7) [36].

Lipases are a group of surface active proteins produced by microorganisms that have amphiphilic properties and catalyse hydrolysis, esterification, and transesterification reactions, involving water-insoluble esters [37]. Other proteins with high surface active properties are the hydrophobins, such as SC3, secreted by filamentous fungi. Due to the well-defined hydrophobic part in the hydrophobin structure and its small molecular size, this protein is an efficient biosurfactant [20].

Lipopeptides are another type of microbially produced biosurfactant, which consist of a cyclic peptide chain bonded to a linear aliphatic acid chain [38]. Compared to small surfactant molecules and large proteins, the lipopeptides have an intermediate size [14]. About 23 types of lipopeptides have been reported over the last two decades, amongst these, surfactin shows the highest surface active properties [15, 39, 40]. Surfactin is reported to decrease the interfacial tension of the water/n-hexadecane system from 43 mN/m to values lowers than 1 mN/m [41]. Other surface active lipopeptides include fengycin and iturins produced by *Bacillus subtilis* [42].

Phospholipids are the major component of the membrane of a microorganism, consisting of phosphate-containing polar head groups attached to non-polar hydrocarbon chains. They stabilise emulsions around neutral pH, by acting both as a mechanical and an electrostatic barrier to coalescence [16]. Besides providing long-term stability in oil-in-water (O/W) emulsions, examples of stable water-in-oil (W/O) emulsions are also available [43].

Mannoproteins are the most commonly found bioemulsifiers, originating from the cell wall of yeasts and some bacteria. Their fraction in the cell wall varies according with the substrate and growth phase of the organism [19]. They consist of mannose polymers covalently bound to a protein backbone and are divided into two classes: the ones with a structural role and enzymes [44].

Besides SACs originating from the microorganism, complex fermentation feedstock can also be expected to contain SACs. Due to the complexity of some feedstocks, it is difficult to predict their effect on the emulsion stability, but molasses and hydrolysed cellulosic

biomass, for example, are known to contain surface active molecules such as betaine and cinnamic acid, respectively [45, 46].

Particle stabilisation: Besides the secretion of SACs, some microorganisms cause or enhance emulsification by adsorption of the cells at the O/W interface, creating Pickering stabilisation. This can occur even in the absence of cell growth or uptake of hydrocarbons [47]. The affinity of the cells for the O/W interface is determined by the composition of the cell wall or cell membrane. When the cell surface is hydrophobic, cells tend to adsorb at the O/W interface [47, 48]. Due to the irreversible nature of particle adhesion at the interface, particle-stabilised emulsions are reported to be stable for months [23].

In Pickering emulsions, the particles can stabilise droplets that are at least one order of magnitude larger than the stabilising particles themselves [49]. Knowing that the microorganism size is generally in the order of micrometres, the smallest droplets that can be stabilised will be in the order of tens of micrometres. This minimum droplet size can be achieved when the complete droplet surface is covered, with a too low particle concentration, the stabilised droplets will be larger than this minimum [50].

The effect of cell adhesion on the interfacial tension between the phases is still a question. Some authors report that cell stabilisation by Pickering does not affect the interfacial tension between the phases because the interface is just mechanically stabilised [47, 51]. However, some works have detected a considerable reduction of the interfacial tension by adsorption of cells [52] or particles [53], even in the absence of biosurfactant production.

In addition to the cell hydrophobicity, the electrostatic character of the cell surface contributes to the stabilising properties of microorganisms. Van der Waals, Lewis acid-base, and especially electrostatic interactions must be considered [24]. By controlling these cell surface properties, the stabilising capacity of the cells might be influenced. Nonetheless, it is important to highlight that the cell surface is highly dynamic, responding strongly to environmental changes (pH and ionic strength) [24]. Most microorganisms are reported to be negatively charged [24, 54], thus they generally experience electric double layer repulsion when approaching to O/W interfaces because most of these interfaces also are naturally

negatively charged as well due to the adsorption of hydroxyl ions at the O/W interface (depending on pH) [13].

2.2.2 Reduction of droplet mobility

High concentrations of sugars or hydrolysed lignocellulosic biomass in the medium result in an increased viscosity [21, 22], as well as high cell concentrations, which can increase the viscosity by an order of magnitude compared to water [55]. This increased viscosity of the medium results in decreased diffusion, hence efficiency, of the biosurfactants, but it decreases the mobility of the oil droplets, resulting in lower coalescence and creaming rates [56].

2.3 Oil recovery from fermentations

The previous section shows that the separation steps described in Appendix B can be impeded by a wide variety of causes. Solutions overcoming these problems can be found in adapting the fermentation process conditions or applying specific process technology, improving one or more of the steps in the separation sequence. Here, we discuss the process technology options that could enhance one of the three steps of the separation: droplet growth, creaming, or formation of a continuous oil phase. However, literature on the large-scale operation of bioprocesses with a second liquid phase is scarce. Therefore, technologies from other fields that deal with emulsions and oil recovery (e.g., petroleum, food, and wastewater engineering) are also discussed. Their applicability in bioprocessing might be limited by the complexity and dynamic nature of fermentation broths, and by the lack of physical/chemical data. Moreover, the compatibility of these technologies with the cells and the fermentation conditions determine the possibilities for process integration and cell reuse, which are necessary for low process costs.

2.3.1 Droplet growth

Already during the fermentation, operating conditions can be adapted to favour droplet growth. In fermentation processes, mixing is required to achieve sufficient mass and heat transfer rates, avoiding adverse local gradients, but the shear forces resulting from mixing

will also influence the droplet size. When the shear by mixing is limited, larger droplets can occur in the system, which can be separated easier [57]. Furthermore, mixing and the related shear forces have been shown to contribute to the amount of released biosurfactants [58]. A compromise might be found so that sufficient mixing is provided for the fermentation and for promoting droplet collisions, but limited in terms of droplet breakage and SAC release.

The medium composition influences the strength of stabilisation caused by charged SACs. Adjusting the salt concentration and process pH can lead to shielding of the droplet surface charge, neutralising electrostatic repulsive forces and enhancing droplet coalescence. Operation at acidic pH is favourable, considering the isoelectric point of microorganisms, which is typically in the acidic range, and the naturally negative charge of oil droplets [13]. Salt concentrations in fermentations are usually sufficient to induce charge neutralisation and eliminate electrostatic repulsion [57]. However, other stabilising mechanisms are not influenced and might still occur.

Besides adapting the process conditions, coalescers could be used to increase droplet size. Most of these techniques originate from the petroleum industry, where they are used to de-oil wastewater streams containing fine droplets (~1 μm). The coalescer consists of a material, often fibres, with affinity for the dispersed phase, at which small droplets are collected and coalesce, until they reach the size at which they detach. The coalescence efficiency has been shown to decrease when particulate matter is present, so the microorganism presence might have an adverse effect [59]. Membranes have been shown to induce coalescence as well. Permeation of an O/W emulsion through a cross-flow membrane increased droplet size from 1.5 to 80 μm, enabling gravity separation afterwards [60]. The presence of microorganisms could limit the applicability of this method as well, because fouling has been observed in many membrane operations in biotechnology [61].

2.3.2 Droplet creaming

When the droplet size is sufficiently large, the buoyancy force induces creaming of the droplets. The most straightforward method to achieve droplet creaming is gravity separation, which can process high volumes in continuous mode. However, this requires large settling

tanks to achieve low liquid velocities and limit turbulence, avoiding back mixing of oil droplets. Inclined plates can be used to retain laminar conditions at higher flow rates, reducing the required tank volumes [62]. Gravity separation is typically used to separate emulsions with a droplet diameter above 100 μm [63], for smaller droplets the buoyancy force is insufficient.

As shown in Appendix B, smaller droplets can be separated by applying a centrifugal field. The typical droplet size that can be separated by centrifugation is one order of magnitude lower compared to gravity settling. Applications in the petroleum industry demonstrate that large scale application for de-oiling of water is possible, but with high investment and maintenance costs [64].

Hydrocyclones are used as a low-cost alternative for centrifuges. The conical shape and tangential inlet of the hydrocyclone create a circular flow pattern, resulting in a centrifugal field in which the oil droplets are concentrated and collected in the overflow [65]. Due to their compactness, hydrocyclones are applied in the offshore industry to de-oil wastewater streams with low oil concentrations (< 1 g/L) [66]. Hydrocyclones have been applied in a biodesulfurisation process treating higher volume fractions (10%) [67], but the increased viscosity at high dispersed phase fractions causes a decrease in hydrocyclone efficiency.

Creaming can also be enhanced by increasing the density difference. In air flotation, the affinity between oil and gas is used to form droplet-bubble complexes, which have a lower overall density, enhancing the creaming rate. The size of the gas bubbles determines the size of the oil droplets that can be removed - the smallest gas bubbles can remove droplets in the range of 1-50 μm [68]. The technique has been mostly applied in wastewater treatment, aiming at low oil concentrations (10-15 mg/L) [69]. Alternatively, SACs might also adsorb at the bubble surface, where it could influence the interaction with oil droplets.

For all of these methods, the viscosity of the continuous phase influences the creaming rate as well. High fractions of dispersed phase and yeast concentrations will result in slowed down creaming. Thus, while high cell concentrations would be beneficial for fermentation productivity, these will adversely affect the creaming rate, requiring a trade-off to be made.

2.3.3 Formation of a continuous oil phase

Depending on the stabilisation of the interface, creaming might result in a concentrated emulsion, requiring an additional step to recover a continuous oil phase. Gravitational methods tend to be inefficient due to the high viscosity of the concentrated emulsion. By contrast, membranes separated emulsions with high volumetric oil fractions [70]. At low trans-membrane pressure, one phase selectively passes the membrane, but above the breakthrough pressure, both phases permeate and the membrane acts as a coalescence filter.

Another option is to target the stabilising component. When the emulsion is stabilised by proteins, denaturing the protein can result in emulsion breakup. Both heat treatment [71] and supercritical carbon dioxide ($scCO_2$) [72] resulted in protein precipitation and emulsion separation. Emulsions stabilised by non-ionic surfactants can also be destabilised by heat treatment. A temperature increase often results in stronger hydrophobic behaviour of the surfactant in an O/W emulsion, making it less soluble in the continuous phase.

The SACs can also be deactivated chemically. By using hydrolases or organisms producing these, the SACs are cut and lose their emulsifying capacity resulting in quick phase separation [73]. Adding other surfactants can result in competitive destabilisation. Due to their stronger affinity for the interface, smaller surfactants can displace macromolecular biosurfactants from the O/W interface [74], with a comparable mechanism to the working of antifoam in fermentations [75]. Furthermore, methanol and ethanol have been shown to improve phase separation in the biodesulfurisation process [76]. Despite their effectiveness, the use of additives can lead to increased processing costs [77] and could have an adverse effect on the viability of the cells, disabling cell reuse. f

2.4 Concluding remarks and future perspectives

Emulsions occur in various fermentation that incorporate an organic liquid phase (Appendix D). When the organic phase is the substrate, emulsification is usually promoted. However, in processes where the organic phase is a product (e.g., advanced biofuel

production, microbial desulfurisation) or an auxiliary phase [e.g., *in situ* product removal (ISPR)], the emulsion formation becomes a hindrance.

For the production of diesel and jet biofuels by microorganisms to be feasible at large scale, process costs should remain low. Metabolic engineering is being used to develop efficient microorganisms that produce and secrete high product titers (e.g., in farnesene fermentations, product titers above 100 g/L have been reported [78]), but developments in scalable process technology seem to be lagging behind. A low-cost product recovery can be particularly challenging, given the multiphase nature of the fermentation mixture.

Emulsification of the produced oil can be a large hurdle for a cheap recovery process. This can be caused by: (i) surfactants and emulsifiers originally present in the fermentation medium or produced by the microorganism; (ii) Pickering stabilisation by the microorganisms or other particles present in the medium; and/or (iii) fermentation medium properties such as viscosity. Separation of the product droplets may require the droplet size to be increased, the creaming rate to be enhanced, and/or concentrated emulsions to be destabilised. Several process technology alternatives addressing these aspects have been discussed. These technologies, although well established in petroleum and wastewater processing, have not been significantly exploited in bioprocessing. The largest potential lays in promoting droplet growth during the fermentation, and in physical separation methods that can be integrated to the fermentation process, allowing for process intensification techniques such as ISPR and cell reuse.

Given the challenges inherent to bioprocesses such as medium complexity, lack of physical/chemical data, cell viability, and susceptibility to microbial fouling, large-scale production of advanced biofuels requires developments in the following areas: (i) integration of microorganism development and process development, so that the microorganism, fermentation medium, and operating conditions are tuned towards promoting droplet growth and minimising stabilising compounds; (ii) cell retention or cell separation from the multiphase mixture during the fermentation, so that cell viability is maintained independently

of the oil recovery method of choice; (iii) studies on (physical) separation methods for oil recovery in a biotechnological environment.

Research programmes in these areas will result in the development of bioprocesses that address the needs of large-scale operation, shortening the time required towards industrial implementation.

Acknowledgements

This work was partly carried out within the BE-Basic R&D Program, which was granted a FES subsidy from the Dutch Ministry of Economic Affairs, Agriculture and Innovation (EL&I). Furthermore, this work was supported by The Fundação de Amparo à Pesquisa e Desenvolvimento de São Paulo–Brazil (FAPESP, Grant Nos. 2012/14003-9 and 2011/51707-1).

Appendix A – The costs of producing advanced biofuel

Currently, first-generation ethanol and biodiesel supply 2% of the global transport energy demand. The biofuel contribution is expected to increase up to 27% by 2050 (www.eia.gov), given the need for fuel replacement in transport vehicles that are not suited for other renewable energy resources (e.g., electricity), as is the case for planes. For this, however, cost- and energy-efficient processes are required.

Little information is available in literature on the overall process for extracellular production of diesel and jet fuel replacements. However, such processes seem to be performed aerobically, making use of conventional fermentation equipment under monoseptic conditions and relying on centrifugation for product recovery [6, 79]. Companies claim target production costs around $0.60 per litre with matured technology [6], which would make them competitive in the diesel and jet fuel market. However, according to Westfall *et al.* [6], most of these technologies are not yet mature and most companies are not producing at full scale yet. A selling price as high as $7.7 per liter was recently reported [80]. As noted by Cuellar *et al.* [81], in order to reach competitive production costs a combination of process improvements will be required: low-cost feedstock, maximised product yield on substrate under anaerobic conditions, cell reuse, and low-cost fermentation and recovery technology [81]. To further illustrate this, let us consider the general stoichiometric reaction for alkane production from glucose:

$$\left(\frac{1}{4}n+\frac{1}{12}\right)\cdot C_6H_{12}O_6 \rightarrow C_nH_{2n+2}+\left(\frac{1}{2}n+\frac{1}{2}\right)\cdot CO_2+\left(\frac{1}{2}n-\frac{1}{2}\right)\cdot H_2O \qquad (1)$$

Assuming that the maximal theoretical yield from this equation can be achieved and considering the production of a long-chain alkane such as octadecane ($C_{18}H_{38}$), about 3 kg of sugars are required per kg of product. At a sugar price of $0.4 per kg (http://ers.usda.gov), this results in $1.2 per kg or $0.9 per litre only on feedstock cost. In mature biofuel processes, 80% of the production cost correspond to the feedstock and 20% is equally distributed among other operating costs and capital charges [82]. This results in capital charges of $0.15 per kg,

which for a production capacity of 100×10^3 ton yr^{-1}, 10% interest and 10-year plant life leads to a maximal investment of $150 million. This is comparable to the investment for a mature sugar cane/ethanol mill with similar production capacity ($100-300 million) [82]. This rough calculation clearly shows that the process technology must be competitive, for these processes to be feasible on a large scale.

Appendix B – Steps in emulsion breakup

In a fermentation producing advanced biofuels, the product is initially present in the fermentation mixture as dispersed droplets in the fermentation broth. To recover the pure product, three steps have to be passed: droplet growth, droplet creaming, and the formation of a continuous oil phase, as shown in Figure I.

Droplet growth can occur by multiple mechanisms. Ostwald ripening is caused by difference in the chemical potential between small and large droplets. Oil from the smaller droplets dissolves easier and will deposit on the larger droplets, thereby causing growth of large droplets at the expense of the smaller droplets [83]. For both flocculation and coalescence, droplets have to collide first. After the collision, the droplets can bounce (no droplet growth), form an agglomerate (flocculation), or merge (coalescence). The result of flocculation is not a larger droplet, but it does increase the effective particle size, which is important for the next step. For coalescence, the film between the droplets must drain and subsequently rupture, forming a larger droplet.

The buoyancy force, caused by the density difference between the dispersed and continuous phases, results in movement of the droplet. For emulsions in which the dispersed phase has a lower density than the continuous phase, this process is called creaming, as opposed to sedimentation for a heavier dispersed phase. The creaming velocity (v_c) of a single droplet in laminar conditions can be described by Stokes law:

$$v_c = \frac{1}{18}\frac{\left(\rho_{oil} - \rho_{aq}\right)}{\mu} g \cdot d_d^2 \qquad (2)$$

The equation shows the importance of the droplet diameter (d_d), and hence the importance of droplet growth as a first step, because the initially formed droplets are expected to be too small to cream effectively. Other parameters of influence are the density difference (ρ_{oil}-ρ_{aq}), the viscosity of the continuous phase (μ), and the acceleration constant (g), which is often increased (e.g., by centrifugation) to enhance creaming rates [56].

In the absence of droplet stabilising components, the creamed droplets will readily coalesce into a continuous oil phase. When the droplet interface is stabilised, a concentrated emulsion – referred to as cream layer – is formed. In such a case, additional steps have to be taken to induce further droplet coalescence and separation of the cream to a continuous oil phase.

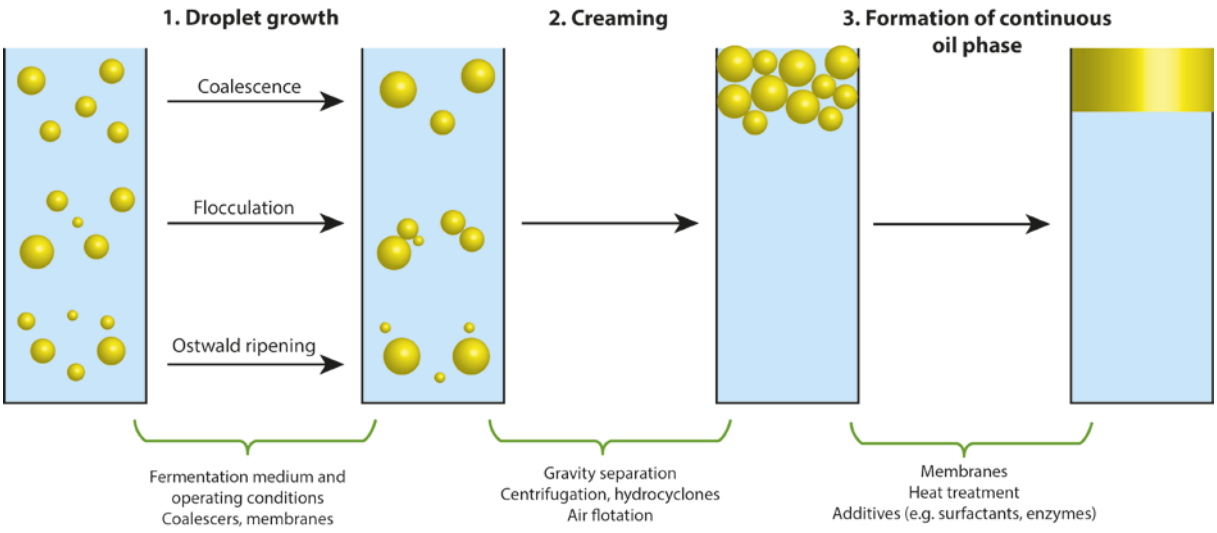

Figure I. The steps in emulsion destabilization. Droplets can grow due to coalescence, flocculation, or Ostwald ripening. This is followed by creaming and formation of a continuous oil phase at the end. Each step can be enhanced by process technology (listed below each step).

Appendix C – Stabilising mechanisms of SACs

Both for droplet growth and formation of the continuous oil layer, coalescence is an important process. As shortly described in Appendix B, coalescence is a three step process: droplet collision, film drainage, and film rupture. Any SACs present will influence the composition of the droplet interface and the coalescence behaviour of the droplets.

Several mechanisms can stabilise the oil droplets against aggregation and coalescence. First, droplet collision can be hindered by an electrostatic repulsive force between equally charged droplets. The effective surface charge of droplets is influenced by the distribution of charged SACs on droplets surface and the degree of ionisation of these groups. The latter is determined by the continuous phase properties such as pH and ionic strength. Overall, SACs decrease the interfacial tension, making the interface more stable and less prone to film drainage. Furthermore, steric hindrance caused by bulky molecules can prevent the droplet surfaces to approach close enough for coalescence [56].

Another form of interface stabilisation is provided by adsorption of amphiphillic macromolecules and particles. The adsorption of these compounds may increase the viscoelasticity and/or mechanical strength of the interfacial film, hindering film disruption and coalescence [56]. Particles may form a rigid barrier whereas flexible macromolecules could form a network surrounding the droplets, leading to the droplets 'immobilisation' [23].

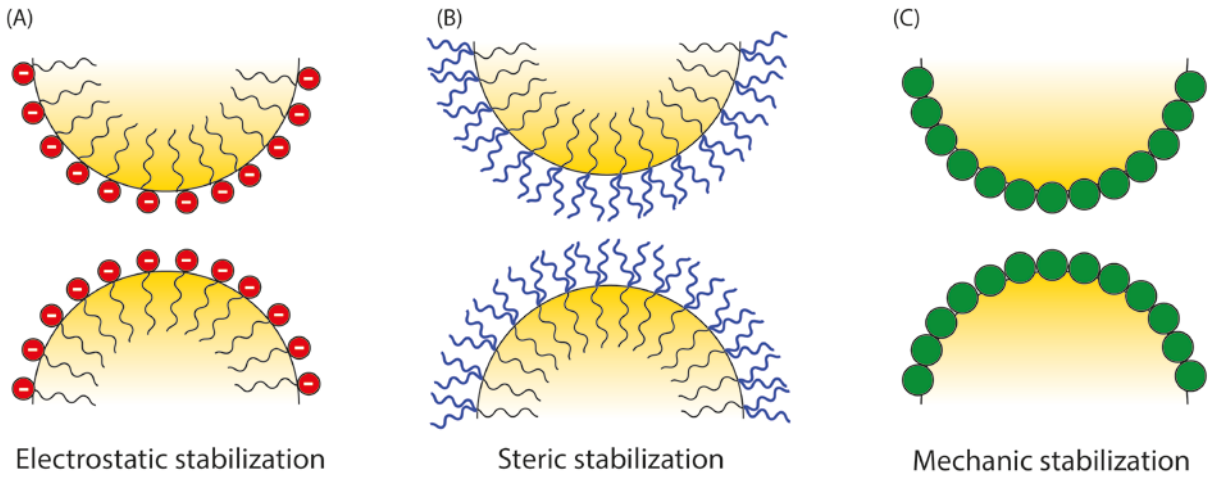

Figure II. Interface stabilizing mechanisms of different SACs. (A) Electrostatic stabilization by charged surfactants. (B) Steric stabilization by uncharged surfactants. (C) Mechanical stabilization by surface active particles.

Appendix D – Occurrence of emulsions in bioprocessing

Emulsions occur in many fermentations that comprise an organic liquid phase. When the organic phase is the substrate, emulsification is usually promoted. However, in processes where the organic phase is a product (e.g., advanced biofuel production, microbial desulfurisation) or an auxiliary phase (e.g., in-situ product removal), the emulsion formation becomes a hindrance.

Fermentations using oils as substrate

The use of oils as main or supplementary carbon source is widely applied in fermentations for the production of antibiotics, lipases, polyhydroxyalkanoates, and lipid-soluble compounds, such as beta-carotene and aromas. Originally, oils were added to antibiotic fermentations as antifoam agents, but later their use was extended to controlling substrate and product toxicity [84-86]. The presence of oil has been reported to both increase and decrease the oxygen transfer in these fermentations [85-87]. Oil substrate uptake requires the action of lipase, which is either secreted to the medium or cell bound. Consequently, the rate of substrate hydrolysis depends on the available area at the O/W interface. Mixing alone results in oil droplet sizes in the range of 100-1000 μm [85, 87], resulting in poor substrate consumption [84]. Several methods for reducing the oil droplet size have been evaluated, including the use of surfactants and pre-emulsification methods, such as membranes and phase inversion by temperature, resulting in mean droplet sizes as low as 0.3 μm [87]. The microorganisms and other particles usually present in these fermentations (e.g., calcium carbonate) have been shown to increase the stability of the oil dispersion [85, 87].

Bioremediation

Following an oil spill in the sea, usually an oil slick is formed. Low molecular weight components either volatilise, or solubilise in water and are metabolised by microorganisms that take up soluble hydrocarbons. However, high molecular weight components are sparingly soluble in water and therefore their degradation rate is often limited by the oil surface area [88]. Degradation of these components mostly involves microorganisms with high cell surface

hydrophobicity, which can adhere on the O/W interface [89], and/or the presence of biosurfactants [90].

Microbial desulfurisation

In microbial desulfurisation, sulfur is removed from fossil fuels by microbial oxidation as an alternative for the energy intensive conventional hydrogen desulfurisation [91]. Generally, the oil fraction in the process is between 10 and 50%. To achieve sufficient mass transfer rates, vigorous mixing is required, which results in emulsion formation. At the laboratory scale, the separation can be achieved by centrifugation, but at a large scale alternatives are required to obtain low production costs [92].

In situ product removal

In situ product removal (ISPR) is applied to overcome the limitations of biotechnological processes caused by a toxic product or substrate, thereby increasing the productivity [93]. When extraction is applied in ISPR, one of the requirements is the biocompatibility of the auxiliary phase [94], resulting in the application of long-chained, nonpolar organic liquids [95]. Industrial application of extractive ISPR has been limited to the production of fine chemicals and pharmaceuticals, mainly because of the high downstream processing costs [93]. The combination of small droplets, required for achieving sufficient mass transfer rates, and stabilising components results in emulsion formation.

References

1. Demirbas, A., *Political, economic and environmental impacts of biofuels: a review.* Appl. Energy, 2009. 86(S1): p. S108-S117.
2. Ro, D.-K., et al., *Production of the antimalarial drug precursor artemisinic acid in engineered yeast.* Nature, 2006. 440(7086): p. 940-943.
3. Schalk, M., *Method for producting beta-santalene*. US20110281257 A1, 2011.
4. Wang, C., et al., *Microbial production of farnesol (FOH): current states and beyond.* Process Biochem., 2011. 46: p. 1221-1229.
5. Renniger, N.S. and D.J. McPhee, *Fuel compositions comprising farnesane and farnesane derivatives and method of making and using same*. 2008, Amyris Biotechnologies, Inc.: United States.
6. Westfall, P.J. and T.S. Gardner, *Industrial fermentation of renewable diesel fuels.* Curr. Opin. Biotech., 2011. 22(3): p. 344-350.
7. Peralta-Yahya, P.P., et al., *Identification and microbial production of a terpene-based advanced biofuel.* Nat. Commun., 2011. 2: p. 483.
8. Warui, D.M., et al., *Detection of formate, rather than carbon monoxide, as the stoichiometric coproduct in conversion of fatty aldehydes to alkanes by a cyanobacterial aldehyde decarbonylase.* J. Am. Chem. Soc., 2011. 133(10): p. 3316-3319.
9. Howard, T.P., et al., *Synthesis of customized petroleum-replica fuel molecules by targeted modification of free fatty acid pools in Escherichia coli.* PNAS, 2013. 110: p. 7636-7641.
10. Schirmer, A., et al., *Microbial biosynthesis of alkanes* Science, 2010. 329: p. 559-562.
11. Domínguez de María, P., *Recent developments in the biotechnological production of hydrocarbons: paving the way for bio-based platform chemicals.* ChemSusChem, 2011. 4(3): p. 327-329.
12. Tabur, P. and G. Dorin, *Method for purifying bio-organic compounds from fermentation broth containing surfactants by temperature-induced phase inversion*. US Patent 20120040396, 2012.
13. Marinova, K.G., et al., *Charging of oil−water interfaces due to spontaneous adsorption of hydroxyl ions.* Langmuir, 1996. 12(8): p. 2045-2051.
14. Deleu, M., et al., *Interfacial and emulsifying properties of lipopeptides from Bacillus subtilis.* Colloid Surf. A, 1999. 152(1–2): p. 3-10.
15. Arima, K., A. Kakinuma, and G. Tamura, *Surfactin, a crystalline peptidelipid surfactant produced by Bacillus subtilis: Isolation, characterization and its inhibition of fibrin clot formation.* Biochem. Biophys. Res. Commun., 1968. 31(3): p. 488-494.
16. Mirtallo, J.M., et al., *State of the art review: intravenous fat emulsions: current applications, safety profile, and clinical implications.* Ann. Pharmacother., 2010. 44(4): p. 688-700.
17. Cameotra, S.S. and R.S. Makkar, *Recent applications of biosurfactants as biological and immunological molecules.* Curr. Opin. Microbiol., 2004. 7(3): p. 262-266.

18. Prieto, L.M., et al., *The production of rhamnolipid by a Pseudomonas aeruginosa strain isolated from a southern coastal zone in Brazil.* Chemosphere, 2008. 71(9): p. 1781-1785.
19. Cameron, D.R., D.G. Cooper, and R.J. Neufeld, *The mannoprotein of Saccharomyces cerevisiae is an effective bioemulsifier.* Appl. Environ. Microbiol., 1988. 54: p. 1420-1425.
20. Lienemann, M., et al., *Structure-Function Relationships in Hydrophobins: Probing the Role of Charged Side Chains.* Appl. Environ. Microbiol., 2013. 79(18): p. 5533-5538.
21. McClements, D.J., *Protein-stabilized emulsions.* Curr. Opin. Colloid In., 2004. 9: p. 305-313.
22. Olofsson, K., M. Bertilsson, and G. Lidén, *A short review on SSF-an interesting process option for ethanol production from lignocellulosic feedstocks.* Biotechnol. Biofuels, 2008. 1(7): p. 1-14.
23. Binks, B.P., *Particles as surfactants - similarities and differences.* Curr. Opin. Colloid In., 2002. 7: p. 21-41.
24. Ly, M.H., et al., *Importance of bacterial surface properties to control the stability of emulsions.* Int. J. Food Microbiol., 2006. 112(1): p. 26-34.
25. Neu, T.R., *Significance of bacterial surface-active compounds in interaction of bacteria with interfaces.* Microbiol. Rev., 1996. 60(1): p. 151-166.
26. Pedetta, A., et al., *Phenanthrene degradation and strategies to improve its bioavailability to microorganisms isolated from brackish sediments.* Int. Biodeter. Biodegr., 2013. 84(0): p. 161-167.
27. Banat, I.M., et al., *Microbial biosurfactants production, applications and future potential.* Appl. Microbiol. Biotechnol., 2010. 87(2): p. 427-444.
28. Jain, R.M., et al., *Isolation and structural characterization of biosurfactant produced by an alkaliphilic bacterium Cronobacter sakazakii isolated from oil contaminated wastewater.* Carbohydr. Polym., 2012. 87(3): p. 2320-2326.
29. Janek, T., M. Łukaszewicz, and A. Krasowska, *Identification and characterization of biosurfactants produced by the Arctic bacterium Pseudomonas putida BD2.* Colloid Surf. B: Biointerfaces, 2013. 110(0): p. 379-386.
30. Berton, C., C. Genot, and M.-H. Ropers, *Quantification of unadsorbed protein and surfactant emulsifiers in oil-in-water emulsions.* J. Colloid Interf. Sci., 2011. 354(2): p. 739-748.
31. Mukherjee, A.K. and K. Das, *Microbial Surfactants and Their Potential Applications: An Overview*, in *Biosurfactants*, R. Sen, Editor. 2010, Springer New York. p. 54-64.
32. Kosaric, N., W.L. Cairns, and N.C.G. Gray, eds. *Biosurfactants and Biotechnology*. Vol. 25. 1987, Marcel Dekker, Inc.
33. Healy, M.G., C.M. Devine, and R. Murphy, *Microbial production of biosurfactants.* Resour. Conserv. Recy., 1996. 18(1–4): p. 41-57.
34. Benincasa, M., et al., *Chemical structure, surface properties and biological activities of the biosurfactant produced by Pseudomonas aeruginosa LBI from soapstock.* A. Van Leeuw. J. Microb., 2004. 85(1): p. 1-8.

35. Lovaglio, R.B., et al., *Rhamnolipid emulsifying activity and emulsion stability: pH rules.* Colloid Surf. B: Biointerfaces, 2011. 85(2): p. 301-305.
36. Pornsunthorntawee, O., et al., *Structural and physicochemical characterization of crude biosurfactant produced by Pseudomonas aeruginosa SP4 isolated from petroleum-contaminated soil.* Bioresource Technol., 2008. 99(6): p. 1589-1595.
37. Treichel, H., et al., *A review on microbial lipases production.* Food Bioprocess. Technol., 2010. 3(2): p. 182-196.
38. Song, C.-S., R.-Q. Ye, and B.-Z. Mu, *Molecular behavior of a microbial lipopeptide monolayer at the air–water interface.* Colloid Surf. A, 2007. 302(1–3): p. 82-87.
39. Rosenberg, E. and E.Z. Ron, *High- and low-molecular-mass microbial surfactants.* Appl. Microbiol. Biotechnol., 1999. 52(2): p. 154-162.
40. Peypoux, F., J.M. Bonmatin, and J. Wallach, *Recent trends in the biochemistry of surfactin.* Appl. Microbiol. Biotechnol., 1999. 51(5): p. 553-563.
41. Lang, S., *Biological amphiphiles (microbial biosurfactants).* Curr. Opin. Colloid Interface Sci., 2002. 7(1–2): p. 12-20.
42. Vater, J., et al., *Matrix-assisted laser desorption ionization-time of flight mass spectrometry of lipopeptide biosurfactants in whole cells and culture filtrates of Bacillus subtilis C-1 isolated from petroleum sludge.* Appl. Environ. Microbiol., 2002. 68(12): p. 6210-6219.
43. Knoth, A., I. Scherze, and G. Muschiolik, *Stability of water-in-oil-emulsions containing phosphatidylcholine-depleted lecithin.* Food Hydrocolloid., 2005. 19(3): p. 635-640.
44. Barriga, J.A.T., et al., *Components of the bioemulsifier from S. cerevisiae.* Enzyme Microb. Tech., 1999. 25(1–2): p. 96-102.
45. Rajakylä, E. and M. Paloposki, *Determination of sugars (and betaine) in molasses by high-performance liquid chromatography: comparison of the results with those obtained by the classical lane-eynon method.* J. Chromatogr. A, 1983. 282(0): p. 595-602.
46. Almeida, J.R.M., et al., *Increased tolerance and conversion of inhibitors in lignocellulosic hydrolysates by Saccharomyces cerevisiae.* J. Chem. Technol. Biotechnol., 2007. 82(4): p. 340-349.
47. Mohebali, G., et al., *Stabilization of water/gas oil emulsions by desulfurizing cells of Gordonia alkanivorans RIPI90A.* Microbiol., 2007. 153: p. 1573-1581.
48. Dorobantu, L.S., et al., *Stabilization of oil-water emulsions by hydrophobic bacteria.* App. Environ. Microb., 2004. 70(10): p. 6333-6336.
49. Dickinson, E., *Use of nanoparticles and microparticles in the formation and stabilization of food emulsions.* Trends Food Sci. Tech., 2012. 24(1): p. 4-12.
50. Chevalier, Y. and M.-A. Bolzinger, *Emulsions stabilized with solid nanoparticles: Pickering emulsions.* Colloid Surf. A, 2013. 439: p. 23–34.
51. Dorobantu, L.S., et al., *Stabilization of oil-water emulsions by hydrophobic bacteria.* Applied and Environmental Microbiology, 2004. 70(10): p. 6333-6336.

52. Huang, X., et al., *Separation and characterization of effective demulsifying substances from surface of Alcaligenes sp. S-XJ-1 and its application in water-in-kerosene emulsion.* Bioresource Technol., 2013. 139(0): p. 257-264.
53. Akartuna, I., et al., *Stabilization of Oil-in-Water Emulsions by Colloidal Particles Modified with Short Amphiphiles.* Langmuir, 2008. 24(14): p. 7161-7168.
54. Poortinga, A.T., et al., *Electric double layer interactions in bacterial adhesion to surfaces.* Surf. Sci. Rep., 2002. 47(1): p. 1-32.
55. Reuß, M., et al., *Viscosity of yeast suspensions.* Eur. J. Appl. Microbiol. Biotechnol., 1979. 8(3): p. 167-175.
56. McClements, D.J., *Food emulsions, principles, practices, and techniques*. 2nd edition ed. Contemporary Food Science, ed. F.M. Clydesdale. 2005, Boca Raton: CRC Press.
57. Walstra, P., *Principles of emulsion formation.* Chem. Eng. Sci., 1993. 48(2): p. 333-349.
58. Desai, J.D. and I.M. Banat, *Microbial production of surfactants and their commercial potential.* Microbiol. Mol. Biol. R., 1997. 61(1): p. 47-64.
59. Sareen, S.S., et al., *Coalescence in fibrous beds.* AIChE J., 1966. 12(6): p. 1045-1050.
60. Hlavacek, M., *Break-up of oil-in-water emulsions induced by permeation through a microfiltration membrane.* J. Membrane Sci., 1995. 102: p. 1-7.
61. van Reis, R. and A. Zydney, *Membrane separations in biotechnology.* Curr. Opin. Biotechnol., 2001. 12(2): p. 208-211.
62. Schlieper, L., et al., *Liquid–liquid phase separation in gravity settler with inclined plates.* AIChE J., 2004. 50(4): p. 802-811.
63. Laleh, A.P., W.Y. Svrcek, and W.D. Monnery, *Design and CFD studies of multiphase separators—a review.* Can. J. Chem. Eng., 2012. 90(6): p. 1547-1561.
64. Grace, R., *Commercial Emulsion Breaking*, in *Emulsions*, L.L. Schramm, Editor. 1992, American Chemical Society. p. 313-339.
65. Young, G.A.B., et al., *Oil-water separation using hydrocyclones: an experimental search for optimum dimensions*. J. Petrol. Sci. Eng., 1994. 11(1): p. 37-50.
66. Meldrum, N., *Hydrocyclones: a solution to produced-water treatment.* SPE Prod. Eng., 1988. 3: p. 669-676.
67. Yu, L.Q., T.A. Meyer, and B.R. Folsom, *Oil/water/biocatalyst three phase separation process*. 1997, Energy Biosystems Corporation.
68. Rubio, J., M.L. Souza, and R.W. Smith, *Overview of flotation as a wastewater treatment technique.* Miner. Eng., 2002. 15(3): p. 139-155.
69. Al-Shamrani, A.A., A. James, and H. Xiao, *Destabilisation of oil-water emulsions and separation by dissolved air flotation.* Water Res., 2002. 36(6): p. 1503-1512.
70. Schroën, C.G.P.H. and J.M. Woodley, *Membrane separation for downstream processing of aqueous-organic bioconversions.* Biotechnol. Prog., 1997. 13(3): p. 276-283.
71. Schmid, A., et al., *Developments toward large-scale bacterial bioprocesses in the presence of bulk amounts of organic solvents.* Extremophiles, 1998. 2(3): p. 249-256.

72. Brandenbusch, C., et al., *Efficient phase separation and product recovery in organic-aqueous bioprocessing using supercritical carbon dioxide.* Biotechnol. Bioeng., 2010. 107(4): p. 642-651.
73. Leppchen, K., et al., *Microbial de-emulsification: a highly efficient procedure for the extractive workup of whole-cell biotransformations.* Org. Process Res. Dev., 2006. 10(6): p. 1119-1125.
74. Wilde, P., et al., *Proteins and emulsifiers at liquid interfaces.* Adv. Colloid Interfac., 2004. 108–109(0): p. 63-71.
75. Prins, A. and K. van't Riet, *Proteins and surface effects in fermentation: foam, antifoam and mass transfer.* Trends Biotechnol., 1987. 5(11): p. 296-301.
76. Choi, O.K., et al., *Enhancement of phase separation by the addition of de-emulsifiers to three-phase (diesel oil/biocatalyst/aqueous phase) emulsion in diesel biodesulfurization.* Biotechnol. Lett., 2003. 25: p. 73-77.
77. Prasad, K., *Cost cutting strategies in downstream processing industry*, in *Downstream Process Technology: A New Horizon In Biotechnology*. 2012, PHI Learning Pvt. Ltd. p. 32-39.
78. George, K.W., et al., *Isoprenoid drugs, biofuels, and chemicals - artemisinin, farnesene, and beyond*, in *Biotechnology of isoprenoids*, J. Schrader and J. Bohlmann, Editors. 2015, Springer International: Heidelberg. p. 355-390.
79. Rude, M.A. and A. Schirmer, *New microbial fuels: a biotech perspective.* Curr. Opin. Biotechnol., 2009. 12(3): p. 274-281.
80. Bullis, K. *Why Amyris is focusing on moisturizers, not fuel, for now*. MIT Technology Review, 2012.
81. Cuellar, M.C., J.J. Heijnen, and L.A.M. van der Wielen, *Large-scale production of diesel-like biofuels - process design as an inherent part of microorganism development.* Biotechnol. J., 2013. 8(6): p. 682-689.
82. Efe, C., A.J.J. Straathof, and L.A.M. Van der Wielen *Technical and economical feasibility of production of ethanol from sugar cane and sugar cane bagasse*. B-Basic Report, 2007.
83. Taylor, P., *Ostwald ripening in emulsions.* Adv. Colloid Interfac., 1998. 75(2): p. 107-163.
84. Large, K.P., A.P. Ison, and D.J. Williams, *The effect of agitation rate on lipid utilisation and clavulanic acid production in Streptomyces clavuligerus.* J. Biotechnol., 1998. 63(2): p. 111-119.
85. Galindo, E., A.W. Pacek, and A.W. Nienow, *Study of drop and bubble sizes in a simulated mycelial fermentation broth of up to four phases.* Biotechnol. Bioeng., 2000. 69(2): p. 213-221.
86. Clarke, K.G. and L.D.C. Correia, *Oxygen transfer in hydrocarbon–aqueous dispersions and its applicability to alkane bioprocesses: a review.* Biochem. Eng. J., 2008. 39(3): p. 405-429.

87. Erler, S., A. Nienow, and A. Pacek, *Oil/water and pre-emulsified oil/water (PIT) dispersions in a stirred vessel: Implications for fermentations.* Biotechnol. Bioeng., 2003. 82(5): p. 543-551.
88. Ron, E. and E. Rosenberg, *Role of biosurfactants*, in *Handbook of hydrocarbon and lipid microbiology*, K.N. Timmis, Editor. 2010, Springer-Verlag. p. 2515-2518.
89. Abbasnezhad, H., M. Gray, and J.M. Foght, *Influence of adhesion on aerobic biodegradation and bioremediation of liquid hydrocarbons.* Appl. Microbiol. Biot., 2011. 92(4): p. 653-675.
90. Lawniczak, L., R. Marecik, and L. Chrzanowski, *Contributions of biosurfactants to natural or induced bioremediation.* Appl. Microbiol. Biot., 2013. 97(6): p. 2327-2339.
91. Babich, I.V. and J.A. Moulijn, *Science and technology of novel processes for deep desulfurization of oil refinery streams: a review.* Fuel, 2003. 82(6): p. 607-631.
92. Monticello, D.J., *Biodesulfurization and the upgrading of petroleum distillates.* Curr. Opin. Biotech., 2000. 11(6): p. 540-546.
93. Lye, G.J. and J.M. Woodley, *Application of in situ product-removal techniques to biocatalytic processes.* Trends Biotechnol., 1999. 17(10): p. 395-402.
94. Straathof, A.J.J., *Auxiliary phase guidelines for microbial biotransformations of toxic substrate into toxic product.* Biotechnol. Progr., 2003. 19(3): p. 755-762.
95. Laane, C., et al., *Rules for optimization of biocatalysis in organic solvents.* Biotechnol. Bioeng., 1987. 30(1): p. 81-87.

Chapter 3. How fermentation broth components influence droplet coalescence and hinder advanced biofuel recovery during fermentation

Abstract

Developments in synthetic biology enabled the microbial production of long chain hydrocarbons, which can be used as advanced biofuels in aviation or transportation. Currently, these fuels are not economically competitive due to their production costs. The current production process offers room for improvement: by utilizing lignocellulosic feedstock, increasing microbial yields, and using cheaper process technology. Gravity separation is an example of the latter, for which droplet growth by coalescence is crucial. The aim of this study was to study the effect of fermentation broth components on droplet coalescence. Droplet coalescence was measured using two setups: a microfluidic chip and regular laboratory scale stirred vessel (2 L). Some fermentation broth components had a large impact on droplet coalescence. Especially components present in hydrolysed cellulosic biomass and mannoproteins from the yeast cell wall retard coalescence. To achieve a technically feasible gravity separation that can be integrated with the fermentation in a future production process, the negative effects of these components on coalescence should be minimised. Redesigning the fermentation medium or adjusting the fermentation conditions will help in decreasing the amount of surface active components in the fermentation broth. This way, coalescence can be stimulated and another step can be made towards economically feasible advanced biofuel production.

This chapter has been published as:

A.S. Heeres, K. Schroën, J.J. Heijnen, L.A.M. van der Wielen, M.C. Cuellar, *Fermentation broth components influence droplet coalescence and hinder advanced biofuel recovery during fermentation,* Biotechnology Journal 2015. 10 (8), p.1206-1215.

3.1 Introduction

3.1.1 Advanced biofuel production

One of the advances in the field of biofuels is the application of synthetic biology to develop microorganisms that produce long chain hydrocarbons, which are also known as advanced biofuels [1-3]. These fuels have been demonstrated in airplanes during the UN Earth Summit in Rio de Janeiro 2012 and public transport busses in São Paulo, Brazil (www.amyris.com). The production of these fuels is done by microorganisms that convert the substrate (e.g., glucose, glycerol) to the biofuel product, which is secreted into the fermentation broth, resulting in a dispersion of product droplets in an aqueous phase from which the product then has to be recovered [4, 5]. For an economically feasible production of the biofuel, the recovery process has to be cheap, so low cost process technology should be used [6]. The initial droplet size after product secretion will be small (probably in the same order of magnitude as the microorganisms) and the recovery of the oil will then follow three steps: (1) droplet growth by coalescence, (2) phase separation by creaming, (3) formation of a continuous oil phase [7]. The coalescence steps are crucial for a low cost recovery process, since these determine the required processing steps. When droplets are stable against coalescence and remain small, expensive methods are required to achieve phase separation [8]. An example is the production of farnesene by engineered yeast, in which the fermentation is followed by two centrifugation steps in combination with addition of a chemical de-emulsifier [9]. These steps are currently required because straightforward coalescence does not occur due to substances in the fermentation broth. In this complex mixture, a wide range of substances is capable of hindering coalescence [7], and this problem could become even more prominent when using hydrolysed cellulosic biomass as a feedstock [10], leading to an even more complex composition of the fermentation broth.

Gravity separation would be a cheaper alternative method to achieve phase separation compared to centrifugation. This method would be feasible when the droplets grow sufficiently in size by coalescence. Additional advantages of gravity separation are the

possibility of integrating it with the fermentation to achieve continuous product removal and the possibility for a cell recycle, both contributing to lower production costs (Heeres, A.S., Cuellar, M.C., Van der Wielen, L.A.M., Integrating fermentation and separation for advanced biofuel production. 10th European Symposium on Biochemical Engineering Sciences, Lille, France 2014).

The main parameter determining the separation rate in gravity separation, represented by the droplet rise velocity (v_d), is the droplet diameter (d_d), with a quadratic dependency on the phase separation rate, as is shown by Stokes' law for the motion of a single droplet (Equation 1). Furthermore, the difference in density of the oil droplets (ρ_o) and the continuous aqueous phase (ρ_w), the viscosity (η) and the gravitational constant (g) play a role in the droplet rise velocity:

$$v_d = \frac{\left(\rho_o - \rho_w\right) g d_d^2}{18\eta} \tag{1}$$

This equation is valid for the rise of a single droplet, but the influence of the parameters extents to more concentrated systems as well. The initial droplet size in the fermentation is dependent on the size of the droplets right after secretion. These small droplets will grow to a steady state droplet size distribution, which is determined by the properties of the dispersion (densities of dispersed and continuous phase, ρ_d and ρ_c, dispersed phase volume fraction, ϕ_d, interfacial tension, σ) and the conditions in the vessel (volume, V, power input, P). The maximum stable droplet diameter (d_{max}) for the steady state distribution can be related to the mechanical power input (volumetric power input, e_v, in a stirred vessel dependent on impeller diameter D and rotational speed N) according to Equation (2), which is valid for dilute dispersions [11]:

$$d_{\max} = C_1 \left(\frac{\sigma^3}{e_v^{\,2} \cdot \rho_c} \right)^{1/5} \tag{2}$$

It was found empirically that this maximum diameter can be related to the Sauter mean diameter (d_{32}) by a factor (C_2). Many experimental studies were aimed at determining this value and its exact value is dependent on the system in which the experiment was performed, but reported values are around 0.5 [12]. With this value for C_2, we can get an estimate of the expected order of magnitude of the droplet size in a large scale fermentation. For the required large volume of the fermenters at an industrial scale, bubble columns have the advantage that no mechanical power input is required (opposed to stirred vessels), so we consider these as most economically feasible reactor type for the industrial production of advanced biofuels. The power input in a large scale bubble column (column height 10 m) is in the order of 750 W/m^3 [13], so according to Equation (2), the steady state Sauter mean diameter would be in the order of 900 μm (σ = 25 mN/m and ρ_c = 997 kg/m^3). This shows that already during the fermentation the initially small droplets from the secreted product can grow to a large steady state value when coalescence is occurring. Equation (2) can be further refined for stirred vessels, by incorporating the Weber tank number ($We_T = \rho_c \cdot N^2 \cdot D^3 \cdot \sigma^{-1}$), and corrected for the viscosity increase due to higher dispersed phase volume fractions with a factor C_3, leading to Equation (3) [14]:

$$\frac{d_{32}}{D} = C_2\left(1 + C_3\phi_D\right)We_T^{-3/5} \tag{3}$$

The constants in the equations change per system for which they are determined, but the equations show the relation between the physical dispersion properties and process parameters and the resulting Sauter mean diameter.

The growth from the initially small droplets to the steady state distribution is caused by droplet-droplet coalescence. When coalescence rates are lower, the balance between droplet breakup and coalescence results in a smaller steady state droplet diameter and the nett droplet growth rate will be lower as well. In that case, rapid gravity separation will become more difficult because the droplets remain smaller for a longer time.

In this paper we will focus on the effects that substances that might be present in the fermentation mixture can have on coalescence, focusing on the effects of individual components. This knowledge could aid optimisation of the fermentation medium and the microorganism, not only aiming at maximal microbial activity, but also taking the product recovery into account in an early stage. When coalescence can be sufficiently promoted during fermentation, low cost gravity separation could be used to make a step towards competitive production of advanced biofuels.

3.1.2 Methods for studying droplet coalescence

The process of coalescence follows three steps: the droplets first collide, then, the interfacial film drains, and finally this film ruptures, resulting in merging of two droplets [15]. The rate of collisions, for the first step of coalescence, is mainly determined by the flow regime in the dispersion, while molecular interactions play a more important role in the latter two steps. Additional substances present in the dispersion, besides water and oil, can influence these steps. Several cases can be distinguished: (1) substances increasing the viscosity of the aqueous phase, changing the collision impact and the drainage of the interfacial film between the droplets, (2) substances that change the charge of the droplets, altering the electrostatic interactions between droplets, and (3) substances that adsorb at the droplet interface and lower the interfacial tension or create a viscoelastic interface, hindering film rupture. Additionally, microbial cells can also hinder coalescence by increasing the viscosity of the continuous phase and by Pickering stabilisation. For Pickering stabilisation, the particles (cells in this case) need to attach to the oil/water (O/W) interface, which depends on their surface properties. With a bacterial adhesion to hydrocarbon (BATH) test, the hydrophobicity of the cells can be determined by measuring the percentage of yeast cells that adheres to a specific amount of O/W interface [16]. Yeast cells are reported to have a low affinity for O/W interfaces (23%) [17] and even cells with an O/W interface affinity of 50% are not capable of adequately stabilizing the O/W interface to form emulsions [16]. Therefore, droplet

stabilization by the cells is not considered in this paper; instead, we focus on components that are either initially present in the fermentation broth, or are excreted into it.

The physics of coalescence are quite well understood, but accurate modelling of this complex process remains difficult, especially when surface active components are present that change the interfacial tension and rheology. Therefore, models describing the coalescence process often rely on an empirical or simplified approach, discerning two factors in the coalescence rate: collision frequency and collision efficiency [18, 19]. The flow regime effects are mainly covered by the collision frequency and the molecular interactions in the collision efficiency. Parameters for these models have to be obtained from experimental data and have an empirical nature, making their application limited. Examples of these are droplet size measurements in stirred vessels. In a stirred vessel, the balance between droplet coalescence and breakup results in a droplet size distribution. By measuring the development of this distribution or an average value derived from it, the overall coalescence behaviour of the system can be studied. Droplet size measurements can be performed with offline methods that determine initial and final droplet size distributions [20, 21]. Online methods such as laser reflection and endoscopes provide an alternative, giving continuous information on the droplet size development in the vessel, but especially at high fractions of dispersed phase the analysis of acquired data becomes difficult [22].

Another approach to obtain online information is to use microfluidic chips, in which flowing dispersions can be studied using optical microscopy [23, 24]. The flow conditions in these chips are better defined than the turbulent conditions in stirred vessels or pipe flows, and they offer the possibility to work with monodisperse emulsions. This makes the chips suitable to study the coalescence frequency of very accurately defined oil droplets [25].

In this paper, the effects of fermentation broth components on droplet coalescence are studied using experiments in both microfluidic chips and stirred vessels. Using the two methods allows us to relate the results in the chip to coalescence in a system that is more similar to the actual process. The two methods might also allow us to distinguish between the different effects that components could have on the coalescence steps.

3.2 Materials and methods

3.2.1 Chemicals

The dispersion consisted of MilliQ water (Millipore, 18.2 MΩ) as a continuous phase and hexadecane (Sigma Aldrich, ReagentPlus 99%) as dispersed phase. Different solutes were selected to represent different types of components that can be present in fermentation mixtures: glucose (Merck, anhydrous for biochemistry) as a typical carbon source in fermentations, potassium chloride (Merck, analytical grade) to simulate the ionic strength in fermentation broth, ethanol (Sigma Aldrich, absolute ≥ 99.8%) as a common by-product of yeast fermentation, mannoproteins (DSM, Claristar®) as emulsifying components originating from the yeast cells, and acetic acid (J.T. Baker, glacial 99-100%), vanillin (Sigma Aldrich, ReagentPlus 99%), and 5-hydroxymethylfurfural (HMF, Sigma Aldrich, Kosher ≥ 99%) as components present in hydrolysed cellulosic biomass. The maximum tested concentrations were based on typical values in fermentations: 10 g/L potassium chloride, 100 g/L ethanol, 100 g/L glucose, 1 g/L mannoproteins, 6 g/L HMF, 1 g/L vanillin, and 5 g/L acetic acid [26, 27], the pH of these solutions was not adjusted to avoid introduction of ionic species that would influence the ionic strength of the solution. Also concentrations of a factor 10 and 100 lower were tested in the microfluidic chips for each of the components.

3.2.2 Interfacial tension measurements

The interfacial tension between hexadecane and the different aqueous solutions were measured with a drop tensiometer (Tracker-S Tensiometer, Teclis Sarl, France). Using a curved needle, a hexadecane droplet (15 μL) was formed in the continuous aqueous phase, so a floating droplet was used instead of a pendant droplet. The balance between the gravitational force acting on a droplet and the interfacial tension determines the shape of the droplet. From the radii of curvature of the pendant droplet, the interfacial tension between the two phases can be calculated using the Young-Laplace equation [28]. To ensure a constant droplet shape, the droplet was formed and left to equilibrate for 10 minutes before recording

the shape, and analysing it by Wdrop software v9.3.3.0 through which the interfacial tension was obtained. The duplicate measurements were performed for all measurements.

3.2.3 Microfluidic chip experiments

The microfluidic chips were manufactured by Micronit B.V., The Netherlands. A detailed description of the microfluidic chips is given by Krebs [24] and the layout is shown in Figure 1. The chips were mounted in a chip holder (Nanoport, Micronit B.V., The Netherlands) and the inflow and outflow were connected to the syringe pumps (NE 1000, New Era Pump Systems, Inc.) by silica capillary tubing (Grace Alltech, inner diameter 150 µm). The experiments were conducted at room temperature.

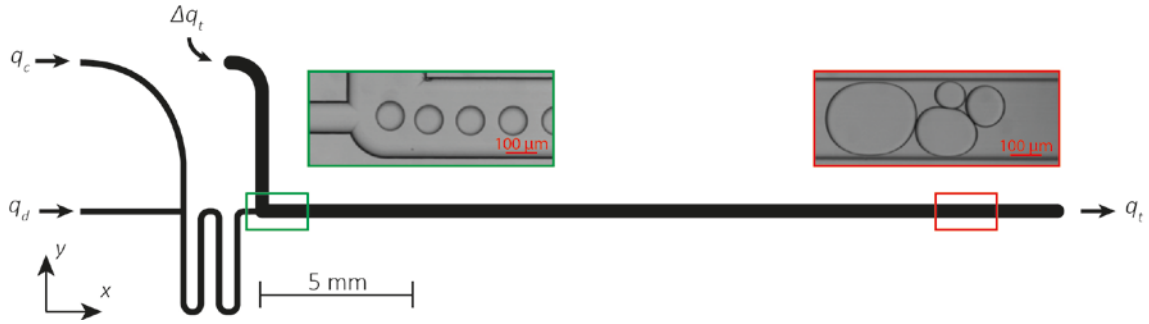

Figure 1. Layout of the microfluidic chip (adapted from [25]). The dispersed phase entered at q_d and the continuous phase entered at q_c. The inlet Δq_t could be used to dilute or change the flow conditions in the coalescence channel. q_t was the outflow. The narrow channels in which the droplets were formed (left) had a width of 100 µm, and the coalescence channel (right) had a width of 250 µm and length of 3.0 cm. All channels had a uniform depth of 45 µm. Two example images are given from the inlet and outlet of the coalescence channel. The coloured boxes show the area in which the images were recorded for the droplet size analysis.

At the T-junction, monodisperse droplets with a diameter of about 100 µm were formed at a dispersed phase flow rate (q_d) of 5 µL/min and continuous phase flow (q_c) of 50 µL/min. The droplets were led through the narrow meandering channel before releasing them into the coalescence channel to make sure that the equilibrium interfacial tension for any of the surface active components was reached [24]. When the droplets entered the broader coalescence channel, the ratio of dispersed and continuous phase flow was adapted by inflow of additional continuous phase (Δq_t,5 µL/min) to create a flow pattern with sufficient collisions between the droplet, which resulted in an oil fraction of 0.083. With these liquid flow rates, the residence time in the coalescence channel is 0.34 s and the liquid velocity 8.9

cm/s, obtaining laminar flow conditions in the channel (Reynolds number of 22). In the broader coalescence channel, the velocity gradient over the width of the channel causes droplet motion not only in the flow direction of the channel (x-direction in Figure 1) but also motion perpendicular to the channel (y-direction in Figure 1). This results in collisions between droplets and depending on interface stabilisation coalescence may occur. Because of the depth of all channels (45 μm), the droplets will be trapped between the top and bottom of the channels adopting a disc-like shape. This makes it possible to convert the increase in droplet area directly to the number of coalescence events. The images for droplet size analysis were acquired at the start and end of the coalescence channel, using a microscope (Axiovert 200 MAT, Carl Zeiss GmbH, 4x magnification) in combination with a high speed camera (Y4-S2, IDT Inc.). The images were recorded in the area shown in Figure 1 by the red box. Per experiment, 5000 images were acquired, using a frame rate of 30 s^{-1} and an exposure time of 10 ms.

The image processing was performed with ImageJ, determining the areas of the droplets recorded and converting these to droplet size distributions. For each experiment, 20 000 droplets were used to construct the droplet size distributions at the end of the coalescence channel. From these distributions and the initial droplet size, the number of coalescence events could be determined using Microsoft Excel and scripts written in Visual Basic by a procedure described in an earlier publication by Krebs [29]. A double sided *t*-test for independent means was performed to determine if there was a statistically significant difference between the reference case (MilliQ/hexadecane) and each other condition, resulting in a *p*-value for the null hypothesis that the mean values for the reference condition and the tested condition were the same.

Each measurement series of a component was performed using increasing solute concentration and in duplicate, except the reference experiment: this experiment was performed 11 times. Between the measurement series, the chip was flushed with 1 M sodium hydroxide solution followed by MilliQ water. To ensure cleanness of the chip, a reference measurement with hexadecane/MilliQ was performed prior to each measurement series.

When additional cleaning of the chip was required, it was again flushed with sodium hydroxide solution and MilliQ water, followed by treatment with an oxygen plasma for 10 minutes (Zepto B Plasma Cleaner, Diener Electronic GmbH).

3.2.4 Stirred vessel experiments

The coalescence measurements at a larger scale were performed in an Applikon 2 L vessel, equipped with two baffles, a heat exchanger (coupled to a thermostat set at 25 °C), and the power input was provided by a six bladed Rushton turbine (Figure 2). The total liquid volume was 1 L and the hexadecane volume fraction was 0.1. Prior to each experiment, the vessel was thoroughly washed with an anionic detergent (Dubro), followed by thorough rinsing with tap water, deionised water, and MilliQ water. In the experiments, the stirring rate was controlled by an Applikon ADI 1012 motor controller. For the first 30 min, the stirring rate was set to 1200 rpm, after which it was decreased to 400 rpm for 90 min. The stirring rate of 400 rpm was chosen to ensure that the oil remained dispersed even at low stirring rate. The factor three decrease in stirring rate lowered the power input in the stirred vessel by a factor 9, resulting in a regime in which only droplet coalescence occurs right after the step change in the stirring rate [30]. In the actual production process, a similar regime change to a coalescence favouring regime will occur when the liquid goes from well-mixed fermentation conditions to gravity separation.

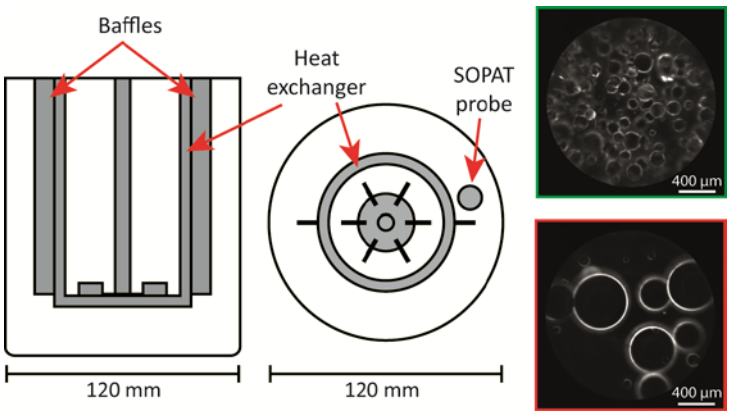

Figure 2. The dimensions of the stirred vessel used for the coalescence experiments with two example pictures of the images recorded during the experiments with a mixture of hexadecane (volume fraction of 0.1) and MilliQ water (top image acquired at 1200 rpm, bottom image at 400 rpm).

During the experiments, images of the droplets were recorded by a SOPAT probe (SOPAT Gmbh) for in situ image acquisition. Every 3 minutes, a trigger of 30 pictures was recorded for the duration of the experiment. After the experiment, the images were analysed using the image analysis software provided by SOPAT Gmbh [31]. At 1200 rpm, air bubbles were incorporated in the mixture and interfered with the image analysis. These were eliminated by setting a maximum particle size of 200 μm, which was validated by manual removal of the air bubbles. At 400 rpm, no more bubbles were incorporated in the mixture and this was not required (see also Results section).

3.3 Results

3.3.1 Effect of fermentation broth components on interfacial tension

Most of the substances did not show any effect on the interfacial tension of the hexadecane/water interface: glucose, potassium chloride, vanillin, and acetic acid left the interfacial tension unchanged. Ethanol is known to influence the surface tension of the air/water interface and it also lowered the interfacial tension from 31.4 mN/m to 25.4 mN/m. HMF and mannoproteins showed a similar decrease, respectively to 26.1 and 26.0 mN/m. These results already show which components have surface active properties, so from which components an effect on coalescence could be expected.

3.3.2 Coalescence measurements in microfluidic chips

The recorded images from the microfluidic chips gave information about the number of coalescence events that occured during the flow through the coalescence channel. The pure hexadecane/water system was used as a reference and in that system close to 60% of the droplets did not coalesce in the coalescence channel (Figure 3). With this number of uncoalesced droplets and the observed variation between experiments, it was expected that differences can be observed with more stable emulsion droplets. The number fractions showed a relatively large standard deviation, especially for the droplets of the initial size (zero

coalescence events). For higher numbers of coalescence events this decreased, because of their lower occurrence, dampening out the standard deviation of the fraction averages.

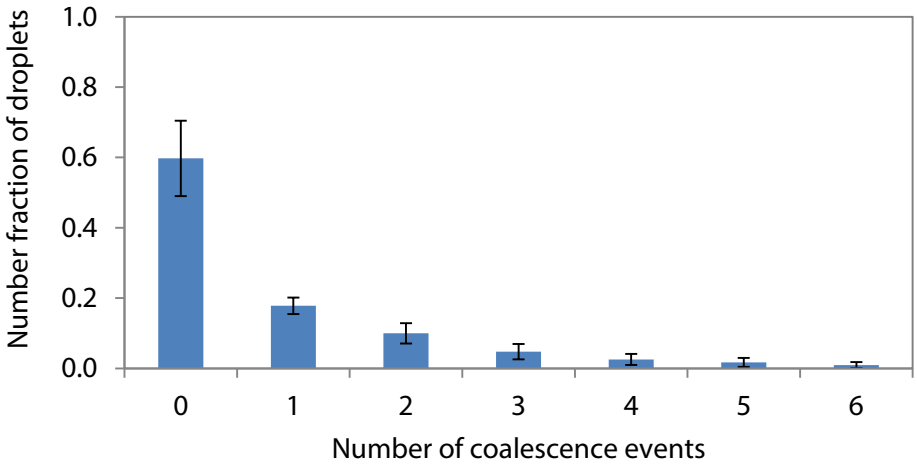

Figure 3. The number of coalescence events that hexadecane droplets underwent in the microfluidic chip with MilliQ water as the continuous phase, which is the reference case for further experiments. The bars represent the standard deviation of the average (total of 11 measurements).

Taking these results as a reference case, we compared them with the results obtained for systems with fermentation mixture components dissolved in the aqueous phase. Since only few droplets underwent three or more coalescence events, only the droplets fractions that had undergone zero, one, and two coalescence events are shown individually in the comparison. The presence of glucose (100 g/L) and potassium chloride (10 g/L) did not result in a significant difference in the droplet size distribution compared to the reference case with MilliQ water and hexadecane (Figure 4A), which could be expected based on their effect on the interfacial tension. For the small droplets (zero and one coalescence events), ethanol did not show a significant decrease in the droplet number fraction, but for droplets that had undergone a larger number of coalescence events, there was a significant decrease (for respectively two, three, four, and five coalescence events, p-values of 0.019, 0.027, 0.057, and 0.047 were obtained). So although there was no clear increase in the number of droplets that did not coalesce, the lack of large droplets showed that ethanol did inhibit coalescence.

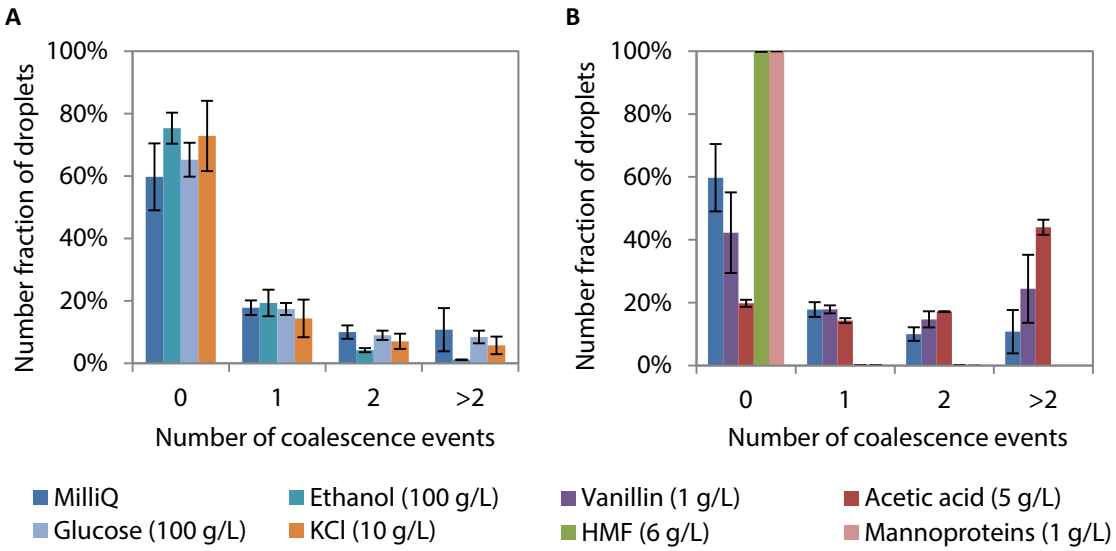

Figure 4. The number fraction of droplets that for a number of coalescence events for different compositions of the aqueous phase. Left (A) the components that occur as in fermentation media or by-products and right (B) the components that occur in hydrolysed cellulosic biomass and a component from the yeast cell wall. The error bars represent the standard deviation in the duplicate experiments. To determine if a component had a significant effect on the coalescence, p-values were calculated for the number fraction of droplets that had undergone zero coalescence events for a certain composition compared to the reference case: ethanol, 0.082; glucose, 0.39; KCl, 0.27; vanillin, 0.21; acetic acid, 0.0068; HMF, 0.0064; mannoproteins, 0.0064.

The substances that could originate from hydrolysed cellulosic biomass and the microorganism influenced the coalescence of the oil droplets stronger (Figure 4B). HMF (6 g/L) and mannoproteins (1 g/L) clearly inhibited coalescence, at the end of the coalescence channel only droplets of the initial size were detected, so the residence time in the coalescence chamber was not sufficient to lead to merging of droplets. For mannoproteins this was expected, since it is known as a good emulsifier [26]. For HMF, an effect could be expected from its influence on the interfacial tension. From the other two components present in hydrolysed cellulosic biomass, acetic acid showed to enhance coalescence, leading to less droplets with no coalescence event and more droplets with a number of coalescence events of more than two. Acetic acid (5 g/L) showed a significant fraction of droplets with 8 coalescence events, respectively 3.5 % (p-value 0.003, result not shown). Vanillin did not cause a significant change in coalescence behaviour compared to the reference case.

In the experiments performed at lower solute concentrations, only two components showed to change coalescence compared to the hexadecane/MilliQ system. At 0.6 g/L, HMF still decreased the number of coalescence events and 96% of the droplets did not coalesce.

Where potassium chloride did not influence coalescence at 10 g/L, at lower concentrations it decreased the number of coalescence events strongly. At 1 g/L and 0.1 g/L, respectively 99.8% and 99.1 % of the droplets did not coalesce.

3.3.3 Coalescence measurements in a stirred vessel

A selection of the substances was tested at a larger scale: mannoproteins (1 g/L), glucose (100 g/L), ethanol (100 g/L), and acetic acid (5 g/L). These components respectively decreased, unaffected, and enhanced coalescence in the microfluidic chip. From the resulting *in-situ* droplet size distribution, the Sauter mean diameter was calculated to see the coalescence behaviour after a step change in stirring rate at 30 min (Figure 5). Only in the experiment with the mannoproteins, the air bubbles present in the dispersion were so small that they did not immediately rise out of the liquid when the stirring rate was lowered, causing the peak in the Sauter mean diameter at 33 min. After about 20 minutes at 400 rpm (t = 50 min), the majority of the gas bubbles had left the liquid and the average gave a true representation of the droplet size.

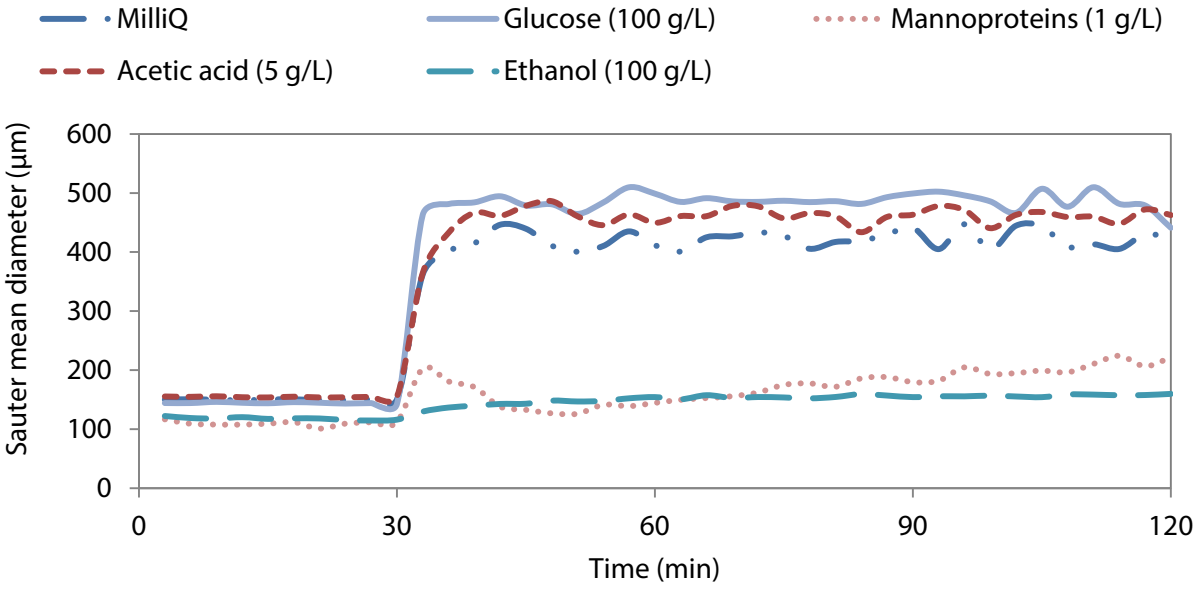

Figure 5. Development of the Sauter mean diameter over time in for a selection of the previously tested substances. The initial stirring rate was 1200 rpm and at 30 min, a step change in stirring rate to 400 rpm was made.

Looking at the increase of the Sauter mean diameter after the step decrease in the stirring rate, we can see that mannoproteins and ethanol strongly retarded the increase of the Sauter mean diameter compared to the mixture with MilliQ water and hexadecane. For both mannoproteins and ethanol the initial droplet size was smaller than for the other tested components, which was also expected from their effect on the interfacial tension. Equation (3) predicts a 10.7 and 11.9 % decrease in the Sauter mean diameter for respectively the mannoproteins and ethanol due to the reduction in interfacial tension (which was decreased from 31.4 to 26.0 mN/m for the mannoproteins and 25.4 mN/m for the ethanol mixture). However, the initial Sauter mean diameter was reduced stronger: from 150 μm in the reference case to 110 μm in the dispersion with the mannoproteins (26.9 % decrease) and to 118 μm in the dispersion with ethanol. The much slower increase of the Sauter mean diameter shows that the coalescence rate was much lower for the two mixtures with ethanol and mannoproteins. In the mixtures with rapid coalescence, the Sauter mean diameter increased with a factor three from one steady state to the other. The same change would be expected for the mixtures with mannoproteins and ethanol and after 1.5 h at the lower stirring rate the Sauter mean diameter was still increasing, so clearly the steady state diameter was not reached within the experiment.

The Sauter mean diameter in the dispersions with glucose and acetic acid showed similar behaviour as the reference case, so the coalescence rate was also similar. The interfacial tension was not influenced by glucose and acetic acid, resulting in larger droplets in the dispersion compared to the mixtures with a decreased interfacial tension.

3.4 Discussion

3.4.1 Comparison of the three experimental methods

Both tested methods allowed us to observe effects of fermentation broth components on coalescence. As expected, interfacial tension measurements provided a suitable initial assessment of the effect on steady state droplet size under operating conditions and showed which components could be expected to influence coalescence. The microfluidic chip and

stirred vessel can then be used to quantify the effect of the components on coalescence. The experiments in the microfluidic chips and stirred vessel showed to focus on different aspects of the coalescence process. In the microfluidic chips, the initial droplet size was similar for all components and there was a focus purely on coalescence. In the stirred vessel, the effect of break-up on the droplet size had to be considered as well. Therefore, the stirred vessel was a closer resemblance to the regimes at fermentation conditions, where coalescence and break-up have to be considered both. The flow rates used in the microfluidic chip resulted in a shear rate of about 580 s^{-1} due to the velocity profile over the coalescence channel [24]. Comparing this to the stirred vessel, the residence time there was orders of magnitude higher (total coalescence time of 1.5 h versus 0.34 s in the chip) and the average shear rate in the vessel varied from 2030 s^{-1} to 390 s^{-1}, at high and low stirring intensity. It must be noted that this is an overall shear rate in the vessel, so locally higher shear rates can occur (near the impeller), resulting in zones with droplet break-up and zones with coalescence. Another difference between the two coalescence experiments is that the microfluidic chips also allowed measuring an enhancement in the coalescence rate, something that could not be detected in the stirred vessel. When the results of the experiments of the interfacial tension measurements, microfluidic chips, and stirred vessel are summarised, the results of the different experiments align well (Table 1).

Table 1. Comparison of the effects of broth components in the different experiments, indicating either no change (0), a decrease (-) or an increase (+) compared to the reference experiment.

Compound	Interfacial tension	Microfluidic chip coalescence	Stirred vessel coalescence	Initial Sauter mean diameter (μm)[a]
Reference	0	0	0	150
Ethanol	-	-	-	118
Glucose	0	0	0	144
KCl	0	0	ND[b]	ND
Vanillin	0	0	ND	ND
Acetic acid	0	+	0	155
HMF	-	-	ND	ND
Mannoproteins	-	-	-	110

a) Steady state Sauter mean diameter at 1200 rpm, before stirring rate decrease.
b) ND: not determined.

3.4.2 The influence of fermentation broth components on coalescence

Looking at the results of the experiments for each of the mixtures, we can see that both the experiments in the microfluidic chips and the stirred vessel showed that some substances potentially present in a fermentation broth influence the coalescence behaviour of oil droplets and others did not:

- Ions are known to have an influence of the droplet charge by changing the effective charge of the droplets. Depending on the ion concentration, the electrostatic repulsion between the droplets can be induced or shielded. At low concentrations (0.1 and 1 g/L), potassium chloride negatively influenced coalescence due to electrostatic repulsion of the droplets, but at a concentration which resulted in a similar ionic strength as fermentation media, the coalescence rate was similar to the pure system. In that case, the ions decreased the electrostatic double layer around the droplets and shielded the electrostatic forces, diminishing electrostatic repulsion between the droplets that could prevent coalescence [32].
- Glucose and vanillin did not show any surface activity in the interfacial tension measurements, as could be expected from their molecular structure. High concentrations of glucose do cause a slight increase of the aqueous phase viscosity but no effect on coalescence was measured [33].

The other tested components influenced coalescence: mannoproteins, ethanol, and HMF negatively influenced coalescence, and acetic acid appeared to enhance coalescence.

- HMF at a concentration as found in hydrolysed cellulosic biomass (6 g/L) completely inhibited coalescence of the droplets in the coalescence channel. Although no report is made about the interfacial activity of HMF, the decrease of interfacial tension shows that it has surface active properties and it is capable of stabilising the droplet interface against coalescence.

- Acetic acid, another component from hydrolysed cellulosic biomass, enhanced coalescence in the microfluidic chips (at 5 g/L). However, when acetic acid was tested in the stirred vessel, no increase in the coalescence rate could be observed and the measured steady state droplets size was similar to that of the reference case, MilliQ water and hexadecane. Because coalescence occurred almost completely within the first three minute interval between measurements, any increase in the coalescence rate could not be seen in the development of the Sauter mean diameter.
- Mannoproteins completely inhibited coalescence in the microfluidic chips at 1 g/L. The residence time of the droplets in the coalescence channel was probably insufficient to achieve film drainage within this time. In the stirred vessel, an increase in the droplet size due to coalescence could be observed due to the much higher residence time in the stirred vessel compared to the microfluidic chip. However, this rate was much too low to reach the expected steady state droplet size within the time of the experiment. As can be seen in Equation 3, when the stirring rate is decreased with a factor 3, the Sauter mean diameter is expected to increase with a factor 3.7. So from the initial steady state droplet size of 100 μm, a new steady state of 370 μm would be expected at 400 rpm.
- Ethanol did not show to have a clear effect on the small droplets in the microfluidic chips, but there was a significant decrease of the number of large droplets. In the stirred vessel, ethanol reduced the increase in the Sauter mean diameter over time. This could indicate that although the experimental conditions in the stirred vessel were chosen to favour coalescence, still significant break-up was occurring, which could be caused by the reduction of the interfacial tension by the ethanol.

These experiments only studied the effects of single components, so any synergistic effects that could occur in complex fermentation mixtures have not been considered. For instance when electrostatic repulsion is stabilising the droplets these synergistic effects are important, because the total ionic strength of the solution has to be considered.

3.5 Concluding remarks & outlook

The experiments showed that a wide range of fermentation broth components can have a significant effect on coalescence, so likely some of these components will be present in the fermentation broth. Interfacial tension measurements can give a first indication of whether coalescence will be influenced in a specific fermentation broth. The fermentation broth could also be used to perform coalescence measurements in a stirred vessel to obtain a first insight in whether coalescence will be affected and the severity of the droplet stabilisation. Experiments in the microfluidic chips are more suitable to identify the exact components responsible for the droplet stabilisation and these could also be used to determine target concentrations for components in the fermentation broth at which coalescence is not negatively influenced. Besides the components causing the stabilisation, the initial droplet size is also of importance. In both type of experiments, an initial droplet size of about 100 μm was used, for which 1.5 h was insufficient to reach a new steady state droplet size with 1 g/L of mannoprotein present. When the initial droplet size is even smaller, one can expect that the required time for droplet growth is even longer.

So, from a product recovery point of view, components that retard coalescence are unwanted. Depending on the components causing the stabilisation, different measures can be taken to lower or avoid their presence in the fermentation broth. For instance by adapting pretreatment methods (in case of feedstock components) or microbial physiology (in case of surface active components released by the microorganism), by minimising stress on the microorganisms due to the process conditions or strain engineering. This will result in easier product recovery, which is not only beneficial for advanced biofuel production, but also for all other processes in which a second liquid phase has to be recovered for a fermentation broth, for instance in extractive fermentations.

Acknowledgement

This work was partly carried out within the BE-Basic R&D Program, which was granted a FES subsidy from the Dutch Ministry of Economic affairs, agriculture and

innovation (EL&I). The authors would like to thank ing. Maurice Strubel for his help setting up the microfluidic chip experiments, dr. ir. Thomas Krebs for his assistance with the image analysis of the microfluidic chip experiment, and prof. dr. Rosiane Lopes da Cunha for facilitating the interfacial tension measurements.

References

1. Lee, S.K., et al., *Metabolic engineering of microorganisms for biofuels production: from bugs to synthetic biology to fuels.* Curr. Opin. Biotechnol., 2008. 19(6): p. 556-563.
2. Rude, M.A. and A. Schirmer, *New microbial fuels: a biotech perspective.* Curr. Opin. Biotechnol., 2009. 12(3): p. 274-281.
3. Zhang, F., S. Rodriguez, and J.D. Keasling, *Metabolic engineering of microbial pathways for advanced biofuels production.* Curr. Opin. Biotechnol., 2011. 22(6): p. 775-783.
4. Schirmer, A., et al., *Microbial biosynthesis of alkanes* Science, 2010. 329: p. 559-562.
5. Dunlop, M.J., et al., *Engineering microbial biofuel tolerance and export using efflux pumps.* Mol. Syst. Biol., 2011. 7.
6. Cuellar, M.C., J.J. Heijnen, and L.A.M. van der Wielen, *Large-scale production of diesel-like biofuels - process design as an inherent part of microorganism development.* Biotechnol. J., 2013. 8(6): p. 682-689.
7. Heeres, A.S., et al., *Microbial advanced biofuels production: overcoming emulsification challenges for large-scale operation.* Trends Biotechnol. , 2014. 32(4): p. 221-229.
8. Van den Broek, W.M.G.T., R. Plat, and M.J. Van der Zande, *Comparison of plate separator, centrifuge and hydrocyclone.* SPE International Conference, Beijing, CN, 1998. http://dx.doi.org/10.2118/48870-MS.
9. Tabur, P. and G. Dorin, *Method for purifying bio-organic compounds from fermentation broth containing surfactants by temperature-induced phase inversion.* US Patent 20120040396, 2012.
10. Wenger, J.W., et al., *Minimizing the cost of cellulosic-biomass-derived Amyris diesel by combining non-native sugar catabolism and xylose isomerase pathways.* SBFC 2014, Clearwater, FL, US, 2014.
11. Levich, V.G., *Physicochemical Hydrodynamics*. 1962. ISBN: 978-0136744405, Englewood Cliffs: Prentice-Hall. 395-471.
12. Zhou, G. and S.M. Kresta, *Correlation of mean drop size and minimum drop size with the turbulence energy dissipation and the flow in an agitated tank.* Chem. Eng. Sci., 1998. 53(11): p. 2063-2079.
13. Roels, J.A. and J.J. Heijnen, *Power dissipation and heat production in bubble columns: approach based on nonequilibrium thermodynamics.* Biotech. Bioeng., 1980. 12: p. 2399-2404.
14. Doulah, M.S., *An effect of hold-up on drop sizes in liquid-liquid dispersions.* Ind. Eng. Chem. Fundam., 1975. 14(2): p. 137-138.
15. Tadros, T.F. and B. Vincent, *Emulsion stability*, in *Encyclopedia of Emulsion Technology*, P. Becher, Editor. 1983, Marcel Dekker: New York. p. 269-272.
16. Dorobantu, L.S., et al., *Stabilization of oil-water emulsions by hydrophobic bacteria.* App. Environ. Microb., 2004. 70(10): p. 6333-6336.

17. Furtado, G.F., et al., *Breaking oil-in-water emulsions stabilized by yeast.* Colloid Surf. B: Biointerfaces, 2015. 128(0): p. 568-576.
18. Chesters, A.K., *The modelling of coalescence processes in fluid-liquid dispersions: a review of current standings.* Chem. Eng. Res. Des., 1991. 69A: p. 259-270.
19. Liao, Y. and D. Lucas, *A literature review on mechanisms and models for the coalescence process of fluid particles.* Chem. Eng. Sci., 2010. 65: p. 2851-2864.
20. Whitby, C.P., et al., *Shear-induced coalescence of oil-in-water Pickering emulsions.* J. Colloid Interface Sci., 2011. 361(1): p. 170-177.
21. Maindarkar, S.N., et al., *Incorporating emulsion drop coalescence into population balance equation models of high pressure homogenization.* Colloid. Surface. Physicochem. Eng. Aspect., 2012. 396: p. 63-73.
22. Maaß, S., et al., *Experimental comparison of measurement techniques for drop size distributions in liquid/liquid dispersions.* Exp. Fluid., 2011. 50(2): p. 259-269.
23. Baret, J.-C., et al., *Kinetic aspects of emulsion stabilization by surfactants: a microfluidic analysis.* Langmuir, 2009. 25(11): p. 6088-6093.
24. Krebs, T., K. Schroën, and R. Boom, *Coalescence dynamics of surfactant-stabilized emulsions studied with microfluidics.* Soft Matter, 2012. 8(41): p. 10650-10657.
25. Tan, Y.-C., Y.L. Ho, and A.P. Lee, *Droplet coalescence by geometrically mediated flow in microfluidic channels.* Microfluid. Nanofluid., 2007. 3: p. 495-499.
26. Cameron, D.R., D.G. Cooper, and R.J. Neufeld, *The mannoprotein of Saccharomyces cerevisiae is an effective bioemulsifier.* Appl. Environ. Microbiol., 1988. 54: p. 1420-1425.
27. Almeida, J.R.M., et al., *Increased tolerance and conversion of inhibitors in lignocellulosic hydrolysates by Saccharomyces cerevisiae.* J. Chem. Technol. Biotechnol., 2007. 82(4): p. 340-349.
28. Rotenberg, Y., L. Boruvka, and A.W. Neumann, *Determination of surface tension and contact angle from the shapes of axisymmetric fluid interfaces.* J. Colloid Interf. Sci., 1983. 93(1): p. 169-183.
29. Krebs, T., K. Schroen, and R. Boom, *A microfluidic method to study demulsification kinetics.* Lab Chip, 2012. 12: p. 1060-1070.
30. Tobin, T., et al., *Determination of coalescence frequencies in liquid-liquid dispersions: effect of drop size dependence.* Chem. Eng. J., 1990. 45: p. 3491-3504.
31. Maaß, S., et al., *Automated drop detection using image analysis for online particle size monitoring in multiphase systems.* Comput. Chem. Eng., 2012. 45: p. 27-37.
32. Elworthy, P.H., A.T. Florence, and J.A. Rogers, *Stabilization of oil-in-water emulsions by nonionic detergents: V. The effect of salts on rates of coalescence in a chlorobenzene emulsion.* J. Colloid Interface Sci., 1971. 35(1): p. 23-33.
33. McClements, D.J., *Food emulsions, principles, practices, and techniques*. 2nd edition ed. Contemporary Food Science, ed. F.M. Clydesdale. 2005, Boca Raton: CRC Press.

Chapter 4. Regime analysis for integrated product recovery in microbial advanced biofuels production

Abstract

One of the recent achievements in biofuel research is the development of microorganisms that produce advanced biofuels. These biofuels form a second liquid phase during fermentation, which creates the opportunity for low cost product separation based on the density difference with the fermentation medium. Integrating product removal and fermentation could contribute to lower equipment and utility costs and it might also enable the recycling of cells. In this paper, the feasibility of gravity separation integrated with biofuel production in a bubble column reactor is studied, using a regime analysis approach. The two crucial subprocesses are droplet coalescence and droplet creaming, but these are hindered by competing subprocesses: emulsification and mixing, respectively. The regime analysis showed that a multi-compartment reactor design is required to benefit from the advantages of integration: cell reuse, lower equipment costs, and easier separation.

This chapter will be submitted as:

A.S. Heeres*, S. Pedraza de la Cuesta*, J.J. Heijnen, L.A.M. van der Wielen, M.C. Cuellar, Regime analysis for integrated product recovery in microbial advanced biofuels production

* Both authors contributed equally

4.1 Introduction

In the search for better biofuels, biotech companies such as REG Life Sciences and Amyris have developed microorganisms that are capable of converting sugars to long-chain hydrocarbon biofuels, also named advanced or drop-in biofuels, using metabolic engineering and synthetic biology [1-4]. These developments are especially relevant for jet fuels, since there are no technical renewable alternatives for airplanes. The biofuels currently produced at commercial scale, ethanol and biodiesel (transesterified lipids) produced from vegetable oils and fats, are either unsuitable as jet fuel and/or limited by feedstock availability. Target production costs for long-chain hydrocarbons of around \$0.60 L^{-1} have been mentioned to make these biofuels an alternative for conventional fuels [4], but selling prices of \$7.7 L^{-1} were recently reported [5]. In order to lower their production costs, a combination of process improvements is required: a) use of a low cost feedstock, b) enabling anaerobic fermentation to maximise product yield on substrate and to avoid aeration related investments and energy cost, c) implementing cell reuse, and d) developing low cost fermentation and product recovery technology [6].

The microbial production of advanced biofuels consists of a fermentation in which the microorganism converts substrate to biofuel and secretes it into the fermentation broth [7], resulting in a four phase mixture consisting of hydrocarbon product (oil) droplets, aqueous fermentation broth, microbial cells, and (fermentation) gas bubbles. Although not much has been reported about the secretion mechanism, the initial size of the oil droplets after secretion can be expected to be at most in the same order of magnitude as the cells (~1 μm). The recovery of the oil droplets follows then three steps: droplet growth by coalescence, phase separation – also named creaming – induced by the density difference, and further coalescence of droplets into a continuous oil phase [8].

In a fermentation process, a wide range of surface active components (SACs) can be present, originating from cells and feedstock [8]. In fact, product droplet stabilisation has been reported in the production of advanced biofuels [9]. The presence of SACs could hinder the coalescence process, preventing droplet growth and leading to product emulsification.

The droplet size that is reached after the first coalescence step, determines the options for the phase separation method. Gravity separation is the most simple and cost effective method to induce creaming, but large droplets are required because the separation is driven by only the gravitational force is used for separation. Enhanced gravity methods (e.g., centrifugation and hydrocyclones) are capable of separating smaller droplets, but these methods are more expensive. Therefore, we will focus on the application of gravity separation.

Next to applying gravity separation, the process costs could be further decreased by integration of product separation with fermentative production in a single unit, potentially decreasing equipment costs. Many large scale fermentation processes are performed in bubble column bioreactors, in which the bubbles (either sparged air in the current aerobic process or gas produced by the microorganisms in an anaerobic case) provide mixing and hence, no mechanical power input is required. This reduces the operating costs and is therefore regarded as the most suitable bioreactor type for large scale production of drop-in biofuels [10]. Integration of the production and separation may have further advantages such as enabling cell reuse and continuous process operation.

Whether product separation can be integrated in a bubble column bioreactor is dependent on the operating conditions. In this paper, the possibility of integrating gravity separation and fermentation into a single piece of equipment is studied by a regime analysis, which takes the effects of operating conditions and scale into account.

4.2 Regime analysis

4.2.1 Concept

Regime analysis is a tool that compares the rates of the different mechanisms involved in a process in order to identify the rate-limiting one. The method divides the overall process in a sequence of steps, or subprocesses, and compares their rates. The subprocess rates are represented as characteristic times, which indicate the time required by a mechanism to smooth out a change [11]. The rates are inversely proportional to their characteristic times, so a subprocess with a low rate has a large characteristic time. One subprocess is considered

faster than the other when its characteristic time is at least one order of magnitude lower [11]. This comparison is done in terms of order of magnitude, since correlations used to determine characteristic times also yield an order of magnitude estimation of these. The subprocess with the largest characteristic time is the rate-limiting one, determining over-all process rate and the regime in which the process operates [12]. By assessing effect of reactor size on the characteristic times, the scale dependency of the process can be determined.

Several scale-up/scale-down studies in literature have used regime analysis as a tool for assessing scale effects, applying it for a variety of processes: gluconic acid production [13], microbial desulfurisation [14], butanol production [15], baker's yeast production [11] and, more recently, Baeyer–Villiger bioconversion of ketones [16, 17] and production of biopharmaceutical proteins [18]. To achieve similar process performance when moving from lab to large scale, the regime should be the same on both scales [12]. Regime analysis can be used to determine if a regime change will take place when the scale of the process is increased.

4.2.2 Subprocess sequence definition

The first step in a regime analysis is to analyse the subprocesses in the production system, which leads to the simplified sequence of subprocesses shown in Figure 1. The microbial production of advanced biofuel starts with the substrate, which is fed to the reactor and mixed in the fermentation broth (1). Microorganisms take the substrate (2), convert it to biofuel (3) and secrete it (4). The recovery of the biofuel begins with small product droplets that grow by coalescence (5). When they reach a critical size, the droplets cream (6) and finally they can form a continuous oil phase on top of the reactor (7).

For conventional fermentation processes, mixing, heat removal, and oxygen transfer are generally considered the rate-limiting subprocesses [19]. In this paper, we will focus the regime analysis on the integration of product separation with its microbial production, which will result in additional subprocesses that have to be evaluated. SACs produced by the microorganisms (e.g., proteins) can stabilise the oil droplets hindering coalescence and leading to product emulsification. In addition, mixing in the reactor (1) competes with the

creaming of the droplets (6) preventing the formation of a continuous oil phase. Because we focus on the integration of the separation process, we take the subprocesses related to the microorganisms not to be limiting.

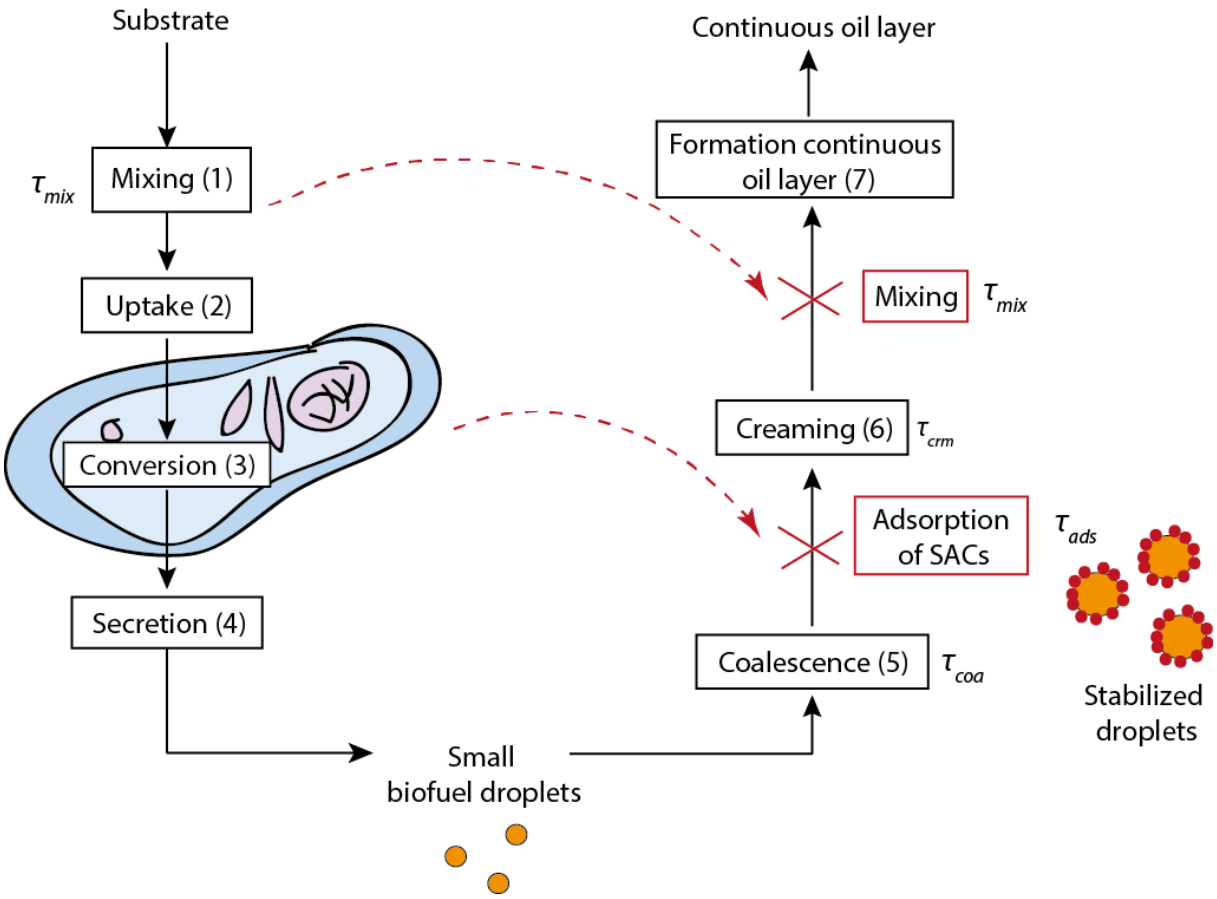

Figure 1. Sketch of the sequence of subprocesses involved in the microbial production (left) and separation (right) of biofuel. Interactions resulting from the integration are represented with dashed lines.

In this study, different process parameters influencing droplet coalescence, droplet creaming, mixing, and adsorption of SACs are assessed by a regime analysis. Integration is considered feasible at operating conditions in which characteristic times of coalescence (τ_{coa}) and creaming (τ_{crm}) are one order of magnitude lower than the characteristic times of adsorption of SACs (τ_{ads}) and mixing (τ_{mix}), respectively:

$$\tau_{coa} < 10 \cdot \tau_{ads} \tag{1}$$

$$\tau_{crm} < 10 \cdot \tau_{mix} \tag{2}$$

Next step is the express these characteristic times as a function of different process parameters. A single process parameter can influence multiple characteristic times. For example, the volumetric power input in the reactor influences the characteristic times of mixing, coalescence, and SAC adsorption, as will be shown in the following paragraphs.

4.2.3 Characteristic times derivation

4.2.3.1 Droplet coalescence

Coalescence is a three stage subprocess (Figure 2): the droplets first collide, then the liquid film between the droplets drains, and finally the film ruptures and the droplets merge [20].

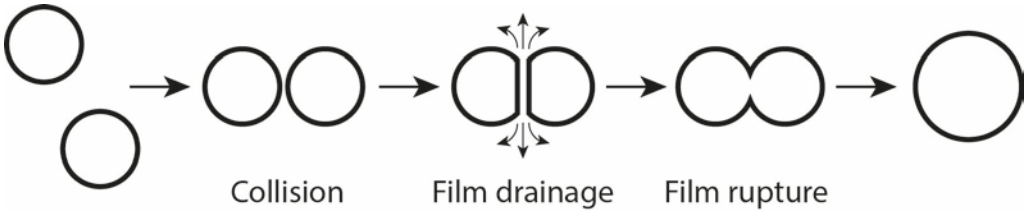

Figure 2. Illustration of the three steps in the coalescence subprocess

When the droplet interface is not stabilised by SACs, film drainage and rupture occur rapidly. Hence, droplet collision is the rate determining step in coalescence of unstabilised droplets [21]. The characteristic time for the coalescence process can be described by the collision time of equally sized droplets is shown in Equation (3) [22]:

$$\tau_{coa} = \frac{d_d^{2/3} \rho_l^{1/3}}{15 \phi_{oil}\ e_v^{1/3}}. \tag{3}$$

The droplet collision rate depends on the volumetric oil fraction (ϕ_{oil}), the droplet diameter (d_d), the overall liquid density (ρ_l), taking into account the volume fractions of oil and water, and the volumetric power input (e_v). The power input in a bubble column is determined by the gas flow rate and the reactor geometry, which are combined in the superficial gas velocity. Equation (4) approximates the volumetric power input by the gas displacement, using the

gravitational acceleration constant (g), overall liquid density and superficial gas velocity (v_{Gs}, volumetric gas flow over cross sectional area of the column) [23]:

$$e_v = g\rho_l v_{Gs}. \tag{4}$$

Ionic strength and pH influence the effective droplet charge, creating or neutralising repulsive electrostatic forces and thereby influencing coalescence. However, at the ion concentrations present in fermentations, the droplet charge is shielded and any electrostatic repulsive forces are eliminated, therefore these do not have to be taken into account [24, 25].

4.2.3.2 Droplet stabilisation

SACs can adsorb at the oil/water interface of the droplets, lowering the interfacial tension, or causing steric or charge stabilisation of the interface, preventing coalescence and droplet growth. The characteristic time for the adsorption of these SACs at a droplet surface is given by Equation (5) [22],

$$\tau_{ads} = \frac{10\Gamma\eta_w^{1/2}}{d_d c_{SAC} e_v^{1/2}}. \tag{5}$$

This equation includes the surface excess concentration (Γ), which is the amount of SACs adsorbing at the oil/water interface, droplet diameter, the concentration of SACs in the bulk (c_{SAC}), and the volumetric power input as a measure for the mixing in the reactor.

4.2.3.3 Droplet creaming

The density difference between the oil droplets and the continuous phase results in a buoyancy force that induces the rising of the droplets, which is also known as creaming. The characteristic time for droplet creaming was defined as the time required for an oil droplet within a swarm of droplets to rise with a certain creaming velocity ($v_{d,swarm}$) over the height of the column (H), as in Equation (6).

$$\tau_{crm} = \frac{H}{v_{d,swarm}}. \tag{6}$$

To obtain the velocity of droplets in a swarm, we first need to calculate the creaming velocity of a single droplet (v_d), which depends on the density difference between oil and aqueous phase (ρ_{aq}), droplet diameter, drag coefficient (C_D) and gravitational acceleration constant as given by Equation (7) [26].

$$v_d = \sqrt{\frac{4g\left(\rho_{aq} - \rho_{oil}\right)d_d}{3C_D\rho_w}}. \tag{7}$$

An initial guess for the creaming velocity can be used to calculate the Reynolds number (Re):

$$Re = \frac{v_d \rho_{aq} d_d}{\eta}. \tag{8}$$

An estimate of the drag coefficient can be determined, using Equation (9) [26].

$$C_D = \frac{24}{Re} + 3Re^{-1/2} + 0.34 \tag{9}$$

By an iterative approach, Equations (7) to (9) are used to determine the creaming velocity of a single droplet. Since high oil fractions are considered, hindered creaming of the oil droplets will occur and droplets should be considered to rise as a swarm instead of single droplets. The Richardson-Zaki equation can be used to correct the droplet creaming velocity for this effect [27]:

$$v_{d,swarm} = v_d(1-\phi_{oil})^n. \tag{10}$$

In this equation, n is a parameter that is dependent on the Reynolds number, droplet diameter, and vessel diameter [28].

4.2.3.4 Mixing

Mixing is the subprocess considered to compete with the droplet creaming. When mixing is too strong, the droplets will move with the bulk liquid instead of creaming to the top of the reactor. The mixing time in a bubble column can be determined by making an

estimation of the circulation time of the liquid in such a column. Groen developed the following correlations for describing the characteristic time of mixing (τ_{mix}) in different flow regimes in a bubble column as function of volumetric power input, bubble diameter, column diameter (D) and the column height (H) [29]. For superficial gas velocities lower than 4 cm/s, the bubble flow is steady and well distributed over the whole reactor, resulting in a homogeneous regime [29]. In this flow regime, the mixing time can be estimated as:

$$\tau_{mix,\mathrm{hom}} = 0.008\left(\frac{D^6}{d_b^4\, e_v/\rho_l}\right)^{1/3}\left(\frac{H}{D}\right)^2 \tag{11}$$

For superficial gas velocities higher than 4 cm/s, the heterogeneous mixing regime is obtained, in which the mixing caused by the bubbles has a more irregular, turbulent pattern [29]. In this case, a distinction must be made for low and high aspect ratio bubble columns. For a bubble column with an aspect ratio between 1 and 3, the mixing time can be described as

$$\tau_{mix,het} = 16\left(\frac{D^2}{e_v/\rho_l}\right)^{1/3} \tag{12}$$

When the aspect ratio of the column is higher than three, Equation (13) gives the characteristic mixing time:

$$\tau_{mix} = 1.496\left(\frac{D^2}{e_v/\rho_l}\right)^{1/3}\left(\frac{H}{D}\right)^2 \tag{13}$$

4.3 Base case definition

The base case for the regime analysis is a continuous fermentation in a bubble column, in which the mixing is provided by gas bubbles. Bubble column bioreactors are often chosen for large scale processes, since they do not require mechanical power input for mixing. The performed regime analysis aims at exploring the possibility of the integration of oil recovery in a fermentation process. Therefore, the analysis is focused on the effects of process conditions on the droplet coalescence and creaming steps, aiming at achieving conditions in

which these steps are enabled. This results in process conditions requirements for the integration of the separation with the fermentation, which are in the end compared to conditions required for fermentations (i.e., mixing requirements), without going into detail in specific fermentation related subprocesses (e.g., substrate uptake, oxygen uptake).

Both bacteria and yeast have been genetically modified to produce advanced biofuels, but yeast cells are generally considered as the most robust microorganisms for industrial fermentation [4]. Therefore the yeast *S. cerevisiae* has been chosen as microorganism for this base case. Current advanced biofuel producing microorganisms operate in aerobic conditions, as metabolic pathways require cofactors regeneration by respiration [30]. However, research for microbial production of bulk chemicals is directed at developing anaerobic metabolic pathways to increase metabolic yields, and potentially decreasing production costs [31]. The regime analysis presented in this study can be applied for both aerobic and anaerobic cases, since gas composition has no effect on mixing. The magnitude of the gas flow can be controlled by the gas inflow (e.g., by a gas recycle).

For the regime analysis, the effect of process parameters and process scale on the characteristic times were evaluated over the specified range, while keeping all other values at their default values. Table 1 summarises the complete set of model parameters values used in the regime analysis, unless specified differently (e.g., when a parameter is varied over a range).

Table 1. Base case parameter values and ranges

Parameter	Base case	Range
V_r (m^3)	1	10^{-2}-10^3
H/D (-)	4	1-15
σ_{oil} (mN/m)	52	
ρ_{oil} (kg/m^3)	776	
ϕ_{oil} (-)	0.1	0-0.4
v_{gs} (cm/s)	5	1-10
d_b (mm)	5	
η_w (mPa·s)	1	
c_{SAC} (mg/L)	0.4	0.1-0.4
Γ(mg/m^2)	3	1-3
d_d	d_{max}	d_{min} - d_{max}

The reactor scale, geometry and superficial gas velocity are the main parameters that determine the reactor design and influence the characteristic times of the subprocesses. The column geometry is determined by the reactor volume (V_r) and aspect ratio (H/D). The reactor volume is varied over the complete range from 10 L to 1000 m^3, with a default value of 1000 L. The aspect ratio is varied from 1 to 15, with a default value of 4.

Mixing is provided by the flow of gas bubbles through the column. The parameter describing the gas flow in a bubble column is the superficial gas velocity. The default value used in the analysis is 5 cm/s and it is varied within a range up to 10 cm/s [32]. Bubbles are assumed to have a diameter (d_b) of 5mm, which is a typical bubble diameter in bubble columns [33].

The physical properties of the drop-in biofuel (interfacial tension, σ_{oil}, and density, ρ_{oil}) are taken similar to those of hexadecane, which is the most abundant component in diesel fuels [34]. The highest applicable oil fraction in biotechnological processes is considered to be 40%, at higher values severe mass transfer limitations can occur locally [35]. The default volumetric oil fraction was 10% and a range up to 40% is evaluated.

The physical properties of the bulk phase, the continuous aqueous phase, are taken similar to those of water. Fermentations at large scale are typically performed at high cell density (50-100 g_{cell}/L). The presence of cells increases the viscosity of the bulk phase. However, for that range of cell concentration viscosity remains in the same order of magnitude of water [36].

Considering the stabilisation of the droplets, the assumption is made that the product is secreted without any stabilising components present at the O/W interface of the initial droplets. The droplets can be stabilised against coalescence by the adsorption of surface active components. One of the best known SACs released by *Saccharomyces cerevisiae* are mannoproteins. These components are potent emulsifiers, being readily released by the microorganisms [37, 38]. In a batch experiment, 0.2 mg of mannoproteins per gram of cell dry weight per hour were released [39]. A continuous process would result in lower concentrations of the surface active component and a default value of 0.4 mg/L was used, the

evaluated range was between 0.1 and 0.4 mg/L. The amount of protein adsorbing at the oil/water interface is given by the surface excess concentration. For different oil/water/protein combinations, the surface excess concentration ranges between 1.5 and 3 mg/m^2 [40, 41], the default value was 3 mg/m^2 and the range of 1 to 3 mg/m^2 was evaluated.

The parameter that comes forward in three of the four subprocesses is the droplet size, which is determined by a combination of process conditions and oil phase properties. This study considers two scenarios with different droplet sizes: d_{min} and d_{max}.

The calculation of minimum and maximum stable droplet size was based on the turbulence in the reactor. Walstra et al. gave Equation (14) for the maximum droplet size (d_{max}) stable to breakup, defined by the interfacial tension (σ_{oil}), the overall liquid density (ρ_l) and volumetric power input (e_v).

$$d_{max} = \left(\frac{\sigma_{oil}^{\ 3}}{\rho_l e_v^{\ 2}} \right)^{1/5} \tag{14}$$

This is the maximum size of the droplets that do not breakup anymore due to the shear forces caused by turbulence. This approach takes the effects of hydrodynamic interactions on droplet collisions into account, which are directly related to the mixing of the droplet (by the power input). This relation, based on the degree of turbulence in the system, was developed for dispersions under isentropic conditions, but also appeared to be valid for lower Reynolds numbers [42, 43].

An expression for the minimum droplet diameter (d_{min}) was developed by Thomas [44], by relating the forces in a turbulent mixture to the force and contact time of two droplets. When the contact time exceeds the time required for film drainage, dependent on the critical film thickness, coalescence takes place. From this condition, Equation (15) was derived, relating d_{min} to the continuous phase viscosity (η_w), the critical film thickness for coalescence (h), interfacial tension (σ_{oil}), and volumetric power input (e_v):

$$d_{min} \sim \frac{\sigma_{oil}^{\ 2} h^2}{\eta_w e_v}. \tag{15}$$

Droplets below this minimum droplet size will have a high chance of coalescence and therefore exist for only a short time. By experimental work of Liu and Li, Equation (15) could be further developed to

$$d_{min} = \left(\frac{\sigma_{oil}^{1.38} B^{0.46} \rho_l^{0.05}}{0.072 \eta_w e_v^{0.89}} \right)^{\frac{1}{3.11}}, \tag{16}$$

eliminating any empirical parameters specifically dependent on the system. It includes the continuous phase density and the van der Waals constant (B =10^{-28} Jm) as a measure for the intermolecular forces [21].

4.4 Results and discussion

The starting points for all characteristic time calculations were the minimum and maximum droplet diameters, which are determined by the power input provided by the gas bubbles. Figure 3 shows the minimum and maximum stable droplet diameters as a function of the superficial gas velocity, calculated using Equations (14) and (16). The largest stable droplets are in the order of millimetres, the minimum droplet diameter was about an order of magnitude lower and both decrease with increasing superficial gas velocity.

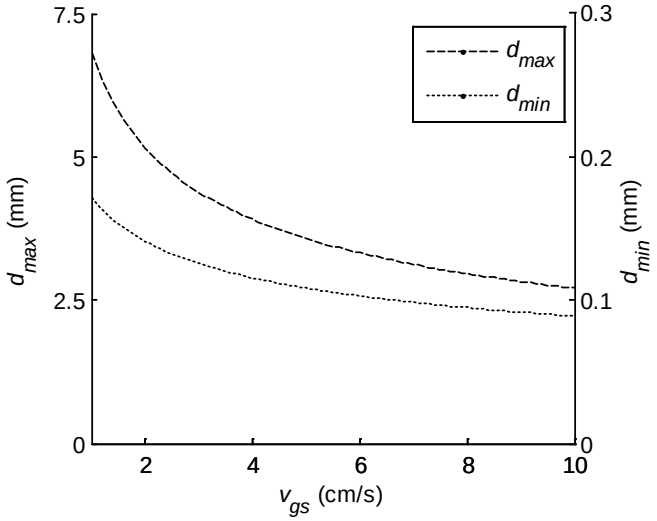

Figure 3. The minimum and maximum droplet diameters at varying superficial gas velocities (V_r = 1m^3, H/D = 4, c_{SAC} = 0.4 mg/L, ϕ_{oil} = 0.1).

4.4.1 Coalescence vs SAC adsorption

The first step in the recovery process is droplet growth by coalescence. Figure 4 compares the characteristic times for coalescence and stabilisation by SAC adsorption for the droplets with the minimum size, showing that coalescence is three orders of magnitude faster than stabilisation of those droplets. This indicates that no emulsification problems are expected for the smallest droplets. Since droplet coalescence slows down with increasing droplet size, coalescence of droplets smaller than d_{max} will be faster than for droplets of size d_{max}. So when coalescence of the droplets with the maximum size is not limiting, coalescence of droplets smaller than this maximum will also occur. However, for the largest stable droplets the characteristic times of SAC adsorption and coalescence are in the same order of magnitude (Figure 5). At a superficial gas velocity higher than 2 cm/s, coalescence is calculated to be faster than adsorption but since there is no order of magnitude difference between the characteristic times, this only indicates that coalescence might be promoted over emulsification with increasing superficial gas velocity. Since the model shows that droplet stabilisation of the smallest droplets is of no concern, from here on we will focus on coalescence of the large droplets.

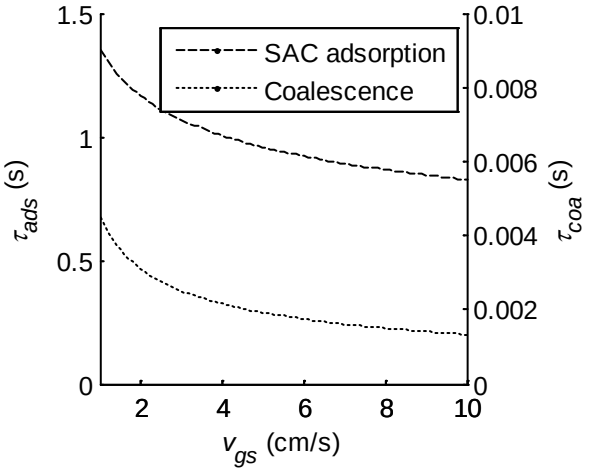

Figure 4. Characteristic times of SAC adsorption and coalescence for d_{min} as a function of superficial gas velocity (V_r = 1m^3, H/D = 4, c_{SAC} = 0.4 mg/L, ϕ_{oil} = 0.1).

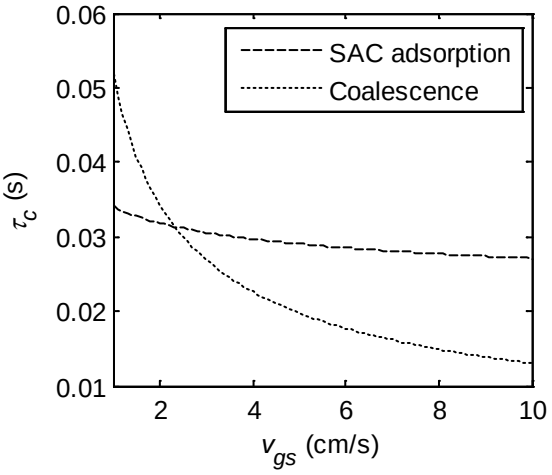

Figure 5. Characteristic times (τ_c) of SAC adsorption and coalescence for d_{max} as a function of superficial gas velocity (V_r = 1m^3, H/D = 4, c_{SAC} = 0.4 mg/L, ϕ_{oil} = 0.1).

As Equations (3) and (5) show, SAC concentration, oil fraction, and surface excess concentration also influence the characteristic times. The former two are in turn influenced by the process conditions, while the latter is a physicochemical property of the emulsifier for the dispersion and hence, is scale independent. When the process operates at high oil fraction, coalescence is promoted (Figure 6). Increasing the oil fraction should preferably be achieved by improved microorganism productivity instead of by operating at higher cell concentrations, since increased cell concentrations will likely lead to higher concentrations of SACs, which in turn enhance droplet stabilisation (Figure 7).

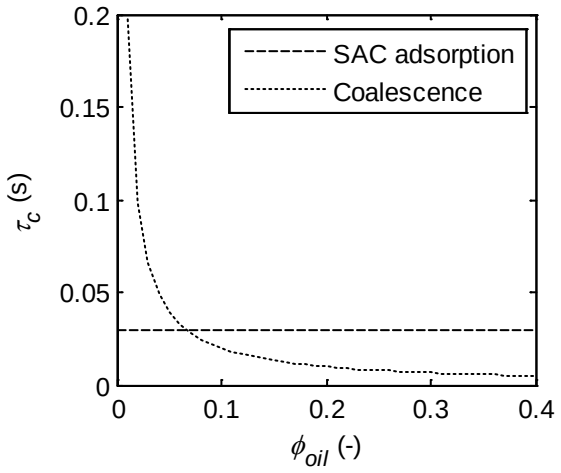

Figure 6. Characteristic times (τ_c) of SAC adsorption and coalescence for d_{max} as a function of volumetric oil fraction (V_r = 1m³, H/D = 4, v_{gs} = 5 cm/s, c_{SAC} = 0.4 mg/L).

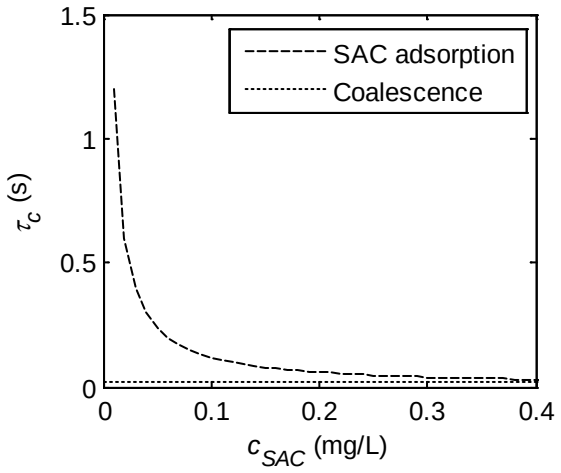

Figure 7. Characteristic times (τ_c) of SAC adsorption and coalescence for d_{max} as a function of SAC concentration (V_r = 1m³, H/D = 4, v_{gs} = 5 cm/s, ϕ_{oil} = 0.1).

The surface excess concentration of the emulsifier describes the minimum amount of emulsifier required to cover the droplet surface. The exact value is dependent on the type of emulsifier and composition of the aqueous and organic phase. The influence of the surface excess concentration on the stabilisation characteristic time is limited. For the considered surface excess range, 1.5-3 mg/m², the order of magnitude of stabilisation remains the same.

In all previous comparisons of the characteristic times for coalescence and emulsification, none of the parameter variations results in one process being conclusively faster than the other. However, when the process is operated at the upper boundary of the oil

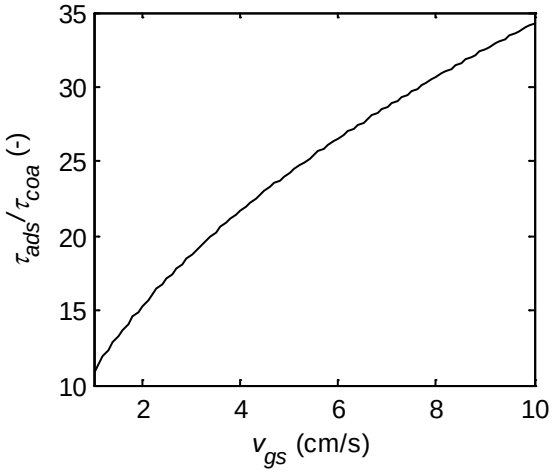

Figure 8. Coalescence is an order of magnitude faster than droplet stabilisation (V_r = 1m^3, H/D = 4, c_{SAC} = 0.1 mg/L, ϕ_{oil} = 0.4).

fraction (0.4) and a low SAC concentration is achieved (0.1 mg/L), an order of magnitude difference between the characteristic times for coalescence and SAC adsorption can be reached, as shown by the ratio of characteristic times in Figure 8. In such conditions, droplet growth by coalescence readily occurs and the droplets might be recovered by gravity separation.

4.4.2 Droplet creaming vs mixing

To facilitate droplet creaming, the characteristic time for creaming must be lower than that for mixing. The superficial gas velocity, determining the power input, influences both creaming and mixing (Figure 9). As mentioned before, two mixing regimes are distinguished: the homogeneous and heterogeneous regime. In the homogeneous flow regime, mixing is gentle and the droplet creaming will occur (results not shown). However, the limited mixing in that case is likely to be insufficient for the fermentation process and therefore we only consider superficial gas velocities in the heterogeneous regime (v_{Gs} > 4 cm/s). When the superficial gas velocity is increased and the heterogeneous regime is reached, τ_{mix} decreases below τ_{crm}. However, there is no order of magnitude difference between them, so none of the subprocesses is conclusively faster than the other.

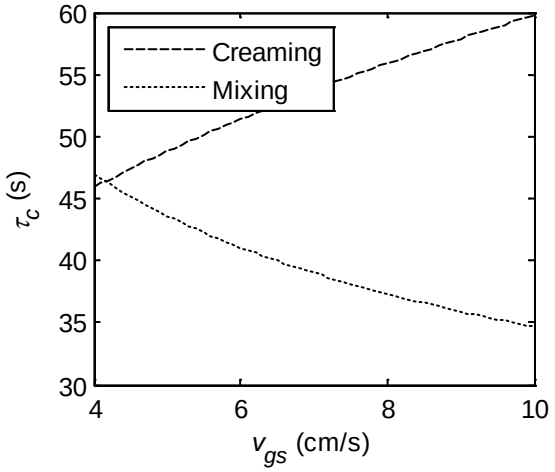

Figure 9. Characteristic times (τ_c) of creaming and mixing for d_{max} as function of superficial gas velocity in the heterogeneous regime (V_r = 1m^3, H/D = 4, ϕ_{oil} = 0.1).

Furthermore, τ_{mix} is strongly influenced by the reactor geometry of the bubble column (both aspect ratio and volume). Only at extreme aspect ratios, an effect on the mixing time can be expected (Figure 10). The influence of the aspect ratio is limited in the lower range and only when it exceeds a value of 3, the τ_{mix} increases. This sudden change is explained by the regimes existing below and above an aspect ratio of 3, as shown in the section describing the mixing time. The mixing and creaming characteristic times are influenced similarly when the reactor volume is increased. Both subprocesses slow down with increasing scale, but droplet creaming is affected stronger than mixing (Figure 11). This suggests that integrated gravity separation will become more difficult at large scale.

This also shows from the ratio of characteristic times at the optimal conditions (Figure 12). When operating at the low end of the heterogeneous regime (5 cm/s) and at extreme aspect ratio (15), the τ_{crm} is close to an order of magnitude lower than the τ_{mix} at lab scale volumes (1 L). But when the reactor volume is increased, this difference is rapidly lost, showing that scale up will cause recovery difficulties. Furthermore, the mixing time at large scale reactors under these conditions is likely to be insufficient for facilitating the fermentation. For example, in lab scale stirred vessel and bubble column the mixing times will be similar [45]. When the reactor size is increased, mixing times will start to differ. In a 20 m^3

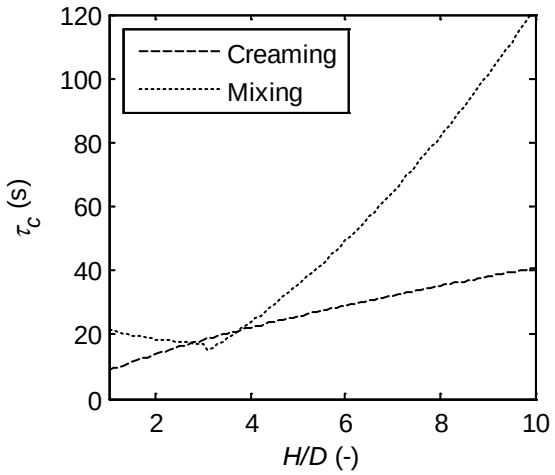

Figure 10. Characteristic times (τ_c) of creaming and mixing for d_{max} as function of aspect ratio (V_r = 1m^3, v_{gs} = 5 cm/s).

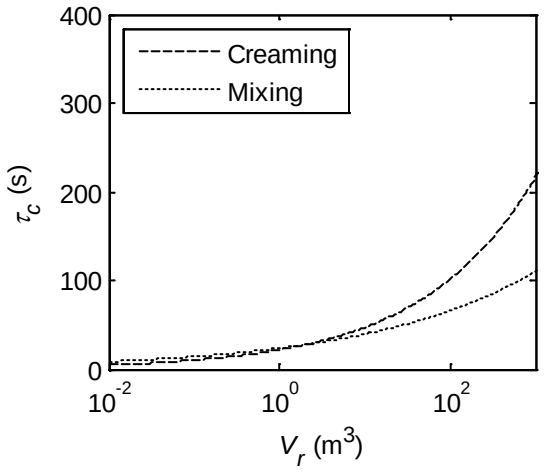

Figure 11. Characteristic times (τ_c) of creaming and mixing for d_{max} as function of reactor volume (H/D = 4, v_{gs} = 5 cm/s).

reactor, mixing times of approximately 50 s can be achieved for stirred vessels [46] and 150 s for high aspect ratio bubble columns (Equation (13)).

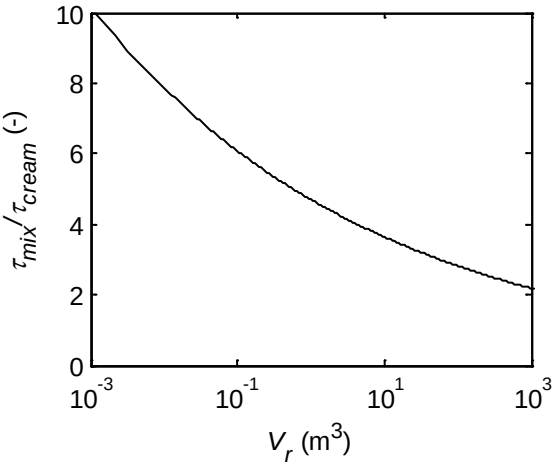

Figure 12. Ratio characteristic times of mixing and creaming for d_{max} (v_{gs} = 5 cm/s, H/D = 15).

4.5 Conclusions

Process integration can contribute to lowering the production costs of advanced biofuels by decreasing the equipment costs. Furthermore, such integration might enable a continuous process configuration and cell reuse, lowering substrate consumption for cell production and possibly lowering the amount of SACs. The most straightforward case of

integration is combining production and gravity separation in a single bubble column. The possibility of this integration was studied by regime analysis. This tool is conventionally used to study a subprocess sequence to determine the rate limiting step, but here was used to identify whether adverse subprocesses (such as mixing and droplet stabilisation by SAC adsorption) would hinder the integration of advanced biofuel production and separation. Parameter variation was used to determine whether operating conditions and reactor geometry can be chosen in a way that the separation can take place, and these conditions had to be compared to conditions required for fermentation from laboratory to production scale.

The first step in the oil recovery, droplet growth by coalescence, is not directly scale dependent. The regime analysis showed the importance of limiting the SAC concentration and obtaining a high oil concentration for coalescence, which both can be related to the microorganism performance. From the perspective of the integrated process, improving the microbial productivity is preferred over increasing the overall productivity by operating at high cell concentrations, because the latter will likely result in increased SAC concentrations. Furthermore, taking the release of SACs by the microorganism into account during strain development could also contribute to enhanced droplet growth. When a high oil fraction is reached and the SAC concentration is limited, droplet growth by coalescence takes place and droplet stabilisation by SACs will not be a problem. This is valid under the earlier made assumption that the secreted product is not initially stabilised. When this is the case, the coalescence subprocess should be described in a different way. In this chapter, the collision frequency is used to obtain an expression for the characteristic time of coalescence, but when the droplets are formed already stabilised, a characteristic time based on the rupture of the stabilising film would be required.

For the next step in the oil recovery, droplet creaming, gravity separation is the cheapest process option. The regime analysis compares the characteristic times for creaming with mixing. When mixing is too strong, the droplets will be back-mixed instead of separated. The analysis showed that it is possible to achieve conditions at lab scale in which droplet creaming is faster than mixing, with a comparable mixing time in the bubble column as in a

lab scale stirred vessel. However, at increased production scale, the limited superficial gas velocities and extreme aspect ratios required to promote droplet creaming over mixing, cause that droplet creaming cannot be promoted while maintaining suitable fermentation conditions. So for large scale integration, the integration of production and separation might only be achieved in a reactor in which two sections with different process conditions (especially superficial gas velocity) are combined, one section for fermentation and one for separation.

Challenges in such a design are to control the hydrodynamics in the different sections and to couple them, while maintaining the microbial cell performance. The design of such an reactor and experimental testing of the scale-up effects are the next steps to be taken in developing low-cost process technology, which in the end is one of the aspects required for economically feasible production of advanced biofuels.

Acknowledgements

This work was partly carried out within the BE-Basic R&D Program, which was granted a FES subsidy from the Dutch Ministry of Economic affairs, agriculture and innovation (EL&I).

Nomenclature

Roman

B	Van Der Waals parameter
C_D	Drag coefficient
D	Diameter
H	Height
Re	Reynolds number
V	Volume
c	Concentration
e	Power input
d	Particle diameter
g	Gravitational constant
h	Critical film thickness
n	Richardson-Zaki parameter
v	Velocity

Greek

Γ	Surface excess concentration
η	Viscosity
ρ	Density
σ	Interfacial tension
τ	Characteristic time
ϕ	Volume fraction

Subscripts

v	Volume specific
b	Bubble
d	Droplet
l	Liquid
r	Reactor
aq	Aqueous
oil	Oil
ads	Adsorption
coa	Coalescence
crm	Creaming
mix	Mixing
max	Maximum
min	Minumum
SAC	Surface active component

References

1. Rude, M.A. and A. Schirmer, *New microbial fuels: a biotech perspective.* Curr. Opin. Biotechnol., 2009. 12(3): p. 274-281.
2. Schirmer, A., et al., *Microbial biosynthesis of alkanes* Science, 2010. 329: p. 559-562.
3. Renniger, N.S. and D.J. McPhee, *Fuel compositions comprising farnesane and farnesane derivatives and method of making and using same*. 2008, Amyris Biotechnologies, Inc.: United States.
4. Westfall, P.J. and T.S. Gardner, *Industrial fermentation of renewable diesel fuels.* Curr. Opin. Biotech., 2011. 22(3): p. 344-350.
5. Bullis, K. *Why Amyris is focusing on moisturizers, not fuel, for now*. MIT Technology Review, 2012.
6. Cuellar, M.C., J.J. Heijnen, and L.A.M. van der Wielen, *Large-scale production of diesel-like biofuels - process design as an inherent part of microorganism development.* Biotechnol. J., 2013. 8(6): p. 682-689.
7. Dunlop, M.J., et al., *Engineering microbial biofuel tolerance and export using efflux pumps.* Mol. Syst. Biol., 2011. 7.
8. Heeres, A.S., et al., *Microbial advanced biofuels production: overcoming emulsification challenges for large-scale operation.* Trends Biotechnol. , 2014. 32(4): p. 221-229.
9. Tabur, P. and G. Dorin, *Method for purifying bio-organic compounds from fermentation broth containing surfactants by temperature-induced phase inversion*. US Patent 20120040396, 2012.
10. Amyris *Amyris's first production facility commisioned*. 2011.
11. Sweere, A.P.J., K.C.A.M. Luyben, and N.W.F. Kossen, *Regime analysis and scale-down: Tools to investigate the performance of bioreactors.* Enzyme Microb. Tech., 1987. 9(7): p. 386-398.
12. Johnstone, R.E. and M.W. Thring, *Pilot plants, models, and scale-up methods in chemical engineering*. 1957: McGraw-Hill.
13. Oosterhuis, N.M.G., *Scale-up of bioreactors: A scale-down approach*, in *Biotechnology*. 1984, Technical University Delft: Delft.
14. Huber, T., et al., *Design and scale up of a reactor for microbial desulphurization of coal: A regime analysis.* Innov. Biotechnol. , 1984. 20: p. 179-189.
15. Schoutens, G.H., *Modelling and design of animmobilized cell process for solvent production*, in *Applied Sciences*. 1986, Technical University Delft: Delft.
16. Law, H.E.M., et al., *Process limitations in a whole-cell catalysed oxidation: Sensitivity analysis.* Chem. Eng. Sci., 2006. 61(20): p. 6646-6652.
17. Melgarejo-Torres, R., et al., *Regime analysis of a Baeyer–Villiger bioconversion in a three-phase (air–water–ionic liquid) stirred tank bioreactor.* Biochem. Eng. J., 2011. 58: p. 87-95.

18. Titchener-Hooker, N.J., P. Dunnill, and M. Hoare, *Micro biochemical engineering to accelerate the design of industrial-scale downstream processes for biopharmaceutical proteins.* Biotechnol. Bioeng., 2008. 100(3): p. 473-487.
19. Garcia-Ochoa, F. and E. Gomez, *Bioreactor scale-up and oxygen transfer rate in microbial processes: An overview.* Biotech. Adv., 2009. 27(2): p. 153-176.
20. Frising, T., C. Noïk, and C. Dalmazzone, *The liquid/liquid sedimentation process: from droplet coalescence to technologically enhanced water/oil emulsion gravity separators: a review.* J. Dispers. Sci. Technol. , 2006. 27: p. 1035-1057.
21. Liu, S. and D. Li, *Drop coalescence in turbulent dispersions.* Chem. Eng. Sci., 1999. 54: p. 5667-5675.
22. Walstra, P., *Principles of emulsion formation.* Chem. Eng. Sci., 1993. 48(2): p. 333-349.
23. Sánchez Pérez, J.A., et al., *Shear rate in stirred tank and bubble column bioreactors.* Chem. Eng. J., 2006. 124(1–3): p. 1-5.
24. Deshiikan, S.R. and K.D. Papadopoulos, *London-van der Waals and EDL effects in the coalescence of oil drops: II. ionic strength and pH effects.* J. Colloid Interface Sci., 1995. 174(2): p. 313-318.
25. Tobin, T. and D. Ramkrishna, *Coalescence of charged droplets in agitated liquid-liquid dispersions.* AIChE J., 1992. 38(8): p. 1199-1205.
26. Reynolds, T.D. and P.A. Richards, *Sedimentation*, in *Unit operations and processes in environmental engineering*. 1996, CL Engineering. p. 219-283.
27. Walstra, P., *Emulson Stability*, in *Encyclopedia of Emulsion Technology. Vol. 4*, P. Dekker, Editor. 1996, Marcel Dekker, Inc.: New York.
28. Janssen, L.P.B.M. and M.M.C.G. Warmoeskerken, *Transport phenomena data companion*. 2001, Delft: VSSD.
29. Groen, D.J., *Macromixing in bioreactors*. 1994, Delft University of Technology: Delft.
30. Ladygina, N., E.G. Dedyukhina, and M.B. Vainshtein, *A review on microbial synthesis of hydrocarbons.* Process Biochem., 2006. 41(5): p. 1001-1014.
31. Weusthuis, R.A., et al., *Microbial production of bulk chemicals: development of anaerobic processes.* Trends Biotechnol., 2011. 29(4): p. 153-158.
32. Almeida, J.R.M., et al., *Increased tolerance and conversion of inhibitors in lignocellulosic hydrolysates by Saccharomyces cerevisiae.* J. Chem. Technol. Biotechnol., 2007. 82(4): p. 340-349.
33. Heijnen, J.J. and K. Van't Riet, *Mass transfer, mixing and heat transfer phenomena in low viscosity bubble column reactors.* Chem. Eng. J., 1984. 28(2): p. B21-B42.
34. Bacha, J., J. Freel, and A. Gibbs, *Diesel Fuels Technical Review*. 2007, Chevron Products Company.
35. Cabral, J.M.S., M. Mota, and J. Tramper, *Multiphase Bioreactor Design*. 2001: CRC press.
36. Reuß, M., et al., *Viscosity of yeast suspensions.* Eur. J. Appl. Microbiol. Biotechnol., 1979. 8(3): p. 167-175.

37. Cameron, D.R., D.G. Cooper, and R.J. Neufeld, *The mannoprotein of Saccharomyces cerevisiae is an effective bioemulsifier.* Appl. Environ. Microbiol., 1988. 54: p. 1420-1425.
38. Cameron, D.R., *Identification and characterisation of mannoprotein emulsifier from Bakers yeast*, in *Department of Biotechnology*. 1992, McGill University: Montreal, Quebec, Canada.
39. Dupin, I.V.S., et al., *Saccharomyces cerevisiae mannoproteins that protect wine from protein haze: their release during fermentation and lees contact and a proposal for their mechanism of action.* J. Agric. Food Chem. , 2000. 48(8): p. 3098-3105.
40. Bos, M.A. and T. van Vliet, *Interfacial rheological properties of adsorbed protein layers and surfactants: a review.* Adv. Colloid Interface Sci., 2001. 91(3): p. 437-471.
41. Tcholakova, S., et al., *Coalescence in β-Lactoglobulin-Stabilized Emulsions: Effects of Protein Adsorption and Drop Size.* Langmuir, 2002. 18(23): p. 8960-8971.
42. Levich, V.G., *Physicochemical Hydrodynamics*. 1962. ISBN: 978-0136744405, Englewood Cliffs: Prentice-Hall. 395-471.
43. Walstra, P. and P.E.A. Smulders, *Emulsion formation*, in *Modern aspects of emulsion science*, B.P. Binks, Editor. 1998, The Royal Socielety of Chemistry: Cambridge. p. 58-74.
44. Thomas, R.M., *Bubble coalescence in turbulent flows.* Int. J. Multiph. Flow, 1981. 7: p. 719-717.
45. Amanullah, A., B.C. Buckland, and A.W. Nienow, *Mixing in the fermentation and cell culture industries*, in *Handbook of industrial mixing: science and practice*, E.L. Paul, V. Atiemo-Obeng, and S.M. Kresta, Editors. 2004, John Wiley & Sons: New Jersey. p. 1071-1110.
46. Hewitt, C.J. and A.W. Nienow, *The scale-up of microbial batch and fed-batch fermentation processes.* Adv. Appl. Microbiol., 2007. 62: p. 105-35.

Chapter 5. Gas bubble induced oil recovery from emulsions stabilised by yeast components

Abstract

In the search of advanced biofuels, microorganisms have been developed that make and secrete long chain hydrocarbons, resulting in a four phase fermentation mixture (cells, aqueous liquid, organic product, and (produced) gas). The product immiscibility offers the potential for a straightforward recovery, but surface active components in the fermentation broth emulsify the product droplets. In the current process, multiple centrifugation steps with chemical de-emulsifiers are used for product recovery, posing economic and environmental burdens on the process. In this paper, an alternative separation method is presented, in which gas bubbles induce coalescence of the emulsified oil droplets, obtaining a continuous oil layer. The oil layer formation was influenced by the gas flow rate, nozzle diameter, column geometry, and emulsion properties, offering the possibility for process optimisation. The developed gas bubble induced oil recovery method does not require chemical additives, uses mild process conditions, and can potentially be integrated with the fermentation, giving a low cost alternative for the conventional recovery method. Using this technology, another step can be made towards economically feasible production of advanced biofuels.

Part of this chapter has been submitted for publication as:

A.S. Heeres, J.J. Heijnen, L.A.M. van der Wielen, M.C. Cuellar, *Gas bubble induced oil recovery from emulsions stabilised by yeast components.*

5.1 Introduction

Synthetic biology has opened the way to microbial production of alkanes or isoprenoids, molecules that are more similar to liquid fossil fuels and have enhanced fuel properties compared to conventional alcoholic biofuels [1-3]. An example is farnesene ($C_{15}H_{24}$), an isoprenoid produced by an engineered yeast strain developed by Amyris. The final product after hydrogenation is farnesane, which is currently being produced at commercial scale and has been certified for diesel and jet fuel blends up to 30% and 10%, respectively (www.amyris.com). Furthermore, progress is being made in the microbial production of alkanes using engineered *Escherichia coli*, which has been performed at pilot scale [4] and is led by REG life sciences (http://www.reglifesciences.com/). In these fermentations, the water immiscible product is secreted into the fermentation broth and dispersed product droplets are formed [5]. To obtain the final product, these droplets will have to be recovered as a continuous oil phase. However, the presence of surface active components in the fermentation broth, originating from the feedstock and the microorganism, hinders coalescence and usually results in formation of emulsions, making product recovery challenging [6, 7]. In the current production of farnesene, these challenges are overcome through multiple centrifugation steps in combination with chemical de-emulsifiers [8]. This approach has a negative effect on cell viability, making complete cell recycle impossible and adding costs and an environmental burden to the process.

Similar challenges are encountered in other fermentation processes with a second liquid phase (product or substrate) and in bioconversions [9, 10]. In the latter, an organic auxiliary phase is added that is used as a sink for the substrate or product, to lower any toxic effects [11]. The proteins released by cells have been shown to adsorb at the interface of the organic droplets, making for instance separation by centrifugation inefficient. Several alternative methods have been studied to overcome the emulsification challenges, such as application of super critical carbon dioxide to denature proteins, addition of chemical de-emulsifiers, or application of enzymes that degrade the surface active components [12-14].

However, the costs associated with these methods make them less suitable for production of low value products, such as the above mentioned advanced biofuels.

To achieve low separation costs, methods requiring additives or expensive process steps should be avoided. Additionally, integration of the product recovery with the fermentation could contribute to lower production costs by reducing equipment costs, by enabling a cell recycle to reduce the substrate requirements, and by lowering the stability of the emulsion through continuous product removal. To be able to recycle the cells, harsh process conditions or toxic additives should be avoided to maintain cell viability. Taking these constraints into account, the options for product recovery become limited.

A method that could fit the requirements is gas flotation. This is a well-known separation method in which gas bubbles are used to remove fine particles or droplets from a dilute aqueous suspension or emulsion. In wastewater treatment of oily waste streams, usually containing mass percentages of oil below 0.1 % and a droplets with a typical size of 1-50 μm [15, 16], this technique is applied to remove emulsified oil droplets that are difficult to separate by gravity. The interaction between oil droplets and gas bubbles is crucial for flotation, because droplets have to attach to the gas bubbles, forming a complex that has a lower overall density and therefore a higher rise velocity [17]. The velocity difference between gas bubbles and oil droplets should not be too large to achieve efficient attachment, leading to a need of very small bubbles. Therefore, different methods have been developed to introduce the bubbles in the system for oil removal from waste water: dissolved air flotation generates bubbles between 30 to 100 μm and jet flotation between 100 to 600 μm [15]. With these small bubbles, the rise of small oil droplets can be accelerated to enhance the separation and the result is clarified water and a concentrated oil/water emulsion.

In multiphase fermentations, in which gas is produced or sparged, the typical oil fractions and droplet sizes are much larger and the organic phase remains dispersed in the aqueous phase due to mixing in the system. When the mixing is stopped, the dispersed oil droplets rise due to the buoyancy force and a concentrated emulsion is formed, which is stabilised by the surface active components from the microorganism and feedstock [18].

There are no reports on the droplet size distributions in advanced biofuel fermentations, but it can be expected that in the same way as for other multiphase fermentations the main the main challenge is not to increase the phase separation of the oil droplets, but to convert the oil droplets in a continuous oil layer by coalescence.

In this project, several separation methods were explored (Appendix A) and in this paper, we present a novel method to convert emulsified oil droplets into an oil layer using gas bubbles. This method avoids the need of additives and harsh process conditions, so fits with the previously set requirements. First, we will introduce the method of recovering liquid oil from an emulsion using gas bubbles in more detail. Next, the effects of process parameters and emulsion properties on this separation method will be evaluated and these results will be used to discuss the underlying physical mechanisms and crucial process parameters for application of the separation method at a larger scale.

5.2 Materials and Methods

5.2.1 Materials

A model multiphase mixture was used in the experiments to study the emulsion behaviour and test the separation method. This mixture was prepared using MilliQ water (18.2 MΩ, MilliPore systems) and baker's yeast (Bruggemans compressed yeast, containing 33 % dry biomass) to create the continuous aqueous phase. There were no nutrients added so the yeast was starved and metabolism was negligible. Hexadecane (Sigma-Aldrich, ReagentPlus) was used as the dispersed phase, which was coloured red using Oil Red O dye (Sigma-Aldrich) to have an absorbance of 1.4 at 515 nm (between 0 and 1.4 the absorbance was linearly correlated to the concentration). The gas phase in the columns was compressed air.

5.2.2 Emulsion preparation

Two types of mixtures were used in the experiment, with a difference in the composition in the aqueous phase. Both mixtures had a hexadecane volume fraction of 10 %, which is close to the highest reported product titer in farnesene production (105 g/L) [19].

The yeast emulsions had a yeast concentration of 10 g/L (dry matter), which is in the range of what would be expected from the process reaction for a good performing strain (see Appendix B).

In the first type of mixture, baker's yeast cells (53 g, wet) were mixed with MilliQ water (1387 g) and hexadecane (160 mL, 124 g) for three hours at a stirring rate of 900 rpm in a 2 L stirred vessel equipped with baffles (P&H, inner diameter of 120 mm) and a six bladed Rushton turbine (diameter of 45 mm), which corresponds to a power input of approximately 5.7 W/L. During mixing, the vessel was open to air and the temperature was maintained at 25 °C by an external cryostat (Lauda Ecoline E300) connected to the reactor. The pH of this mixture was not controlled but it was measured to be 4.3 at the end of the stirring period (Metrohm 691 pH meter).

The second type of mixture used in the experiments had an aqueous phase based on the supernatant of a yeast suspension, so no cells were present anymore. This eliminated biological variations in the mixture due to the microorganisms and assured constant properties of the emulsion. This supernatant was prepared by mixing the baker´s yeast (320 g, wet) and MilliQ water (1200 g) in the same stirred vessel as used for the emulsion preparation at 1100 rpm for 3 h, while maintaining the temperature at 25 °C. Afterwards, the whole cell suspension was centrifuged at 20,000 rpm for 20 minutes (Sorvall RC 5B plus) and the resulting supernatant was stored frozen at -20 °C until use. This supernatant had a protein concentration of 0.26 g/L, which was measured using a BCA assay (INTERCHIM UPTIMA BC Assay Protein Quantitation Kit). After thawing the supernatant at room temperature, an emulsion was prepared by mixing supernatant (100 g) with hexadecane (123.68 g) and MilliQ water (1340 g) by the same procedure as for the emulsion containing yeast cells (3 h, 2 L vessel, 900 rpm, 25 °C). The pH of the aqueous phase was not controlled but it was measured to be 4.5 in the experiments. The previously mentioned conditions for preparation of the emulsion without yeast cells were the reference conditions used in the experiments, unless mentioned otherwise. The effect of emulsion preparation on the oil recovery was studied as well with the variations mentioned in Table 1.

Table 1. An overview of the reference parameters used for preparation of the emulsions without yeast cells and the tested variations.

Emulsion parameters	Reference value	Variations
Stirring rate (rpm)	900	1200
Supernatant amount (g)	100	150
Oil volume fraction (-)	0.1	0.05, 0.2

5.2.3 Separation experiments

After preparation of an emulsion in the stirred vessel, the mixture was pumped to the custom made glass columns in which the separation took place (inner diameter: 36 mm, height: 600 mm) at room temperature. These columns were equipped with a stainless steel bottom plate with a single nozzle (plate thickness: 2 mm, nozzle diameter, d_{nozzle}: 0.3 mm) to sparge the gas bubbles into the system. The gas flow in the columns was controlled by Brooks mass flow controllers (0-1 L/min). The columns were filled with 300 mL of the prepared emulsion. During the oil layer formation process, pictures were taken every 15 minutes for manual image analysis to determine the change in volume of the oil layer formed on top of the columns over time. The columns were provided with a white background to improve the visibility of the different phases in the columns. After two hours, the gas flow was stopped and the mixture was left to separate by gravity for one hour, during which the unrecovered oil droplets formed a concentrated emulsion (cream) below the oil layer. The volumes of the phases were measured by heights of the oil, cream, and aqueous layer directly in the column. Samples of the resulting cream layer were taken, using a glass Pasteur pipet with the tip removed to create a larger opening, which could be further analysed for oil content or protein concentration to come to the surface excess protein concentration, using the methods described in the following sections. Table 2 summarises the reference values of the process parameters for the separation process and the experimentally tested variations.

Table 2. An overview of the reference separation conditions and the tested variations of the process parameters.

Process parameters	Reference value	Variations
Column height (cm)	30	15, 55
Superficial gas velocity (cm/s)	0.1	0.2, 0.5, 1.0
Nozzle diameter (mm)	0.3	0.1, 1, 3

5.2.4 Analytical methods

5.2.4.1 Emulsion sample preparation

To prepare the cream layer samples for both protein and oil fraction measurements, the emulsion had to be broken first. The protein that was attached to the interface had to be solubilised, creating a good phase separation. To achieve this, an equal volume of aqueous urea buffer was added (4 M urea, 10 mM $NaHCO_3$, 0.1 mM EDTA, pH 12) and the samples were set in a shaker (200 rpm, 25 °C, Sartorius CERTOMAT BS-1) overnight. After centrifugation to compress the droplets (10 min at 5000 rpm, 4000 g, Heraeus Multifuge 1-sr), the complete tube and its contents were frozen at -20 °C and stored until further analysis. After the samples were thawed at room temperature, the formed organic and aqueous layers could be further analysed for respectively oil fraction and protein concentration.

5.2.4.2 Surface and interface tension measurements

The interfacial tension of the different surfaces and interfaces (oil/air, aqueous/air, oil/aqueous) were measured using a Krüss 0 2160 ring tensiometer. Measurements were performed in duplicate and at room temperature.

5.2.4.3 Protein measurement

The protein concentration in the aqueous layer, after the cream sample preparation procedure, was measured using a BCA assay (Interchim Uptima BC Assay Protein Quantitation Kit), according to the enhanced protocol provided with the assay: 2 mL of assay were mixed with 100 µL of sample and heated for 30 min at 50 °C, followed by measurement of absorbance at 595 nm (Hewlett Packard 8453 UV-Vis spectrophotometer).

5.2.4.4 Oil fraction measurement

The oil fraction in the sample was determined making use of the red colour of the organic layer and the Beer-Lambert law. First, a known amount of uncoloured hexadecane was added to after taking the sample. After following the emulsion sample procedure

described earlier, complete phase separation of the organic and aqueous phase was achieved. The organic layer was a mixture of the coloured hexadecane from the sample and the added uncoloured hexadecane. By measuring the absorbance of the organic phase at 515 nm (Hewlett Packard 8453 UV-Vis spectrophotometer) and knowing the amount of uncoloured hexadecane that was added, the amount of hexadecane in the sample could be calculated. To be able to make this calculation, a calibration line was prepared consisting of different ratios of the coloured hexadecane used in the experiment and uncoloured hexadecane.

5.2.4.5 Droplet size measurements

The droplet size in the emulsion was determined from pictures that were acquired in the stirred vessel during the emulsion preparation using a SOPAT particle size measurement system (SOPAT Gmbh), which consisted of a probe that could be placed in the stirred vessel coupled to a computer system. The exact configuration of the probe in the vessel can be found in [7]. During the three hours of emulsion preparation, 30 pictures were acquired every five minutes, starting at 5 min and ending at 175 min. The accompanying particle detection software was used to measure the size of the droplets in the pictures. For the yeast containing emulsions, an additional step was required, in which false positives (detected gas bubbles) were manually removed. The detected particles were converted to size distributions and values for the Sauter mean diameter. The number of pictures was sufficient to have more than 1000 droplets per data point. For droplet size measurements in the cream layer, a sample (5 mL) was taken from the cream layer in a Falcon tube using a glass Pasteur pipet with the tip removed. The cream was then pumped (Masterflex peristaltic pump, model 77521-57) through a custom made flow cell with a channel depth of 4 mm to which the SOPAT camera probe was connected.

5.2.4.6 Bubble size measurements

The bubble size in the separation column was determined in columns filled with the yeast supernatant without the presence of hexadecane, because this decreased the visibility of the gas bubbles. Pictures were acquired with a digital camera (Nikon D3200) at a height

between 25 and 30 cm in the column and the column was lit from below. A custom made Perspex block with a cylindrical cut out was placed against the columns to eliminate the optical distortion due to the curvature of the columns. The size of the bubbles was measured manually using ImageJ (v1.49). Since the larger bubbles were not spherical anymore they were considered to be ellipsoids and their minimum and maximum diameters were measured (Figure 1). Between 60 and 100 bubbles were measured for each tested condition, until the Sauter mean diameter did not show a change anymore.

Figure 1. An example of the pictures from which the bubble size was determined, the red lines represent the measured diameters of the bubbles. The chart shows the development of the Sauter mean diameter while increasing the number of measured bubbles (d_{nozzle} = 3 mm, v_{Gs} = 0.1 cm/s)

The measured bubble size was used to estimate the bubble area formation rate, the gas holdup, and the bubble area present in the separation columns. For the first, the bubble surface area introduced to the system (in cm^2/s) was calculated using the determined diameter of the bubble and the gas flow rate. Due to the low superficial gas velocities in the columns the gas holdup in the columns was very low and could not be measured accurately in the experiments. Instead, the gas holdup (ε_G) was calculated by dividing the superficial gas velocity by the bubble rise velocity [20]. The bubble rise velocity was estimated using an empirical correlation from [20], in which the deformation of larger bubbles is taken into account. From the bubble rise velocity, the surface area of the bubbles (A_b) in system was calculated using the volume of gas in the column (calculated from the gas holdup) and the bubble diameter ($A_b = 6\ V_g/d_b$).

5.2.4.7 Column image analysis

During the separation process, pictures of the columns were acquired every 15 min using a digital camera (Nikon D3200). From these pictures, the volume of the continuous oil layer was determined by manually measuring the height of the layer using IrfanView v4.33. In the experiments in which an oil layer was formed, the gas holdup in the columns was very low (1.3 % at most), so this effect was neglected. Furthermore, the images were used to quantitatively describe the colour gradient in the column that could be visually observed in the experiments (as in Figure 5). This gradient reflects the gradient in hold-up of oil droplets. First, the images were vertically aligned and cropped to remove the background. The column images were corrected for the variations in light using the background. The image processing was performed in MATLAB R2014b, resulting in colour gradients that allowed to compare the different columns in the experiments. Appendix C shows the followed procedure and illustrates it with an example picture.

5.3 Results

5.3.1 Characterization of the model emulsions

After the three hours of mixing of the hexadecane and the aqueous phase, the droplets in the emulsion were sufficiently stabilised by the surface active components to avoid coalescence. When a shorter stirring time was used, the droplet interface was not sufficiently stabilised and the emulsion could be readily separated by centrifugation. The emulsion develops over time, as can be seen from the decrease of the Sauter mean diameter over time (Figure 2). Droplet breakup itself is a quick process, but the newly formed interface has to be stabilised to prevent coalescence. The adsorption of the stabilising components takes time and therefore, we can observe the gradual decrease in Sauter mean diameter over time.

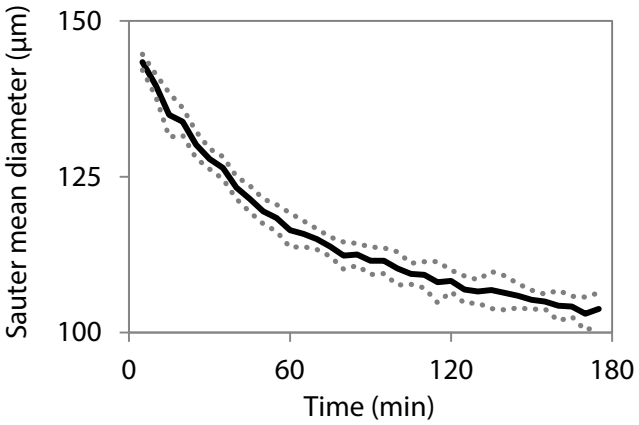

Figure 2. The development of the Sauter mean diameter during emulsion preparation for the emulsion prepared with yeast supernatant (average of 6 experiments, the dotted lines display the standard deviation of the measured values).

Besides the stirring rate and emulsion preparation time, the final Sauter mean diameter of the oil droplets is also determined by the amount of surface active components. In the emulsions prepared with the supernatant, the amount of surface active components could be well controlled at a constant value by addition of the amount of yeast supernatant and this gave an accurate reproducibility of the final Sauter mean diameter: 103.7 µm with a standard deviation of 2.2 µm (6 experiments). When yeast cells were used to prepare the emulsion, a much broader distribution in the final Sauter mean diameter as obtained: 88.9 µm with a standard deviation of 13.3 µm (7 experiments).

5.3.2 Behaviour of emulsion in gravity separation

Although the droplet size was slightly smaller in the emulsions with the cells, the emulsions with and without cells showed comparable behaviour during (enhanced) gravity separation. When the emulsion was transferred to a column without gas flow, the droplets rose quickly to the top of the column, creating a stable concentrated emulsion (cream, Figure 3A). Within 10 minutes, the majority of the oil was present in this layer, which could be expected from the droplet size: the smallest droplets had a size of about 50 µm, which would result in a Stokes rise velocity of 0.4 mm/s. So within 13 minutes such a droplet would rise from bottom to top in the column. After one hour of gravity separation, the cream had a gel like structure and complete coalescence into a continuous oil layer did not occur, even after a

prolonged time (+24 h). Proteins are known to create a visco-elastic droplet surface, which allows the droplets to deform when compressed [21]. This was indeed observed when the cream was left standing for 72 h: the gravitational force compressed the droplets but coalesce did not occur (Figure 3C).

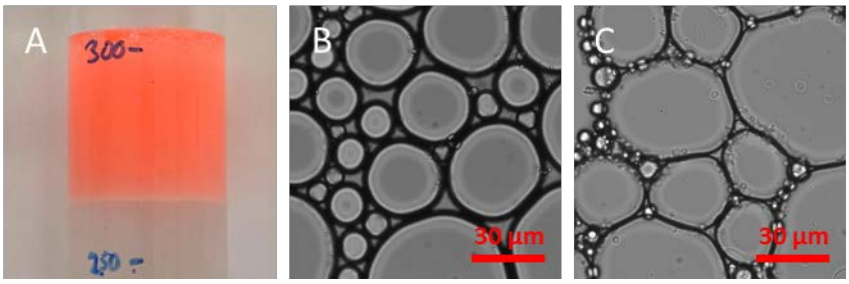

Figure 3. Different pictures of the cream layer formed in a emulsion with yeast cells: (A) the formed cream layer after gravity separation of the emulsion, (B) a microscope picture of the cream layer after 1 h of gravity separation, and (C) a microscope picture of the cream layer compression by gravity for 72 h.

As observed in research about emulsion formation in fermentations, centrifugation is inefficient to induce coalescence of the stabilised droplets and to separate the cream into oil and aqueous phase [13, 14]. These type of emulsions can reach very low volume fractions of the aqueous phase after centrifugation (< 0.01%) without formation of a continuous oil phase [22], so extensive film drainage can take place without film rupture occurring. Centrifugation (4000 g) resulted in the formation of a thin oil layer, containing 4% of the oil, while the majority of the oil remained emulsified as deformed droplets. So even when droplet collision and film drainage were forced, complete coalescence was prevented by the stabilising components at the oil/water (O/W) interface that prevented film rupture. By measuring the total amount of protein and the amount of protein in the aqueous phase of the cream layer formed after gravity separation of the yeast emulsion, the amount of adsorbed protein in the cream could be calculated, which was found to be 145 ± 33 mg/L. Knowing the oil droplet Sauter mean diameter and the oil fraction in the cream (0.55 ± 0.07, after 1 h of gravity separation), the measured surface excess concentration of proteins at the O/W interface could be calculated (4.5 ± 1.1 mg/m^2). This surface excess concentration is at the higher end of the range reported in literature for protein stabilised emulsions (1.5 – 4 mg/m^2) [23, 24], so also in

our model emulsions proteins are likely to have a major contribution to the stabilisation of the oil droplets leading to a stable cream layer.

5.3.3 Gas bubble induced oil recovery in the reference experiment

Film rupture was the crucial step that had to be induced to obtain a continuous oil layer from the emulsion. When the emulsions were transferred from the stirred vessel to a column in which a superficial gas velocity (v_{gs}) of 0.1 cm/s was applied, a continuous oil layer was formed on top of the column. Similar to the emulsion behaviour discussed in the previous paragraph, the two emulsions (with cells and yeast supernatant) showed similar amounts of continuous oil layer being formed. After the two hours of aeration at 0.1 cm/s, 20 mL of the initially dispersed oil droplets had coalesced into the continuous oil layer (of the total 30 mL added). When the gas flow was then stopped, the remaining oil droplets (containing the remaining 10 mL of oil) formed a cream layer below the continuous oil phase due to gravity separation (Figure 4). The droplet size in this cream layer was only a bit larger or smaller than the droplet size of the original emulsion (for example, 91 vs. 88 μm), suggesting that droplet-droplet coalescence was not occurring during the aeration. When the experiment was continued overnight (21 h) with air sparging, all oil droplets coalesced into the continuous oil layer (not shown).

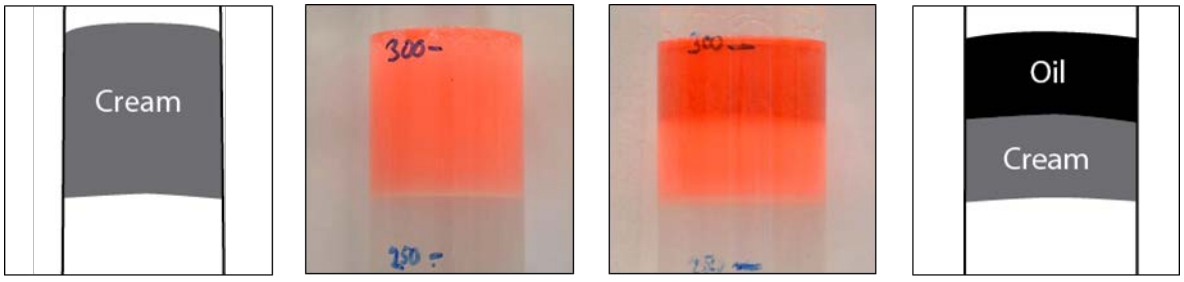

Figure 4. Pictures and schematic drawings of the results of gravity separation(left) and two hours of gas bubble induced oil recovery at a superficial gas flow of 0.1 cm/s followed by 1 h of gravity separation without air (right) and using a emulsion with yeast cells.

The experiments performed using yeast supernatant had an enhanced visibility in the dispersed phase, which allowed for better visual observations during the separation process.

Besides the enhanced visibility, the use of yeast supernatant also eliminated biological variations among experiments that could affect the emulsion behaviour. Furthermore, in the experiments with yeast, a foam layer could be formed that contained part of the oil. This did not happen for the reference conditions (with a superficial gas velocity of 0.1 cm/s), but at high superficial gas velocities (>0.5 cm/s) a foam layer was formed. For these reasons, the supernatant emulsion was used in the following experiments to study the phenomena in the oil formation process.

When the emulsion was transferred to the aerated separation columns, two phenomena occurred: the formation of a continuous oil layer started and a concentration gradient of the dispersed droplets over the height of the column was observed (Figure 5). This axial dispersion of the oil droplets occurred due to back mixing induced by the gas bubbles that counteracted the upwards motion of the droplets caused by the buoyancy force. This way, the flow of gas bubbles prevented the formation of a cream layer, contrary to what was observed in the system without air.

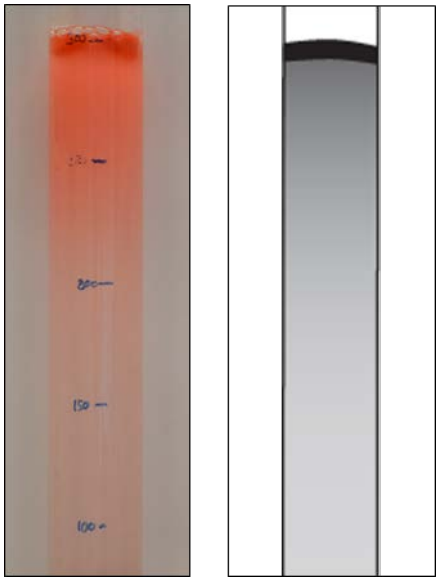

Figure 5. A picture and schematic drawing of the column during the separation process (at 45 min) with a superficial gas velocity of 0.1 cm/s, showing the concentration gradient of dispersed oil droplets in an emulsion with yeast supernatant.

While gas bubbles were supplied to the column at a superficial gas velocity of 0.1 cm/s, the continuous oil layer at the top of the column increased over time (Figure 6). When the

volume of this oil layer was determined from the pictures, the rate with which the height of the continuous oil layer increased appeared to be constant over the two hours of the experiment (10 mL/h, Figure 7). So for this period of time, the coalescence rate of droplets into the continuous oil layer was constant.

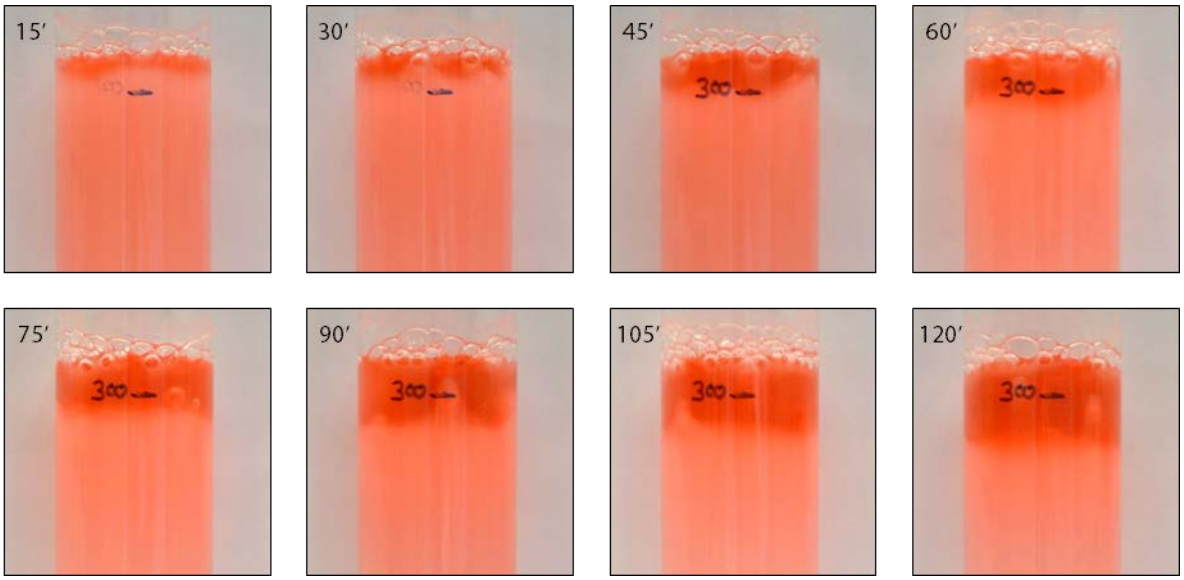

Figure 6. The formation of the continuous oil layer over time, during two hours at a gas flow of 0.1 cm/s in an emulsion with yeast supernatant.

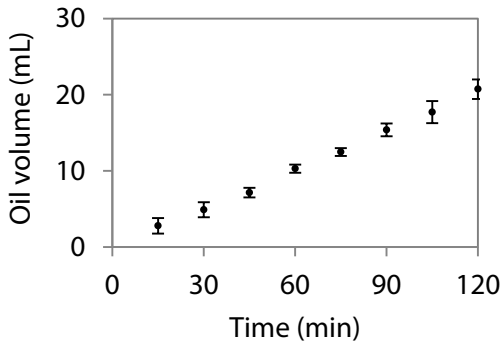

Figure 7. The volume of the continuous oil layer over time, during two hours of separation at a superficial gas velocity of 0.1 cm/s in an emulsion with yeast supernatant. The mixture contains 30 mL of oil, reaching an oil recovery of 66 % (presented values are an average value of 6 experiments, error bars give standard deviation of average).

The observations in this experiment show that the gas bubbles had at least two effects: (1) the bubbles caused axial dispersion of the droplets over the column height due to back mixing and (2) the bubbles induced film rupture of the stabilising interface, increasing the continuous oil layer over time. These observations will be used in the following sections to

determine and discuss the influence of varying process parameters or emulsion properties on the oil recovery, leading to a better understanding of the process of bubble induced oil recovery.

5.3.4 Separation process parameters

Using the yeast supernatant emulsion, the effect of different process parameters was studied (Table 2). With the above observations, changing the properties of the gas phase is the most obvious parameter of the process that can be optimised. The gas phase in the column can be characterised by the number of gas bubbles and the size of the gas bubbles, but these are difficult to control directly. However, the superficial gas velocity in the column and the nozzle diameter at the bottom of the columns could be controlled accurately and the combination of these two parameters determines the number of bubbles and their size (Table 3). At the 0.3 mm nozzle, the influence of superficial gas velocity on the bubble diameter was minor, while the nozzle diameter had a strong effect when the superficial gas velocity remained constant. However, the two largest nozzles (with 1 and 3 mm diameter) showed a similar bubble size at the same superficial gas velocity. Furthermore, the bubble surface area present in the columns and introduced in the columns per unit of time both showed the same pattern for the variations in superficial gas velocity and nozzle diameter. Increasing the superficial gas velocity led to an increase in the bubble surface area present in the system and

Table 3. The bubble Sauter mean diameter ($d_{32,b}$), standard deviation (σ) and the calculated bubble surface flow into the column ($F_{A,b}$), gas holdup (ε_G), bubble surface area in the column (A_b) for the different tested combinations of superficial gas velocity and nozzle diameter (the reference case is in bold).

v_{Gs} (cm/s)	d_{nozzle} (mm)	$d_{32,b}$ (mm)	σ (mm)	$F_{A,b}$ (cm^2/s)	ε_G (-)	A_b (cm^2)
0.1	**0.3**	**3.6**	**0.48**	17.9	0.4%	21.2
0.2	0.3	4.5	0.68	28.7	0.8%	33.6
0.5	0.3	3.8	0.77	84.9	2.1%	102.6
1.0	0.3	4.5	1.75	143.4	4.2%	174.0
0.1	0.1	1.7	0.53	37.9	0.4%	43.8
0.1	1	6.5	1.68	9.9	0.4%	10.8
0.1	3	6.3	1.15	10.2	0.4%	11.2

introduced into the system. Increasing the nozzle diameter decreased the surface area of the bubbles. Comparing the surface area of the bubbles to the surface area of the oil droplets initially present in the system (30 mL oil with an average droplet diameter of 104 μm gives 1.7 m^2 droplet interface), shows that the oil droplet surface area is several orders of magnitude larger.

Increasing the superficial gas velocity from its reference value (0.1 cm/s) resulted in a lower amount of oil being recovered after 2 hours of separation (Figure 8A). At 0.2 cm/s, a continuous oil layer was still obtained, although it was lower than the reference case. When the gas flow was increased even further (to 0.5 cm/s and 1.0 cm/s) the mixing induced by the gas bubbles was too severe to form a continuous oil layer. Instead, some coalescence into larger droplets (with a size of several millimetres) occurred but these were continuously mixed back into the columns and these bigger droplets were recovered after the gravity separation as a cream layer containing these large droplets (with about 30% of the oil in the columns). The superficial gas velocity had a strong influence on the axial dispersion of the oil droplets in the columns, which could be visually observed as a colour gradient over the column. At 0.1 cm/s, the magnitude of the axial dispersion and the rise velocity of the droplets were in the same order of magnitude, resulting in a concentration gradient over the height of the column. When the superficial gas velocity was increased to 0.2 cm/s or higher, the axial dispersion was also increased and no droplet concentration gradient could be observed anymore (Figure 8B). The decrease in colour intensity at ca. 27 cm is an artefact in the image analysis, caused by light that shone through the liquid surface at the top of the column affecting the intensity of the pixels at the top of the column.

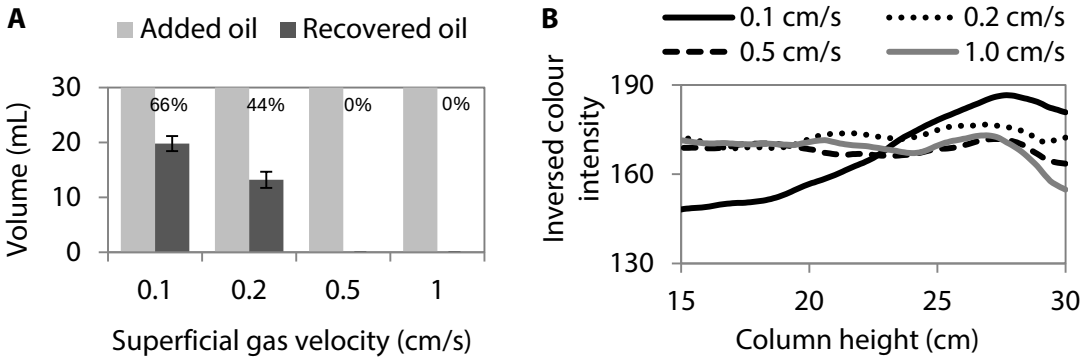

Figure 8. (A) The total volume of oil, the volume of oil recovered as a continuous oil layer, and the recovery yield after 2 hours of separation for different superficial gas velocities followed by gravity separation (d_{nozzle} = 0.3 mm, h_{column} = 30 cm) and (B) the colour intensity gradient over the column height.

By changing the diameter of the nozzle, the size of the gas bubbles could be changed. With a constant gas flow rate, the bubble size will increase with increasing nozzle diameter, resulting in a decreased number of bubbles and a decreased surface area of the gas bubbles. The trend in the amount of recovered oil was not unambiguous: the highest amount of oil was recovered with the standard nozzle diameter (0.3 mm). Both the larger (1 and 3 mm) and smaller (0.1 mm) nozzle diameters resulted in a smaller amount of continuous oil (Figure 9A). The change in nozzle diameter also caused a difference in the axial dispersion of the droplets: a concentration gradient was observed for the two smallest nozzle diameters and with the larger nozzle diameters the droplets were dispersed homogeneously below the continuous oil layer (Figure 9B).

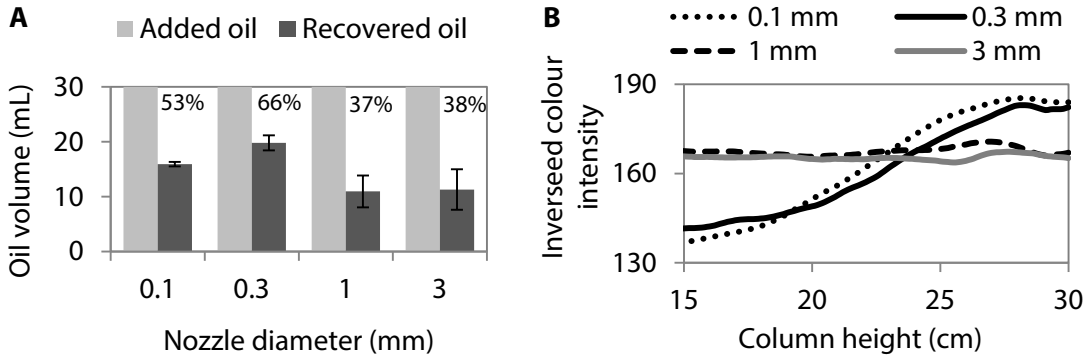

Figure 9. (A) The total volume of oil, the volume of oil recovered as a continuous oil layer, and the recovery yield after 2 hours of separation with different nozzle diameters followed by gravity separation (v_{gs} = 0.1 cm/s, h_{column} = 30 cm) and (B) the colour intensity gradient over the column height.

When the height of the column was increased while keeping the dispersion properties constant, the absolute amount of oil varied in the columns. Because a superficial gas velocity of 0.1 cm/s was used, similar axial dispersion behaviour was observed as discussed previously. Only in the lowest column the droplet concentration gradient could not be observed (not shown). The amount of oil that was recovered in the smaller column was lower, as could be expected from the lower amount of oil present in the column, but the percentage of oil in the oil layer was similar to the reference case. In the larger column, the amount of recovered oil did not increase (Figure 10A). The oil formation rates (mL/h) were initially similar for the three columns (Figure 10B), but in the smaller column the it decreased after approximately 45 minutes. The oil formation rates in the reference and taller columns were constant and equal to each other.

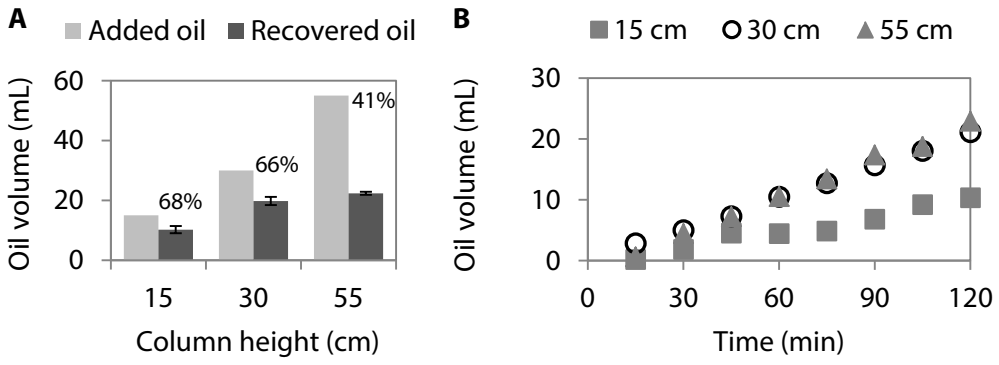

Figure 10. (A) The total volume of oil, the volume of oil recovered as a continuous oil layer, and the recovery yield after 2 hours of separation followed by gravity separation for different column heights (v_{gs} = 0.1 cm/s, d_{nozzle} = 0.3 mm) and (B) the volume of the continuous oil layer over time.

In the experiments, the gas bubble induced oil recovery was followed by a 1 h gravity separation to determine the volumes of the different layers. When a 1 h gravity separation was done before the gas bubble induced oil recovery, the amount of oil recovered in the oil layer was decreased from 19.8 mL to 10.5 mL. This shows that the separation process is more efficient when it is used before gravity separation.

5.3.5 *Effect of dispersion properties*

Besides the process conditions, the properties of the dispersion also influenced the separation. The effect of variations in oil volume fraction, protein concentration, and droplet size on the formation of the oil layer after 2 hours of separation were tested (Figure 11). When the oil fraction was lowered, the final amount of recovered oil was lower because there was simply less oil in the system. Similar as increasing the column height, increasing the oil fraction in the dispersion did not have a large impact on the amount of oil coalescing into the continuous oil layer. Looking at the development of the continuous oil layer over time (Figure 12), all oil formation rates were initially the same (10 mL/h), but after approximately 60 minutes the oil formation slowed down for the dispersion with a 0.05 oil fraction.

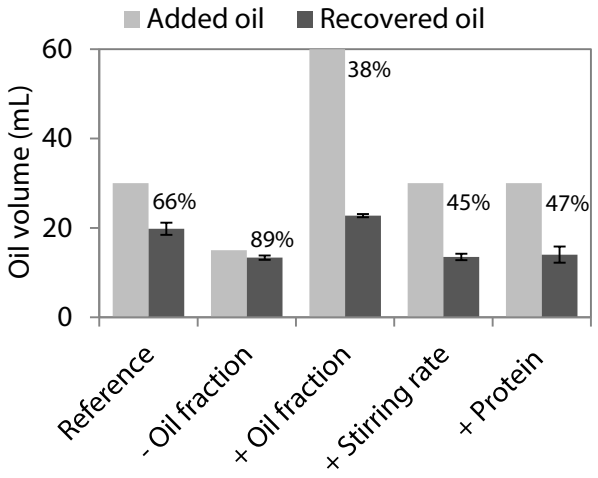

Figure 11. The total volume of oil, the volume of oil recovered as a continuous oil layer, and the recovery yield after 2 hours of separation followed by gravity separation with different dispersion properties (v_{Gs} = 0.1 cm/s, d_{nozzle} = 0.3 mm, h_{column} = 30 cm).

Increasing the stirring rate and increasing the protein concentration in the preparation procedure of the emulsion caused a similar decrease in the amount of recovered oil (Figure 13). When the stirrer speed was increased from 900 rpm to 1200 rpm, the Sauter mean diameter of the dispersed oil droplets was decreased from 104 μm to 87 μm. Smaller droplets experience a lower buoyancy force, so their tendency to move upwards towards the oil layer will be lower, possibly lowering the oil formation rate. The increase in the protein

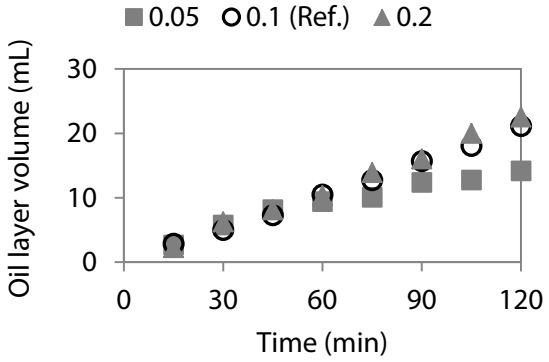

Figure 12. The volume of the continuous oil layer over time for different oil volume fractions in the dispersion (v_{Gs} = 0.1 cm/s, d_{nozzle} = 0.3 mm, h_{column} = 30 cm).

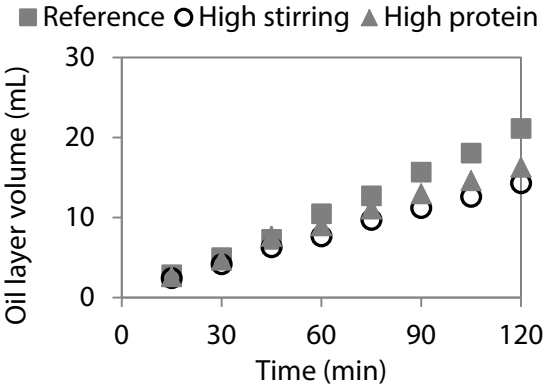

Figure 13. The volume of the continuous oil layer over time for the reference case, the emulsion with smaller droplets due to a higher stirring rate, and the emulsion with an increased protein concentration.

concentration led to a 30% decrease in the amount of recovered oil after the 2 hours of the experiment. Although the amount of proteins was increased with 50%, the Sauter mean diameter showed only a slight decrease (to 99 μm). So the surface area of the droplets did not increase proportional with the amount of surface active components, meaning that a higher surface coverage could be achieved, leading to stronger surface stabilisation and therefore less rapid coalescence.

5.4 Discussion

5.4.1 How gas bubbles induce coalescence

Two effects of the gas bubbles were readily observed in the columns during the separation: they induced formation of a continuous oil layer and caused back mixing of the

dispersed oil droplets. Coalescence of the dispersed oil droplets did not occur readily as was shown in the experiments without gas bubbles, so the gas bubbles facilitated coalescence into oil. Surfaces are known to be able to facilitate coalescence, depending on the physical properties of the surface and emulsion [25]. The gas bubbles provide a hydrophobic surface, so the hydrophobic oil droplets prefer contact with gas surface over contact with the aqueous phase. Whether the oil droplets indeed enter the water/gas (W/G) surface depends on the interfacial and surface tensions of the three interfaces in the system. According to Robinson and Woods, from the measured values of the interface and surface tensions (σ_{WG} = 70.0 mN/m, σ_{OG} = 27.3 mN/m and σ_{OW} = 25.5 mN/m) the oil droplets in this system can be expected to enter the W/G interface [26, 27]. Because the surface active components have a preference for an hydrophobic/hydrophilic interface, the oil/gas (O/G) interface formed after entering of a droplet will not be covered with surface active components and coalescence can occur [28].

A prerequisite for entering of the droplets into the W/G interface is rupture of the stabilising film at the O/W interface. The type of proteins attached at the interface has a strong influence on the required film rupture. When the O/W interface is stabilised by random coiled proteins, multiple small holes are formed when the droplet comes into contact with the gas phase. The oil can move through these holes and the droplet can then enter into the W/G surface. To achieve the entering of droplets that are stabilised by globular proteins, local stresses are required to induce film fracture, for instance by shear or dilatational deformation [28]. The motion induced by the rising gas bubbles in the system could cause the deformation of the droplets and thereby provide the necessary forces for film rupture.

With the above discussed phenomena, a mechanism for gas bubble induced coalescence can be suggested. Since the volume of the oil layer increases, the oil droplets have to come in close proximity of the continuous oil layer, but as the gravity separation experiments showed, when stabilised oil interfaces come into contact with each other, coalescence does not occur (Figure 14, step 1). Before a gas bubble can facilitate coalescence, it must first collide with the oil droplet close to the main O/W interface (step 2). With film

rupture occurring, the oil can move into the bubble surface and an unstabilised oil surface is created (step 3). Now coalescence of the oil droplet into the oil layer can occur through the uncovered oil surface (step 4) and the coalescence process is completed and the bubble rises further through the oil layer and leaves the system (step 5). When the droplets coalesce into the oil layer, the total O/W interface in the system decreases. Where the proteins that are initially adsorbed at the O/W interface move to remains a question.

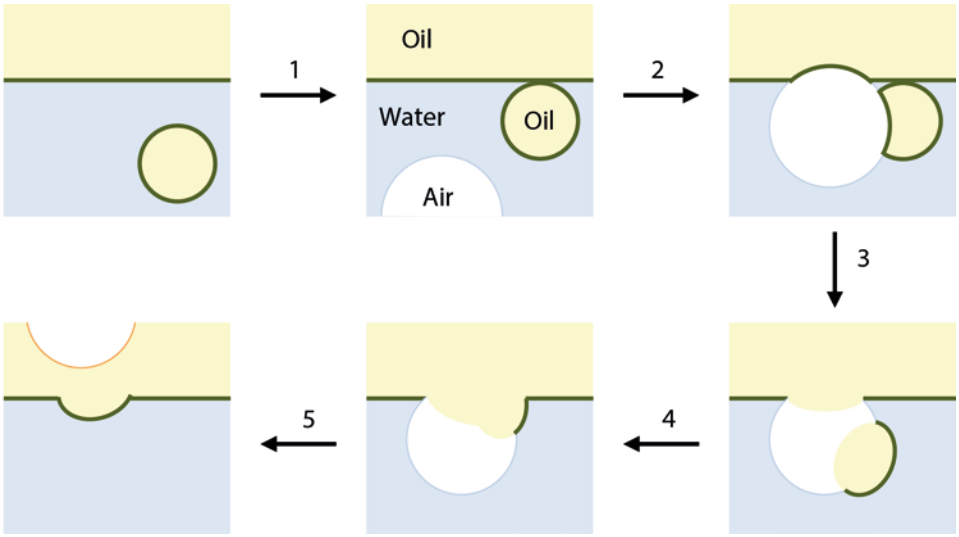

Figure 14. A sketch of the suggested mechanism of gas bubble induced coalescence. (1) Coalescence of a stabilised oil droplet does not occur when it comes into contact with the main O/W interface, (2) a gas bubble collides with the O/W interface and the oil droplet, (3) the stabilising film ruptures and the oil enters into the bubble surface, creating an unstabilised oil surface, (4) the droplet coalesces into the oil layer through the unstabilised surface, (5) coalescence of the oil droplet into the oil layer is completed and the bubble leaves through the oil layer. Important note: for visibility, this sketch is not to scale. The oil droplets will be almost two orders of magnitude smaller.

5.4.2 Limiting axial dispersion is more important than inducing coalescence

According to the proposed coalescence mechanism, increasing the bubble surface area will enhance the oil layer formation. However, increasing the gas flow rate also increased the axial dispersion in the column, what resulted in a more homogeneous distribution of the droplets throughout the column and a lowered droplet concentration below the main O/W interface. This negatively affected the oil layer formation and the results suggest that axial dispersion should be limited, at least to the degree at which the oil concentration at the top is sufficient to achieve the maximum oil formation rate (Section 5.4.5).

Increasing the nozzle diameter while keeping the gas flow constant led to less and larger bubbles and increased the axial dispersion in the columns. As could be expected from the increase of axial dispersion and decrease of bubble surface area, the amount of recovered oil was also lowered. When bubble surface area in the system was increased by increasing the superficial gas velocity, the amount of recovered oil still decreased. So, the detrimental effect of the higher gas flow in the system was stronger than any positive effect of the increase in bubble surface area on coalescence.

5.4.3 More bubble surface area does enhance coalescence

Comparing the experiments in which axial dispersion was strong, the effects of variations in the droplet concentration over the height in the column are cancelled out and the effect of the bubble surface area is isolated. The experiments with larger nozzle diameters (1 and 3 mm, v_{Gs} = 0.1 cm/s) and higher superficial gas velocity (0.2 cm/s, d_{nozzle} = 0.3 mm) all had strong axial dispersion and a homogeneous distribution of the oil droplets over the column height. Of these three, the experiment with the higher superficial gas velocity and smaller nozzle size yielded the largest amount of oil after two hours of separation, 13.2 mL versus 11.0 and 11.3 for the experiments with the 1 and 3 mm nozzle. Due to the higher gas flow and smaller nozzle, more and smaller bubbles were formed in this system and thereby the bubble surface area introduced into the system was higher, 29 cm^2/s versus 10 cm^2/s for the larger nozzles. The higher oil recovery achieved with this higher bubble surface area indicates that increasing the bubble surface area can indeed enhance the oil recovery, but it is not linearly related to the amount of bubble surface area introduced in the columns. Furthermore, as discussed before, the adverse effects of stronger axial dispersion can outweigh this benefit.

5.4.4 Is there a minimum bubble size?

However, there seems to be a lower limit to the positive effects of decreasing the size of the bubbles and increasing their number. Even though the bubbles were small, the number of bubbles was high, and there was little axial dispersion, the experiment with the smallest nozzle

diameter (0.1 mm) had a lower oil formation rate than the experiment with a nozzle diameter of 0.3 mm. In the pictures, it was observed that the bubbles created with the smallest nozzle diameter were spherical, where for all other nozzle diameters the bubbles deformed. In those deformed and larger droplets, the bubble wake will be larger and higher shear forces will occur [29]. Based on the previously discussed coalescence mechanism, the smaller gas bubbles could be less efficient in inducing the shear forces that are required for the droplets to enter into the W/G interface, setting a lower boundary for the gas bubble size.

5.4.5 The kinetics of bubble induced oil recovery

The previous discussion shows that by changing gas phase parameters (flow rate, bubble size), the separation process can be influenced, creating the possibility for optimisation. For the reference conditions used in the experiments (v_{Gs} = 0.1 cm/s, d_{nozzle} = 0.3 mm), there seems to be a maximum oil formation rate that the bubbles in the system can induce (10 mL/h). Both increasing the column height and oil fraction in the dispersion led to an increased total amount of oil in the system, which could result in an increased oil concentration below the main O/W interface. However, an increase in the volume fraction of oil droplets did not result in a clear increase in the oil formation rate of oil droplets into the continuous oil layer, as shown clearly by the experiments with varying oil fraction (Figure 12). Only in the experiment with an oil volume fraction of 0.05, the oil formation rate decreased after 1 h when 60% of the oil was recovered as a continuous oil layer. This reduction in the amount of oil droplets in the column could have decreased the droplet concentration sufficiently so that the droplet concentration was insufficient to fully use the coalescence capacity of the gas bubbles.

Besides the gas phase, the emulsion composition influenced the oil formation rate. The experiments with a higher stirring rate, resulting in smaller droplets, or higher protein concentration showed a lower oil formation rate under the reference column conditions. Since the gas bubbles remained unchanged, these results show that the gas bubbles have more difficulties inducing coalescence of smaller droplets and more stabilised droplets. This shows

the importance of choosing process conditions for the fermentation that also promote the formation of large droplets and minimise the amount of stabilising components.

5.5 Conclusions and outlook

Fermentations with the product as a second liquid phase have great potential for simple product recovery, but coalescence of product droplets into a continuous oil layer is crucial for this. The presence of surface active components in the fermentation broth can prevent film rupture, inhibiting coalescence. Especially for low cost, high volume products such as advanced biofuels it is important that a low cost solution for the product recovery is developed. In this paper, a new method is presented that uses gas bubbles to induce coalescence of oil droplets into a continuous oil layer. This method uses mild process conditions and does not require any expensive de-emulsifiers that could also be harmful for the microorganisms in the system. This creates the possibility of integrating bubble induced oil recovery in the fermentor, enabling cell recycle and potentially decreasing the process costs significantly.

The mechanism by which the gas bubbles cause the formation of a continuous oil layer is not completely understood, but the gas bubbles are thought to have at least two effects: causing axial dispersion and facilitating coalescence. Adapting the parameters of the gas phase, by changing nozzle diameter or superficial gas velocity, influenced the performance of the separation. Although increasing the bubble surface area in the columns can lead to an enhanced oil recovery, this positive effect can be outweighed by the negative effect of increased axial dispersion in the column. At this moment the main challenge seems to be to maximise the amount of gas bubbles in the system to facilitate coalescence, while minimising the axial dispersion caused by the flow of these gas bubbles.

These challenges will also be very important when scaling up the separation process, where the changes in the geometry and the gas distribution will have a large influence on the overall hydrodynamics and on the separation process. Integrating the separation with the fermentation will also require a change in the operation mode from batch to continuous. How

such a continuous in and out flow affects the oil recovery should be studied, to arrive at an optimal design for a reactor in which the fermentation and separation are integrated.

When these steps are taken, a better assessment can be made for the applicability of the developed separation method in the production of advanced biofuels. At this moment, the gas bubble induced oil recovery is a promising separation technique that could lower downstream processing costs, resulting in an economically more feasible production of advanced biofuels.

Acknowledgments

This work was carried out within the BE-Basic R&D Program, which was granted a FES subsidy from the Dutch Ministry of Economic affairs, agriculture and innovation (EL&I). The authors would like to thank Renco Beunis MSc, Robbert Binneveld MSc, and Emilio Ruano MSc for their contributions in developing the gas bubble induced separation method and the analytical methods.

List of symbols

$d_{32,b}$	Gas bubble Sauter mean diameter
v_{Gs}	Superficial gas velocity
d_{nozzle}	Nozzle diameter
ε_G	Gas holdup
A_b	Bubble surface area in column
$F_{A,b}$	Flow of bubble surface area
h_{column}	Column height
σ_{WG}	Water/gas surface tension
σ_{OG}	Oil/gas surface tension
σ_{OW}	Oil/water interfacial tension

Appendix A – Discussion on the explored alternative separation methods

Several methods aiming at recovering oil from fermentation broths have been explored, especially aiming at low cost methods that can be integrated in large scale advanced biofuel fermentations. When the droplets become sufficiently large to achieve droplet creaming by gravity, a stable cream layer will be formed and a second coalescence step is required to form an oil layer. Literature discussing fermentations with an organic phase showed that instead of coalescence into an oil layer, often a concentrated emulsion (cream) is obtained. In our model emulsion, such a cream layer was formed after gravity separation as well. Using the developed model mixture and the developed analytical techniques, alternative options for the prevention emulsion formation or recovery of the oil from the emulsion were explored:

- De-emulsifiers in combination with centrifugation – at large scale, the oil is being recovered via this method. Also for our model emulsion, the addition of surface active molecules (ethanol, octanol, SDS) showed to enhance the efficiency of centrifugation. However, as discussed before, a method without the need for centrifugation and de-emulsifiers is preferred.
- Hydrocyclones – centrifugal forces can also be generated by creating a spiral flow, which is done in hydrocyclones. They have clear advantages (e.g., no moving parts, easily scalable by number) and are used in places with space limitations, for instance in the offshore industry. The main application of hydrocyclones is in the removal of fine oil droplets, which cannot be removed by gravity separation, aiming at a clean water stream. Since we aim at recovering a pure oil phase, while there is already rapid gravity separation and we have relatively high oil fractions, the application of hydrocyclones did not result in separation of the oil.
- Cooling-thawing – after gravity separation, the obtained cream layer could be separated by a cool and thaw cycle, as done during the analytical procedure in which the complete phase separation had to be achieved. Since the hexadecane in

our model emulsion had a melting point of 18 °C, cooling the cream below this temperature resulted in freezing of the hexadecane. Upon heating, a continuous oil layer was formed. A cause for this coalescence could be the formation of crystals when the hexadecane froze, these could puncture the stabilising film and induce complete coalescence when melted again. For components with a lower melting point than water this process also worked: when a model emulsion with farnesene instead of hexadecane was cooled to -20 °C, the farnesene remained liquid and the continuous water phase froze. Upon melting, separation of the oil was again achieved. However, at a large scale, such a process would be very energy intensive so it was discarded for further study and only used in the analytical procedures.

- Gas bubble induced oil recovery – flotation is a well-known technique to remove small particles or droplets and obtain a clarified waste water stream. The goal of this technique is to enhance the rise velocity of the droplets, however in our model mixture that was not required because it separated already quickly by gravity. However, when supplying gas bubbles to the emulsion, the formation of a cream layer was prevented and a continuous oil layer was formed.

The gas bubble induced oil recovery method does not require de-emulsifiers and uses mild process conditions, this technique showed potential for application at large scale and was studied in further detail in this chapter.

Appendix B – Short cut calculations of biomass concentration

No data has been published about the biomass specific productivities for the production of advanced biofuels at an industrial scale. To come to an estimate of the microorganism concentration in a process for the production of advanced biofuels (farnesene is taken as an example), the following analysis was made based on heuristics and publicly available information. In an optimal scenario, the microorganism generates the energy that it requires from the formation of farnesene, directly coupling farnesene production to microbial growth. *Saccharomyces cerevisiae* can produced farnesene from acetyl-CoA via the mevalonate pathway [5]:

$$9\ Acetyl-CoA + 9\ ATP + 6\ NADPH \rightarrow C_{15}H_{24} + 3\ CO_2 \quad (1)$$

This acetyl-CoA has to be formed from pyruvate. Because cytosolic acetyl-CoA is required, it cannot be simply decarboxylated in a wild type *Saccharomyces cerevisiae*, but instead, pyruvate is converted to acetaldehyde and acetate in the native pathway. This results in a nett ATP consumption during the formation of farnesene and is therefore unfavourable for the microorganism. Kozak et al. developed an alternative pathway for the generation of cytosolic acetyl-CoA [30]. Amyris patented the bypass of the native acetyl-CoA production [31], obtaining a different reaction for the formation of cytosolic acetyl-CoA from glucose:

$$C_6H_{12}O_6 \rightarrow 2\ Acetyl-CoA + 2\ CO_2 + 2\ ATP + 4\ NADH \quad (2)$$

Furthermore, they slightly adapted the mevalonate pathway, by implementing an enzyme that uses NADH instead of NADPH as cofactor, yielding the overall reaction for the formation of farnesene from acetyl-CoA:

$$9\ Acetyl-CoA + 9\ ATP + 6\ NADH \rightarrow C_{15}H_{24} + 3\ CO_2 \quad (3)$$

Combining the two, we arrive to a reaction in which glucose is converted into farnesene:

$$4.5\ C_6H_{12}O_6 \rightarrow C_{15}H_{24} + 12\ CO_2 + 12\ NADH \quad (4)$$

ATP can be generated from oxidising the NADH, assuming a P/O ratio of 1. This results in the overall ATP generating reaction, in which glucose is converted to farnesene.

$$4.5\ C_6H_{12}O_6 + 6\ O_2 \rightarrow C_{15}H_{24} + 12\ CO_2 + 15\ H_2O + 12\ ATP \tag{5}$$

On the other hand, we have the anabolic reaction in which 1 mol of biomass is formed [32]:

$$0.175\ C_6H_{12}O_6 + 0.2\ NH_4^+ + 1.5\ ATP \rightarrow C_1H_{1.8}O_{0.5}N_{0.2} + 0.05\ CO_2 + 0.45\ H_2O + 0.2\ H^+ \tag{6}$$

Combining the catabolic and anaerobic reaction leads to the growth reaction, in which the formation of farnesene is coupled to microbial growth:

$$\begin{aligned} &0.7375\ C_6H_{12}O_6 + 0.75\ O_2 + 0.2\ NH_4^+ \rightarrow \\ &\quad C_1H_{1.8}O_{0.5}N_{0.2} + 0.125\ C_{15}H_{24} + 1.55\ CO_2 + 2.325\ H_2O + 0.2\ H^+ \end{aligned} \tag{7}$$

When a typical maintenance rate of 0.05 $mol_{ATP}/(mol_x \cdot h)$ is assumed, the specific substrate consumption rate (q_s), specific product rate (q_p), and specific water production rate (q_w) as a function of the specific growth rate (μ) can be derived from Equations (5) and (7):

$$q_s = -0.7375\ \mu - 0.01875 \tag{8}$$

$$q_p = 0.125\ \mu + 0.004167 \tag{9}$$

$$q_w = 2.325\ \mu + 0.0625 \tag{10}$$

When we consider the reactor to be operated at a constant volume and a diluted glucose feed (e.g., a second generation feedstock) with a glucose content of 180 g/kg (and a molar ratio of water and glucose in the feed of w = 45.65), we need the water outflow rate ($F_{w,out}$) and the biomass production rate (R_x) to come to a biomass concentration in the reactor. The water outflow from the reactor is a combination of the water in the feed and the produced water:

$$F_{w,out} = \frac{M_w}{\rho_w} R_P \left(\frac{q_w}{q_p} + w \frac{q_s}{q_p} \right) = \frac{M_w}{\rho_w} R_p \frac{\left(2.325 + 0.7375w\right)\mu + 0.0625 + 0.01875\ w}{0.125\mu + 0.004167} \tag{11}$$

In which M_w is the molecular weight of water, ρ_w the density of water, and R_p the overall product formation rate (moles of farnesene per hours). The production rate of biomass (R_x) as a function of the specific growth rate and the product formation rate can be calculated using the stoichiometry from the process and catabolic reaction:

$$R_x = R_p \frac{\mu}{q_p} = R_p \frac{\mu}{0.125\mu + 0.004167} \tag{12}$$

Combining Equations (11), (12) and the biomass balance gives the biomass concentration in the effluent:

$$c_x = \frac{R_x}{F_{w,out}} = \frac{\rho_w}{M_w} \frac{\mu}{\left(2.325 + 0.7375w\right)\mu + 0.0625 + 0.01875\ w} \tag{13}$$

This equation shows that at higher growth rates, more biomass will be produced and a higher biomass concentration will be obtained, which will have a negative effect on the economics of the process. However, higher biomass concentrations will result in a lower reactor volume due to the higher volumetric productivity, in a future analysis this trade-of will have to be studied. For the range of specific growth rates from 0.005 to 0.06 h^{-1}, we obtain a biomass concentration of 253-1083 mol_x/m^3 (note, this is per m^3 water, not m^3 broth), which corresponds to 6.2-26.7 g_x/L in dry weight. So the concentration in the experiments (10 g/L) is in the same order of magnitude as could be expected in the process.

Appendix C – Quantification of the colour gradient in the columns

In this appendix, the quantification of the colour gradient in the columns during the gas bubble induced oil recovery is illustrated with an example. Figure 15 shows the original picture and how the picture was cropped for the image analysis.

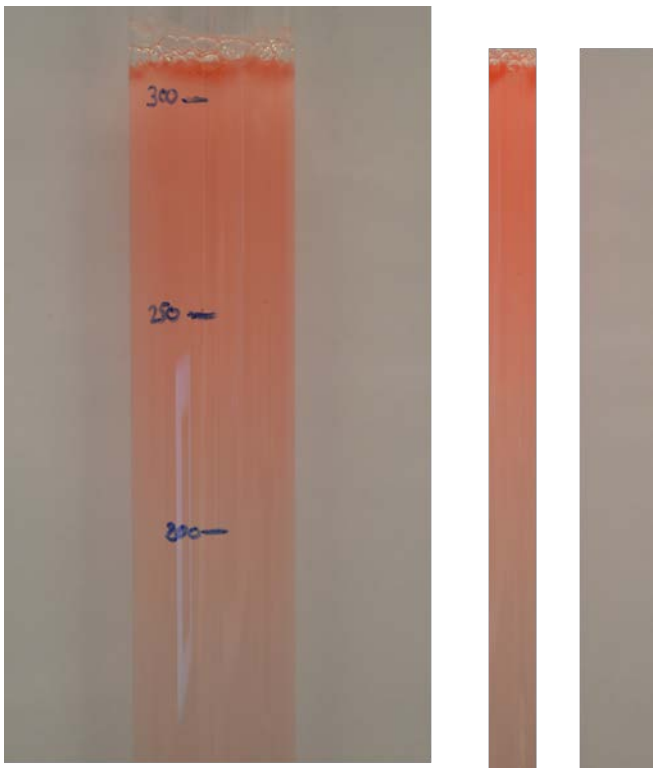

Figure 15. (left) An image from the column under reference conditions, made at 15 minutes. (middle) The cropped column image. (right) the white background for the correction of light intensities.

The column gradient and white image were loaded into MATLAB as a multidimensional array, containing the values for the red, green, and blue (RGB) pixels as three matrices. Each matrix was averaged over the width of the picture, yielding three vectors (for red, green and blue) with the average pixel value (Figure 16). The length of these vectors was equal to the height of the images in pixels.

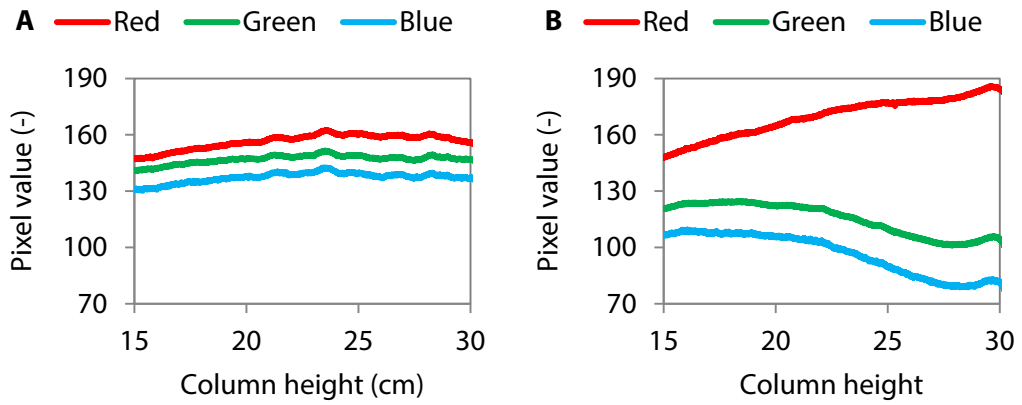

Figure 16. (A) the width averaged pixel values of the white background (B) the width averaged pixel values of the column picture.

The pixel values of the white background (Figure 16A) show that the light intensity over the height is not constant, there is an increase with increasing height and a slight decrease towards the top of the column. The colour gradient of the column (Figure 16B) was corrected for this inhomogeneity using the pixel values of the white background. First, the white background was normalised by dividing it by its average value. Then, the column values were corrected by dividing them by the normalised background vector (Figure 17A). Because the intensity of the green and blue pixels decreased with increasing redness, the green and blue vector were inverted by subtracting the maximum value a pixel can have (255) with the green and blue vectors (Figure 17B). Of the three resulting vectors, the inverted blue vector was used to compare the different columns.

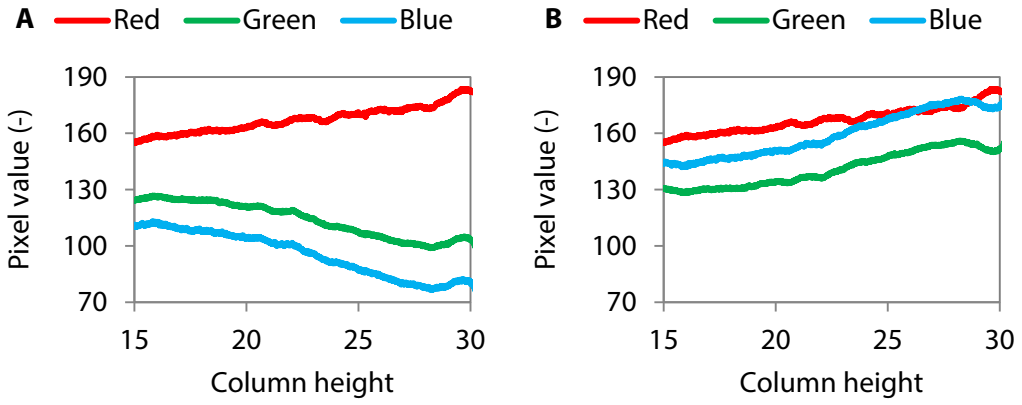

Figure 17. (A) the pixel values of the column corrected with the white background vector (B) the pixel values of the column, the green and blue vectors have been inverted.

References

1. Lee, S.K., et al., *Metabolic engineering of microorganisms for biofuels production: from bugs to synthetic biology to fuels.* Curr. Opin. Biotechnol., 2008. 19(6): p. 556-563.
2. Rude, M.A. and A. Schirmer, *New microbial fuels: a biotech perspective.* Curr. Opin. Microbiol., 2009. 12(3): p. 274-81.
3. Zhang, F., S. Rodriguez, and J.D. Keasling, *Metabolic engineering of microbial pathways for advanced biofuels production.* Curr. Opin. Biotechnol., 2011. 22(6): p. 775-783.
4. Domínguez de María, P., *Recent developments in the biotechnological production of hydrocarbons: paving the way for bio-based platform chemicals.* ChemSusChem, 2011. 4(3): p. 327-329.
5. Chandran, S.S., J.T. Kealey, and C.D. Reeves, *Microbial production of isoprenoids.* Proc. Biochem., 2011. 46(9): p. 1703-1710.
6. Heeres, A.S., et al., *Microbial advanced biofuels production: overcoming emulsification challenges for large-scale operation.* Trends Biotechnol. , 2014. 32(4): p. 221-229.
7. Heeres, A.S., et al., *Fermentation broth components influence droplet coalescence and hinder advanced biofuel recovery during fermentation.* Biotechnol. J., 2015: p. n/a-n/a.
8. Tabur, P. and G. Dorin, *Method for purifying bio-organic compounds from fermentation broth containing surfactants by temperature-induced phase inversion*. 2012, Amyris Inc.: US.
9. Malinowski, J.J., *Two-phase partitioning bioreactors in fermentation technology.* Biotechnol. Adv., 2001. 19(7): p. 525-538.
10. Schewe, H., M.A. Mirata, and J. Schrader, *Bioprocess engineering for microbial synthesis of isoprenoids*, in *Biotechnology of isoprenoids*, J. Schrader and J. Bohlmann, Editors. 2015, Springer International: Heidelberg. p. 251-286.
11. Lye, G.J. and J.M. Woodley, *Application of in situ product-removal techniques to biocatalytic processes.* Trends Biotechnol., 1999. 17(10): p. 395-402.
12. Brandenbusch, C., et al., *Process boundaries of irreversible scCO2-assisted phase separation in biphasic whole-cell biocatalysis.* Biotech. Bioeng., 2015. 112(11): p. 2316-2323.
13. Leppchen, K., et al., *Microbial de-emulsification: a highly efficient procedure for the extractive workup of whole-cell biotransformations.* Org. Process Res. Dev., 2006. 10(6): p. 1119-1125.
14. Choi, O.K., et al., *Enhancement of phase separation by the addition of de-emulsifiers to three-phase (diesel oil/biocatalyst/aqueous phase) emulsion in diesel biodesulfurization.* Biotechnol. Lett., 2003. 25: p. 73-77.
15. Rubio, J., M.L. Souza, and R.W. Smith, *Overview of flotation as a wastewater treatment technique.* Miner. Eng., 2002. 15(3): p. 139-155.

16. Al-Shamrani, A.A., A. James, and H. Xiao, *Separation of oil from water by dissolved air flotation.* Colloid. Surface. Physicochem. Eng. Aspect., 2002. 209(1): p. 15-26.
17. Ralston, J., D. Fornasiero, and R. Hayes, *Bubble–particle attachment and detachment in flotation.* Int. J. Miner. Process., 1999. 56(1–4): p. 133-164.
18. Schmid, A., et al., *Developments toward large-scale bacterial bioprocesses in the presence of bulk amounts of organic solvents.* Extremophiles, 1998. 2(3): p. 249-256.
19. George, K.W., et al., *Isoprenoid drugs, biofuels, and chemicals - artemisinin, farnesene, and beyond*, in *Biotechnology of isoprenoids*, J. Schrader and J. Bohlmann, Editors. 2015, Springer International: Heidelberg. p. 355-390.
20. Heijnen, J.J. and K. Van't Riet, *Mass transfer, mixing and heat transfer phenomena in low viscosity bubble column reactors.* Chem. Eng. J., 1984. 28(2): p. B21-B42.
21. Tadros, T.F. and B. Vincent, *Emulsion stability*, in *Encyclopedia of Emulsion Technology*, P. Becher, Editor. 1983, Marcel Dekker: New York. p. 269-272.
22. van Aken, G.A., F.D. Zoet, and J. Diederen, *Composition of thin films between emulsion droplets stabilized by protein, as measured in highly concentrated emulsions.* Colloid Surf. B: Biointerfaces, 2002. 26(3): p. 269-279.
23. Bos, M.A. and T. van Vliet, *Interfacial rheological properties of adsorbed protein layers and surfactants: a review.* Adv. Colloid Interface Sci., 2001. 91(3): p. 437-471.
24. Tcholakova, S., et al., *Coalescence in β-Lactoglobulin-Stabilized Emulsions: Effects of Protein Adsorption and Drop Size.* Langmuir, 2002. 18(23): p. 8960-8971.
25. Hotrum, N.E., et al., *Elucidating the relationship between the spreading coefficient, surface-mediated partial coalescence and the whipping time of artificial cream.* Colloid. Surface. Physicochem. Eng. Aspect., 2005. 260(1–3): p. 71-78.
26. Hotrum, N.E., et al., *Monitoring Entering and Spreading of Emulsion Droplets at an Expanding Air/Water Interface: A Novel Technique.* J. Colloid Interf. Sci., 2002. 247(1): p. 125-131.
27. Robinson, J.V. and W.W. Woods, *A method of selecting foam inhibitors.* J. Soc. Chem. Ind., 1948. 67(9): p. 361-365.
28. Hotrum, N.E., et al., *Flow and fracture phenomena in adsorbed protein layers at the air/water interface in connection with spreading oil droplets.* Langmuir, 2003. 19(24): p. 10210-10216.
29. Clift, R., J.R. Grace, and M.E. Weber, *Bubbles, drops, and particles*. 1978, New York: Academic Press.
30. Kozak, B.U., et al., *Replacement of the Saccharomyces cerevisiae acetyl-CoA synthetases by alternative pathways for cytosolic acetyl-CoA synthesis.* Metabolic Engineering, 2014. 21: p. 46-59.
31. Gardner, T.S., et al., *Production of acetyl-coenzyme a derived isoprenoids*. 2013.
32. Heijnen, J.J., *A therodynamic approach to predict black box model parameters for microbial growth*, in *Biothermodynamics*, U.v. Stockar, Editor. 2013, EPFL Press: Lausanne.

Chapter 6. Final discussion, concluding remarks and outlook

6.1 The future challenges in advanced biofuel production

The fermentative production of advanced biofuels provides an opportunity for a renewable alternative for fossil fuels, especially for the aviation industry for which a sustainable liquid fuel with a high energy density is required. As sketched Chapter 1, there is room for improvement in different areas of the production process to lower the production costs of these advanced biofuels. Further developments in the feedstock, microorganism, and process technology will help in creating a more economically competitive advanced biofuel production process. The main focus of this research was on the latter of the three, the process technology, but the influence of adapting the feedstock or microorganism on the process should not be disregarded. Ideally, the feedstock and microorganism should be improved, already taking the further process development into account.

The hydrocarbon production by fermentation offers the potential for simple recovery of the product, because of the extracellular and immiscible nature of the product. This results in a four phase fermentation mixture consisting of cells, gas bubbles, water and organic liquid (with a typical density difference between 0.11 and 0.24 kg/L). In principle, a mixture of oil and water is easy to separate and follows the following three steps (Figure 1):

1. Droplet growth – Since the product is secreted by the microorganisms, the initial droplets can be expected to be small. So this first step is required to reach a droplet size that can be separated. In a simple oil and water mixture, the droplet surface is not stabilised and coalescence of the droplets occurs readily.
2. Droplet creaming – The buoyancy force will cause droplets to rise when they are sufficiently large. So the first coalescence step will determine if passive gravity separation is applicable. The droplet creaming results in an oil rich layer at the top and an oil depleted aqueous layer at the bottom.

3. Oil layer formation – When the droplets cream to the top, another coalescence step is required to form a continuous product layer and achieve complete separation. Again, when the droplet surface is not stabilised, coalescence will occur readily and the continuous oil layer will be formed rapidly.

So coalescence is a very important mechanism in the recovery of oil from an advanced biofuel fermentation mixture, because it influences droplet growth and oil layer formation. The extent to which coalescence readily occurs determines the type of process steps that are required for this recovery process.

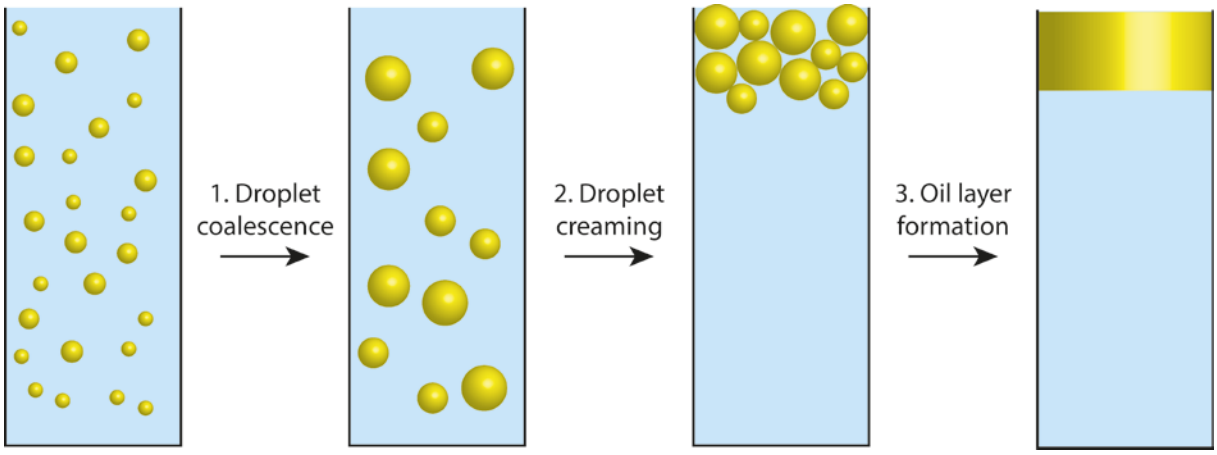

Figure 1. A sketch of the three steps in separation of oil from an emulsion.

Unfortunately, the complexity of the fermentation mixture will be much higher than a simple oil and water mixture and, as discussed in Chapter 2, a wide range of the components in fermentation mixtures have surface active properties, which could diminish coalescence. Furthermore, the process conditions (turbulence due to mixing) and the fact that the oil is produced microbially will also complicate the separation. In Chapter 3, it is experimentally confirmed that a number of the typical fermentation broth components indeed stabilise the oil/water interface against coalescence. Especially the components originating from the microorganism or complex feedstocks hinder coalescence, resulting in a decrease of the droplet-droplet coalescence rate of several orders of magnitude. These findings stress the importance of taking the recovery process into account when implementing a new feedstock, developing a microorganism, or changing fermentation conditions; already in that stage one

should aim at minimising the amount of surface active components in the mixture. However, most likely there will always occur some droplet stabilisation in in the fermentation process and additional steps will be required to convert these stable oil droplets into a continuous oil phase.

6.2 Experimental approach in this research project

6.2.1 Model emulsion

6.2.1.1 The behaviour of the model emulsion

Due to lack of access to an engineered microorganism that produced the advanced biofuel at process relevant titers, a model emulsion was used in this research to study the separation process. The main requirement of a model system is that it gives a good representation of the actual system. Although little has been reported about the nature of emulsions in fermentations in general and the nature of emulsions in advanced biofuel production in particular, the macro-properties of the emulsions (e.g., stability against gravity, gel-like structure, volumetric oil fraction) obtained in those processes and the model emulsion are comparable. Even though the product is secreted by the microorganism and the initial droplet size must be small, it has been suggested that droplet separation can be observed when the mixing is stopped in advanced biofuel fermentations [1, 2]. This behaviour is similar to the model emulsion used in the experiments, in which the droplet size is also sufficiently large to have droplet creaming due to the gravitational force. So the behaviour of the model emulsions and advanced biofuel fermentation emulsions seem to be similar, but when an actual producing strain becomes available, this is the first check that has to be made.

6.2.1.2 Proteins as main stabilising component

In fermentations incorporating an organic phase, proteins have also been reported to be an important cause of emulsion stabilisation [3, 4]. When proteins adsorb at the oil/water interface, they stabilise the interface by forming a visco-elastic interface, preventing film rupture. Depending on the type of protein, the affinity for the oil/water interface could vary,

but the stabilising mechanism remains the same [5, 6]. Proteins also have been reported as one of the main stabilisers in emulsions obtained in advanced biofuel fermentations and the addition of proteases decreased the emulsion stability [7]. The product secretion mechanism of the microorganisms could also influence the stabilising components. When intracellular product globules as a whole are secreted, there might be some biosurfactants or phospholipids around these small droplets [8]. However, their possible influence appears to be limited, given the observations that droplet creaming in the process occurs readily and therefore droplet-droplet coalescence must occur in the fermentor.

The exact composition of the stabilising components in the model emulsion used in this thesis remains unknown, but proteins originating from the yeast cells were (one of) the main stabilisers. Also for the model emulsion addition of proteases resulted in a decrease of the emulsion stability. An attempt was made to analyse the composition of the proteins, using a combination of liquid chromatography/mass spectrometry after treating the emulsions samples with trypsin to partially digest the proteins. From the peptide fragment spectra, the present proteins were identified using SwissProt database. This analysis could not identify a main responsible for the stabilisation, instead, a wide range of different yeast proteins (100+) were found to be present in the emulsion. Furthermore, the following experimental observations also support the hypothesis that proteins are the main cause of stabilisation in the model emulsions:

- Protein measurements in the cream layer gave a surface excess concentration of 4.5 mg/m^2, which is in the range of protein stabilised emulsions (Chapter 5).
- The cream layer was stable against centrifugation (Chapter 5). Instead of coalescence into a continuous oil layer, extensive film drainage occurred which is known behaviour of protein stabilised emulsions [9].
- The yeast cells appear to be unable to cause Pickering stabilisation (as argued in Chapter 3 and 5), the cells do not attach at the oil/water interface.

So looking at the macro-behaviour of the model emulsions with the available information about the emulsions in advanced biofuel production, the model emulsion seems to give a good representation of the actual challenges faced in advanced biofuel production.

6.2.1.3 The pro's and cons' of a yeast cell free model mixture

In the experimental study, two types of model emulsions were used: an emulsion with yeast cells and an emulsion with supernatant from yeast cells. The first seems to be a better representation of the fermentation mixture due to the presence of cells, but the yeast cells did not have the ability to stabilise the oil/water interface by Pickering stabilisation, so their presence is not required for a good mimic of the emulsion stabilisation. Furthermore, the presence of yeast cells caused large variations in the experimental results (Chapter 5). One possible cause could be the variations in the age of the used pressed yeast and thereby the amount of surface active components in the system (Figure 2),

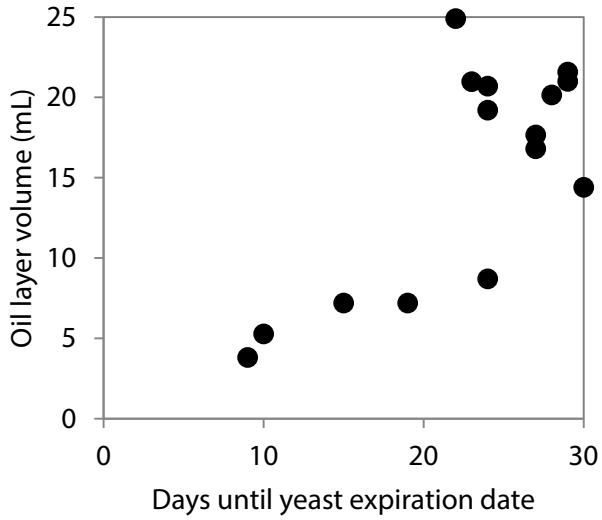

Figure 2. The different amounts of oil recovered by gas bubble induced oil recovery under standard conditions (v_{Gs} = 0.1 cm/s, d_{nozzle} = 0.3 mm) with emulsions that were prepared with changing yeast age.

Furthermore, the yeast cells can keep releasing surface active components into the system during the experiment, causing their amount to increase over time. By using yeast supernatant, a fixed amount of surface active components could be added and the experimental variations were eliminated so that the effects of individual parameters could be

isolated. An additional advantage of the cell free emulsion was that it allowed for improved visual observations. The model emulsions used in this research appeared to give a good mimic of challenges encountered in the advanced fermentations and are therefore very useful for studying the improvement opportunities and separation methods for the product recovery, which can be implemented in the production process in a later stage.

6.2.2 Analytics

Besides developing a model emulsion to study the phenomena in the separation process, the analytical tools to characterise the emulsions had to be developed as well, since this was the first project working with emulsions in the department. The main properties of the emulsions that had to be characterised were the oil content, the amount of surface active components, and the droplet size (Figure 3). The multiphase nature of the system already caused a challenge in obtaining an representative sample, especially when sampling from the cream layer. However, this could quite easily be overcome by taking a sufficiently large sample volume and using a pipet with a large opening. With this approach, samples could be taken for analysis of the oil content and amount of surface active components.

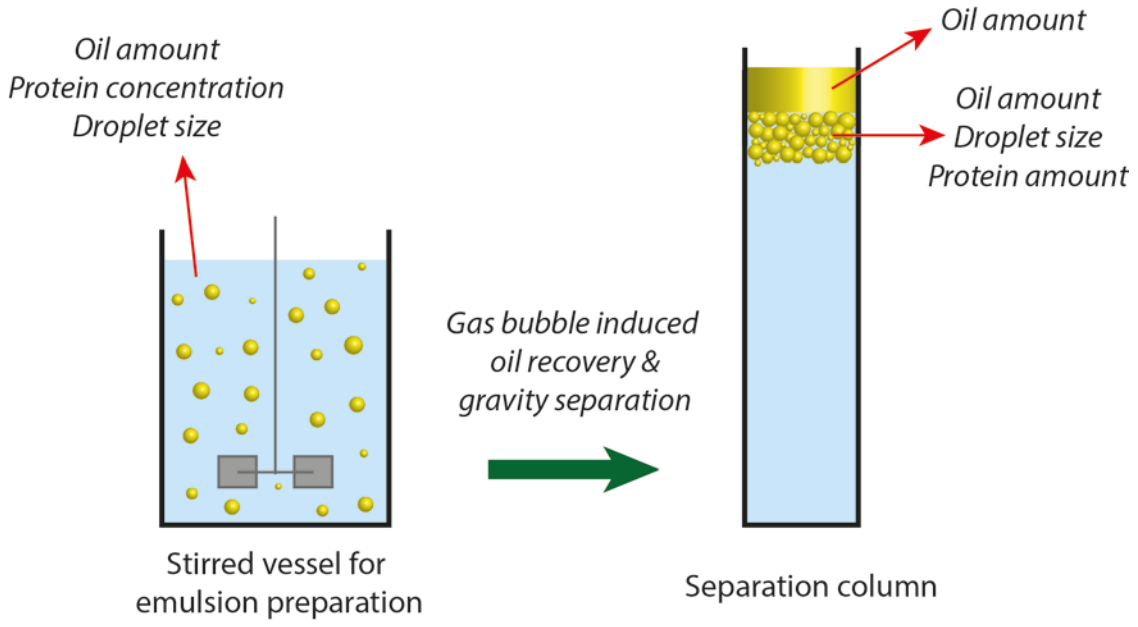

Figure 3. Different properties that were determined during the gas bubble induced oil recovery experiments.

6.2.2.1 Oil fraction measurements

The first attempt for determining the oil fraction was done on a mass basis: a known amount of sample was centrifuged with de-emulsifiers (SDS or ethanol) to break the emulsion, after which the organic layer could be removed and weighted. However, accurate removal of the organic phase and achieving complete de-emulsification was difficult. A second method used gas chromatography to determine the amount of organic phase (hexadecane) in the emulsion. Again, the emulsion had to be broken completely and the organic phase was extracted and diluted with heptane. The procedure of emulsion breaking and dilutions was labour intensive and the duplicate experiments showed large deviations in the results. When a comparison was made between using plastic disposables or glass tubes and pipets, it was found that a large part of these deviations were caused by the use of plastics (Falcon sample tubes, pipet tips) when processing the samples. The cause of these deviations was unknown, but in analysis of isoprenoid compounds, also only glass is used. So therefore the use of plastic components was avoided and glass ware should be used.

Finally, a less laborious method was developed, using photo spectrometry in combination with the presence of Oil Red O in the organic phase (as described in Chapter 5). A known amount of uncoloured hexadecane was added to the samples, which allowed to calculate the amount of coloured hexadecane that was present in the original sample. This method did not require high dilutions of the sample and decreased the amount of waste produced. When the dye cannot be added to the organic phase during the process (e.g., during fermentation), the approach can be inverted: addition of a known amount of coloured hexadecane to an uncoloured sample before the emulsion breakup procedure.

In the experiments, most of the oil was present in the oil layer or in the cream layer after gravity separation. The aqueous layer was clear, so the amount of oil in that bottom layer could be neglected. To come to an accurate oil mass balance, the volumes of the oil and cream layers and the oil fraction of these layers had to be quantified accurately, from which the mass could be calculated with the oil density and the oil volume fraction. However, in the emulsions with yeast cells, a foam could be formed on top of the liquid surface, which

contained a significant amount of oil. To be able to set up a closing mass balance for that situation, the amount of oil in the foam should also be quantified.

6.2.2.2 Quantification of surface active components

For determining the surface active components in the emulsion, the first challenge is to remove them from the interface into the aqueous layer in which they can be characterised or measured. Using an aqueous urea buffer in combination with a freezing/thawing cycle (as described in Chapter 5), destabilised the emulsion and solubilised the proteins that were adsorbed at the oil/water surface. In that aqueous phase, the protein concentration could be determined using an assay (e.g., Bradford or BCA), but due to the amount of urea buffer that had to be added, the protein concentrations were in the bottom range of what could be detected with the assays, so the method could be improved further by decreasing the amount of buffer required for the solubilisation of the proteins, or using another method to measure the protein concentration. Furthermore, in this research we have been focussing on proteins, which provide a very large contribution to the emulsion stability, but a more thorough characterisation could also identify other stabilisers, this would be especially interesting when an advanced biofuel fermentation broth is available.

6.2.2.3 Droplet size measurements

Initially, the droplet size was measured using an available offline microscope in combination with image analysis software. Such an offline method has well known disadvantages: taking the sample could alter the droplet size distribution and the droplet size in the sample can change over time due to coalescence. Different analytical techniques were studied, aiming at *in situ* measurement of the droplet size, so eliminating the need for sampling. Different optical probes are available to acquire images of the emulsion *in situ*, but the main challenges for these instruments are related to the automated analysis of the pictures and acquiring good quality images. In systems with high oil fractions or high yeast concentrations, getting sufficient light in the system for the pictures can be difficult. Furthermore, high oil fractions result in overlapping droplets in the pictures, which make

automated image analysis of the pictures difficult. The instrument from SOPAT was able to provide sufficient lighting for the pictures (in very dense systems back lighting can be applied) and the image analysis software was capable of dealing with high oil fractions and the presence of cells. So this instrument provided a good solution for measurement of the droplet size. However, when such an instrument is placed into a reactor, it influences the local hydrodynamics. Furthermore, there is the risk of fouling, either by growing microorganisms in a fermentation or oil droplets sticking to the lens of the probe. The latter is especially problematic when this occurs during a fermentation. To clean the lens, the probe has to be removed from the reactor and placed back again, while maintaining aseptic conditions. This might be done by creating a separate chamber on the reactor, in which the probe can be sterilised after retracting it from the reactor and cleaning (http://www.knick.de).

6.3 How to separate oil in advanced biofuel production

Currently, multiple centrifugation steps are used in combination with chemical de-emulsifiers to achieve separation of the product [7]. Substitution of the centrifugation step by an alternative method and avoiding the use of the chemical de-emulsifier can both decrease the process costs. Gravity separation would be the obvious alternative to achieve the phase separation of the product. This method has the additional advantage that it might be integrated with the fermentation process, decreasing equipment costs, enabling the recycle of cells and limiting the stability of the dispersion (enhanced coalescence) by continuous removal of the droplets. The regime analysis in Chapter 4 showed that sufficient droplet growth can be achieved under fermentation conditions, but that the broth mixing due to gas flow in bubble columns at large scale will be too severe for direct integration of gravity separation. So for integration of gravity separation in the fermentator, a gas free compartment in the fermentor is required

6.3.1 *Alternative separation methods*

When the droplets can become sufficiently large, phase separation by gravity can be achieved in a gas free compartment leading to a stable cream layer. The second coalescence step (Figure 1) to convert the cream layer into a continuous oil layer has to occur to achieve a complete separation. Within this project, several methods have been studied aiming at the recovery of oil from fermentation broths (Chapter 5, Appendix A) before the study of bubble induced oil recovery. These methods are summarised in Figure 3.

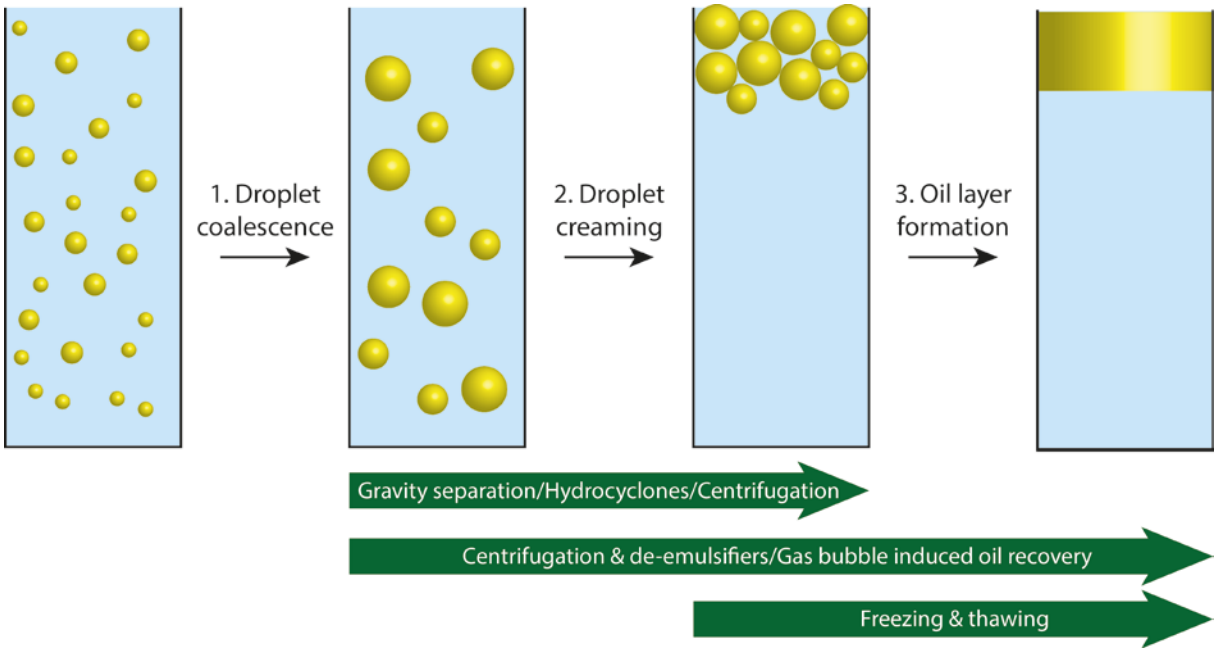

Figure 4. The explored separation methods and their place in the separation process where they act.

Literature discussing fermentations with an organic phase showed that instead of coalescence into a continuous oil layer, a concentrated emulsion (cream) is often obtained. In our model emulsion, such a cream layer was formed after gravity separation as well, so the most challenging step is to form the oil layer from the stabilised droplets. With the goal of developing a low cost alternative for centrifugation that does not require de-emulsifiers, the gas bubble induced oil recovery was studied in more detail (as discussed in Chapter 5).

6.3.2 Bubble induced oil recovery

Although the method of bubble induced oil recovery has been studied in Chapter 5, there is no certainty on the underlying physical mechanism. The varied process parameters show clearly that the number and size of the gas bubbles have a large influence on the formation of an oil layer, along with the properties of the dispersion (oil fraction, concentration of surface active components). In Section 5.1.1, a mechanism is suggested in which the gas bubble surface facilitates coalescence by inducing film rupture and offering a hydrophobic surface. The experimental results suggest there is a maximum oil formation rate that was achieved in the laboratory setup, but with the knowledge of this moment, the reason for this maximum rate is not clear. When the separation mechanism is understood more thoroughly, the cause for the maximum oil formation rate could become clear and further improvements could be made to increase the rate.

The separation method was tested with the two different model emulsions (with yeast cells and with supernatant) and the experiments with yeast supernatant provided most insight in the effect of different process parameters. A major difference between the two model emulsions was the formation of foam in the experiments with the yeast cell supernatant. Especially at higher superficial gas velocities, a large foam layer was formed that contained a significant amount of oil (>50% of the total oil in the system). Besides the oil, also a large amount of water was present in this foam. Although it does not deliver liquid containing only oil, this foaming could also be interesting for further research, using the foam formation as method to achieve a first oil concentration step. However, applying a first concentration step might not be beneficial for the gas bubble induced oil recovery. When the droplets were allowed to gravity separate for 1 hour and form a cream layer before the gas bubble induced oil recovery was started, the volume of the oil layer after two hours of separation was halved. So the gas bubble induced oil recovery seems to be more efficient when it is directly applied to a diluted emulsion. Therefore, integrating the separation process with the fermentation could also enhance the separation process.

6.4 Towards an integrated process at large scale

6.4.1 Integration in the fermentor

The developed separation process shows the potential to be integrated in the fermentor, which offers several advantages:

- The equipment costs can be lowered when the fermentation and separation are done in one piece of equipment.
- Continuous removal of the product reduces the residence time of product droplets in the fermentation broth. This reduces the available time for stabilisation of the interface by the surface active components, leading to reduced emulsion stability and an easier separation.
- Because of the mild process conditions and absence of de-emulsifiers, cell viability can be maintained. This makes a cell recycle possible, which lowers the substrate requirement for the production of cells and lowers the fermentor volume.

Keeping the cells intact is also beneficial for the separation itself, since it limits the amount of surface active components released by the cells. When the gas bubble induced separation method was tested for a patent application with a model emulsion containing homogenised cells, no oil could be separated anymore. In an actual fermentation process, the complexity of the mixture composition will be higher than in the model emulsions used in the experiments. Furthermore, the process conditions will also influence the amount of surface active components in the emulsion.

When the fermentation has to be integrated with the separation, a conflict in the mixing regimes comes forward, which is similar to the previously discussed integration of gravity separation. The gas flow rate of the separation process is at least one order of magnitude lower than for the fermentation, so for a feasible integration into a single reactor, a two-compartment design has to be made (Figure 4). In such a compartmentalised reactor, the fermentation broth, including the cells, can be continuously circulated and reused. The

conditions in the fermentation compartment can then be optimised for the cells, but in the separation compartment, concessions will have to be made to achieve the separation (e.g., mixing or oxygen transfer). This could result in less favourable conditions for the microorganism and therefore, the residence time of the microorganisms will likely have to be limited. So the flow through the separation section has to be balanced in a way that a sufficiently short residence time of the cells in the separation section is achieved (to avoid shortage of oxygen and substrate) and the droplets still get sufficient time to separate.

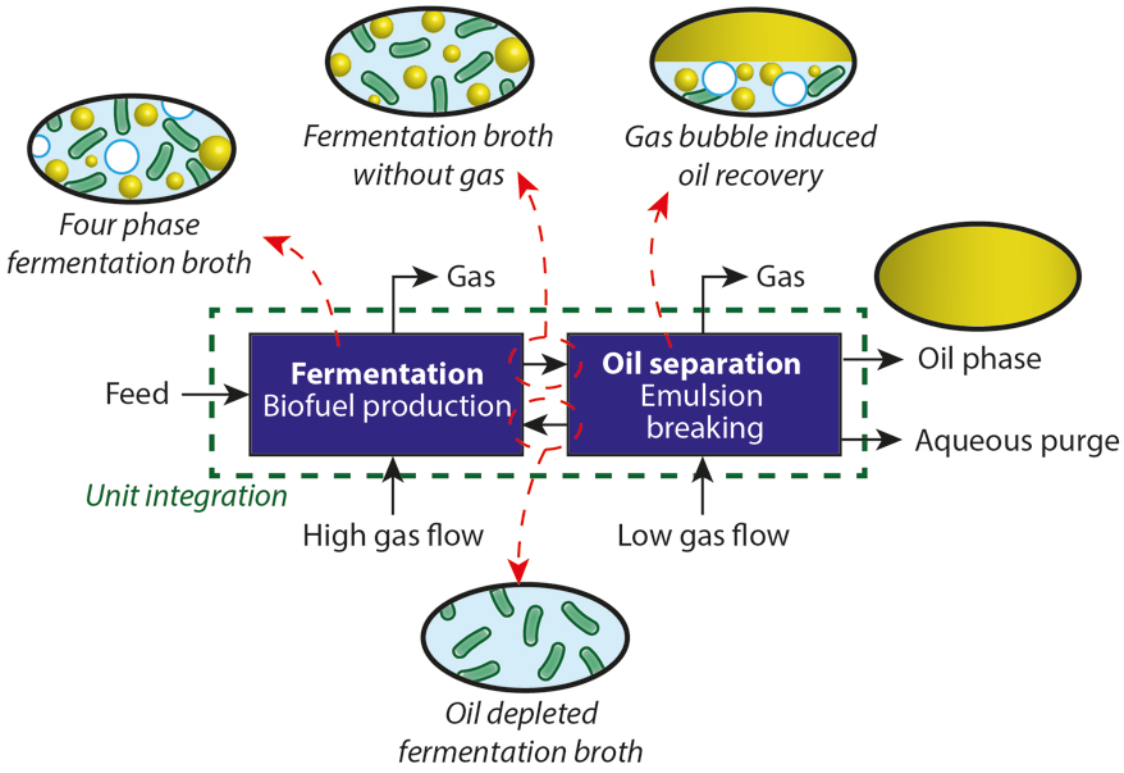

Figure 5. A block scheme of the two compartment reactor including the different composition in the different compartments and flows.

In the small scale columns, a recovery rate of approximately 10 mL/h is being achieved, which corresponds to about 7.7 g/h. The volume of the columns was 300 mL, so that results in a volume specific separation rate of 25 g/(L·h). This is higher than the typical volumetric productivity of developed fermentation processes, which is usually in the order of magnitude of 1 g/(L·h) (0.35 g/(L·h) has been reported for amorpha-4,11-diene, a

sesquiterpene produced via a similar pathway as farnesene) [10]. So if the processes could be integrated directly, the separation rate is sufficient to separate the formed product. For the two-compartment reactor, this calculation shows that is likely that the volume of the fermentation section can be larger than the volume of the separation section. Another comparison can be made when the separation rate is considered as a flux of oil droplets coalescing into the main oil phase through the O/W interface. With the diameter of the columns in the laboratory scale experiments, an oil recovery rate of 10 mL/h corresponds to an area specific oil recovery rate of 1 $mL/cm^2/h$. An industrial scale reactor with a volume of 600 m^3 will have a cross sectional are of 26 m^2 (diameter 5.8 m, aspect ratio 4), through which a recovery rate of 0.26 m^3/h could be achieved (scaling by area). This separation rate can balance a volumetric productivity in the bioreactor of 0.35 g/L/h, so it seems to be in the same order of magnitude as the volumetric productivity. However, at this moment the exact scale up mechanism of separation process scales up is unknown, so this should be subject of future research.

The model emulsion did not show extensive foaming, but for scale up this could become a challenge. In a fermentation process, the amount of surface active components will not be constant over time and it might increase over the course of the fermentation. These surface active components will want to adsorb at an interface and in the bubble induced separation process, the bubble surface will be present as an additional surface. When the available surface active components adsorb at this W/G interface, a foam layer could be formed, adding complexity to the system. Such a foam layer can contain a significant amount of oil, as mentioned before. To which extent this will influence the separation process will have to be addressed in future research as well.

6.4.2 Process scale up

A better understanding of the separation mechanism is also necessary for a rational scale up of the process. One could expect that because the coalescence of the dispersed droplets is likely to happen at the interface of the continuous oil layer and the aqueous phase,

the coalescence rate might scale with the area of this interface. This would set a clear scaling parameter for the separation rate, around which the integrated equipment could be designed. When increasing the cross sectional area, the further geometry of the separation section will change as well. The laboratory experiments showed the importance of the axial dispersion of the oil droplets in the separation section. These experiments were executed in columns with a small diameter and high aspect ratio, which limited the mixing and axial dispersion of the droplets throughout the column. Limiting axial dispersion enhanced the recovery of oil up to a certain extent, but when the size and diameter of the separation compartment are increased, the hydrodynamics and axial dispersion in the separation compartment will be harder to control. By implementing internal structures, scale independent hydrodynamic conditions could be achieved in the separation compartment. Limiting axial dispersion of the droplets will inevitably lead to limitation of mixing, which will also influence other (microbial) processes in the separation section.

6.5 Outlook

How the developed process of gas bubble induced oil recovery will develop further depends on the outcome of future research. At this moment, the developed method shows potential to contribute to a cheaper and more sustainable production process for advanced biofuels. Further research into the scalability of this method and the technical feasibility for the integration of this method with the fermentation will learn how this research will influence the future production of advanced biofuels.

References

1. Cherry, J., *Amyris synthetic biology: Purposeful, predictable, profitable*, in *37th Symposium on Biotechnology for Chemicals and Fuels*. 2015: San Diego, CA, United States.
2. Keasling, J.D., et al. *Production of fatty acids and derivatives thereof.* WO 2007/136762 A2, 2011.
3. Lennie, S., P.J. Hailing, and G. Bell, *Causes of emulsion formation during solvent extraction of fermentation broths and its reduction by surfactants.* Biotech. Bioeng., 1990. 35(9): p. 948-950.
4. Schmid, A., et al., *Developments toward large-scale bacterial bioprocesses in the presence of bulk amounts of organic solvents.* Extremophiles, 1998. 2(3): p. 249-256.
5. McClements, D.J., *Protein-stabilized emulsions.* Curr. Opin. Colloid In., 2004. 9: p. 305-313.
6. Bos, M.A. and T. van Vliet, *Interfacial rheological properties of adsorbed protein layers and surfactants: A review.* Adv. Colloid Interface Sci., 2001. 91(3): p. 437-471.
7. Tabur, P. and G. Dorin. *Method for purifying bio-organic compounds from fermentation broth containing surfactants by temperature-induced phase inversion*. US Patent 20120040396, 2012.
8. Walther, T.C. and R.V. Farese Jr, *The life of lipid droplets.* Biochim. Biophys. Acta, 2009. 1791(6): p. 459-466.
9. van Aken, G.A. and F.D. Zoet, *Coalescence in highly concentrated coarse emulsions.* Langmuir, 2000. 16(18): p. 7131-7138.
10. Straathof, A.J.J., *Transformation of biomass into commodity chemicals using enzymes or cells.* Chem. Rev., 2014. 114(3): p. 1871-1908.

Curriculum Vitae

Arjan Heeres was born on the 19th of September 1986 in Vlissingen, the Netherlands. After completing atheneum at the S.S.G. Nehalennia in Middelburg, he moved to Delft to start his studies at the Delft University of Technology. After acquiring a bachelor degree in chemical engineering and bioprocess technology, he continued with the biochemical engineering programme. During the two-year programme, he did an internship at the R&D department of DSM Food Specialties, working on increasing downstream processing yields of lactic acid starter cultures. The graduation project was done under supervision by Dr. C. van den Berg, Dr. A.J.J. Straathof, and Prof. Dr. Ir. L.A.M. van der Wielen on the production of butyl butyrate by simultaneous clostridial fermentation, lipase-catalysed esterification, and ester extraction.

In July 2011, he started as a PhD student at the Delft University of Technology in the current Bioprocess Engineering with Prof. Dr. Ir L.A.M. van der Wielen and Prof. Dr. Ir. J.J. Heijnen as promotors and M.C. Cuellar as co-promotor. Within this project, he worked on the development of a process in which the production and separation of advanced biofuels are integrated, as presented in this thesis.

After working for Delft Advanced Biorenewables for a short project on the implementation of the developed separation method at a larger scale he now works as a bioprocess engineering consultant for TMC.

Acknowledgements

A little over four years ago, after a nice MSc project with the BPE section I decided that I wanted to keep learning at the university and that opportunity was there in the BioProcess Engineering group. An exciting new line of research on the production and recovery of advanced biofuels was started, led by Maria. The project title seduced me (many would follow), but the project turned out to be even better than the title suggested. I owe this mainly to the great supervision I had. Maria, I was lucky enough to have had you as my supervisor, I cannot imagine a supervisor being more committed and helpful than you have been to me, I hope you look back to this adventure with the same pleasure as I do!

Talking about supervision, I also had two promotors, who founded this project, and I thank them for their contribution during the project. Sef, working together with you was very inspiring to me; it was great to share a bit in your experience and to get your thorough review of the work I did (sometimes within minutes…). Luuk, I am very grateful that you made everything in this project possible and for now and then pushing me in the right direction. I don't think many PhD students get the opportunities that I got in my project (working at other universities/pilot experiments/conferences). These opportunities were the cherries that have created many of the lasting experiences and memories.

But already without these cherries, the cake would have been very, very nice! This is due to the great people that have been part of the BPE group in the past four years. Camilo, thanks for all the coffees we had at 10.30 and 15.30, your broad interest in everything made all the conversations we had a pleasure. Too bad you suddenly disappeared while I was in Brazil, but luckily Carlos was also always up for a coffee. It was always nice to talk about the business at BT, NBA results, or the speech of Donald Trump of the previous day and I appreciated your always constructive attitude. Besides in Delft, colleagues also play a crucial role when travelling to conferences. Visiting Brazil, going from waterfalls to some kind of Swiss mountain village, with Susana and the raki in Istanbul with David and Alex also created everlasting memories. Furthermore, I want to thank everyone of the BPE group for being

grateful test dummies for everything that I whipped up in my oven, it was a pleasure to share all the cake with you!

I also had the joy of working together with a lot of students on my project: Bert, Renco, Robbert, Leonor, Wouter, and Nikos, it was a pleasure to work with each of you. I always enjoyed the discussions we had about your projects, while appreciating a good cup of coffee, and I think working with you was one of the aspects of my PhD that learnt me the most! I also want to thank Susana, Filippo, Kumaran, and Rita for their contribution to the project and although my work with DAB was technically not part of my PhD, I also want to express my gratitude to Fabiënne, Rob and Kirsten; it was great to work with you for three more months on this project with you.

As I mentioned before, I got the opportunity to visit and experience how it is to work at two other universities. In Wageningen, Karin and Thomas welcomed us enthusiastically and Marcel helped me out with every issue I had with those delicate microfluidic chips, thanks for the hospitality! Some might argue that Wageningen is far away, but the other adventure was even further away. Caroline, Rosiane and all the others, you made me really feel at home during the 3 months that I got to be in Campinas. You all have been so kind and helpful with everything and you gave me the true Brazilian experience.

Besides drinking coffee, eating cake, and travelling, some work had to be done as well. I could not have done what I did in the past four years without all the support that I got from people in the department. First of all, thank you, Stef and Max, for always being there and willing to help searching through the building when I again needed some piece of equipment that no one ever used. Furthermore, I owe the people from the workshop, Marcel, Arno, Carlo and Ruud, a lot of gratitude for making everything that I could not find laying around in the building and always being prepared to offer a helping hand on a short notice. I think you are a great example of why BT is such a nice department to work at: everyone is always very supporting and helping you to achieve what you want to achieve!